GENOMIC DNA DETECTION BASED ON ELECTROCHEMICAL LABEL OF GOLD NANOPARTICLES ENCAPSULATED POLYELECTROLYTE MICROCAPSULE

MISS NAPHAT KHUNRATTANAPORN

A THESIS SUBMITTED IN PARTIAL FULFILLMENT

OF THE REQUIREMENTS FOR

THE DEGREE OF MASTER OF SCIENCE (BIOTECHNOLOGY)

SCHOOL OF BIORESOURCES AND TECHNOLOGY

KING MONGKUT'S UNIVERSITY OF TECHNOLOGY THONBURI

2012

Genomic DNA Detection Based on Electrochemical Label of Gold Nanoparticles Encapsulated Polyelectrolyte Microcapsule

Miss Naphat Khunrattanaporn B.S. (Agro-Industrial Biotechnology)

A Thesis Submitted in Partial Fulfillment of the Requirements for
the Degree of Master of Science (Biotechnology)
School of Bioresources and Technology
King Mongkut's University of Technology Thonburi
2012

Thesis Committee

…….. Chairman of Thesis Committee
(Sukunya Oaew, Ph.D.)

……. Member and Thesis Advisor
(Assoc. Prof. Werasak Surareungchai, Ph.D.)

……. Member and Thesis Co-Advisor
(Patsamon Rijiravanich, Ph.D.)

……. Member
(Mithran Somasundrum, Ph.D.)

……. Member
(Asst. Prof. Chamras Promptmas, Ph.D.)

Thesis Title	Genomic DNA Detection Based on Electrochemical Labels of Gold Nanoparticle Encapsulated Polyelectrolyte Microcapsules
Thesis Credit	12
Candidate	Miss Naphat Khunrattanaporn
Thesis Advisors	Assoc. Prof. Dr. Werasak Surareungchai Dr. Patsamon Rijiravanich
Program	Master of Science
Field of Study	Biotechnology
Division	Biotechnology
Faculty	School of Bioresources and Technology
B.E	2555

Abstract

The spiky gold capsules were successfully fabricated as electrochemical labels to enhance the sensitivity of oligonucleotide and genomic DNA detection by increasing the numbers of gold nanoparticles entrapped in polyelectrolyte microcapsules (PAA-capsule). PAA-capsules were prepared by layer-by-layer assembly of alternating oppositely charged polyelectrolytes onto polystyrene-co-acrylic acid (PSA) templates. The templates were removed by dissolution in an organic solvent to lease hollow shell polyelectrolyte microcapsules. The capsule interior was loaded with polyallylamine (PAA) via pH manipulation. Gold loading into the PAA-capsule to produce spiky gold capsules were performed by two steps: preparation of the seed mediated method and the incubation in growing solution method. The spiky gold capsules were found to contain approx. 1.02×10^{11} Au^{3+} molecules per capsule. DNA hybridization detections using the spiky gold capsule as labels was performed using stem loop DNA (SL-DNA) probes. The probe contained a digoxigenin (DIG) label at one end. The other end of the SL-DNA probe contained a thiol group, enabling assembly with a spiky gold capsule. After DNA hybridization, the stem loop straightens out, hence enabling to an anti-DIG coated magnetic latex at one end and a spiky gold capsule at the other. The quantity of gold attracted to the probes could then be measured by differential pulse anodic stripping voltammetry. A detection limit of 1.84 aM was achieved, the lowest quantity of target oligonucleotide. The genomic DNA of *E. coil* BL21, ATCC8739 and O157:H7 was detected in real samples (milk and fermented palm juice) with detection limits of 2-4 CFU mL^{-1} for an assay time of approx. 105 min.

Keywords: Genomic DNA Detection/ Spiky gold Capsule/ Stem loop DNA/ Gold Nanoparticles/ Anodic Stripping Voltammetry.

หัวข้อวิทยานิพนธ์	การตรวจวัดจีโนมิกดีเอ็นเอด้วยฉลากเคมีไฟฟ้าพอลิอิเลคโทรไลท์ไมโครแคปซูลที่บรรจุอนุภาคทองนาโน
หน่วยกิต	12
ผู้เขียน	นางสาวนภัทร คุณรัตนาภรณ์
อาจารย์ที่ปรึกษา	รศ.ดร. วีระศักดิ์ สุระเรืองชัย
	ดร. พรรษมณฑ์ ริจิรวนิช
หลักสูตร	วิทยาศาสตรมหาบัณฑิต
สาขาวิชา	เทคโนโลยีชีวภาพ
คณะ	ทรัพยากรชีวภาพและเทคโนโลยี
พ.ศ.	2555

บทคัดย่อ

งานวิจัยนี้เป็นการสร้าง และศึกษาฉลากเคมีไฟฟ้าแคปซูลบรรจุอนุภาค Spiky gold (spiky gold capsule) เพื่อเพิ่มความไวต่อการตรวจวัดโอลิโกนิวคลีโอไทด์ และจีโนมิกดีเอ็นเอ โดยการเพิ่มจำนวนอนุภาคทองนาโนที่บรรจุในพอลิอิเล็กโทรไลท์แคปซูล (PAA-capsule) ทำการเตรียม PAA-capsule ด้วยเทคนิคการตรึงแบบชั้น-ต่อ-ชั้น ที่อาศัยแรงดึงดูดทางไฟฟ้าสถิต (electrostatic interaction) ของพอลิอิเลคโทรไลท์ที่มีประจุตรงข้ามลงบนแม่พิมพ์อนุภาคพอลิสไตรีน-โค-อะคิลิกแอซิด (PSA) จากนั้นทำการละลายแม่พิมพ์ PSA ออก ด้วยสารละลายอินทรีย์ได้เป็นพอลิอิเลคโทรไลท์แคปซูลที่มีช่องว่างภายใน ต่อมาทำการบรรจุสารพอลิเอริลเอมีนภายในได้โดยกายปรับเปลี่ยน pH ได้เป็น PAA-capsule ในการบรรจุอนุภาคทองเข้าสู่ PAA-capsule เพื่อสร้าง spiky gold capsule สามารถเตรียมด้วยวิธี seed mediated method และตามด้วยวิธีการบ่มภายในสารละลาย growthing solution ตามลำดับ พบว่าภายใน spiky gold capsule หนึ่งอนุภาคมีปริมาณโมเลกุลของ Au^{3+} สูงถึง 1.02×10^{11} โมเลกุลต่อแคปซูล ในการตรวจวัดดีเอ็นเอไฮบริไดเซชั่นได้ทำการใช้ฉลาก spiky gold capsule ร่วมกับโพรบสเต็มลูปดีเอ็นเอ (SL-DNA) ที่มีการติดสารดิกออกซิจีนิน (DIG) ที่ปลายด้านหนึ่งของโพรบ ส่วนปลายอีกข้างหนึ่งของโพรบติดหมู่ thoil ซึ่งสามารถเชื่อมติดกับ ฉลาก spiky gold capsule ได้ เมื่อมีการไฮบริไดซ์เซชั่น โครงสร้างของสเต็มลูปดีเอ็นเอจะยืดยาวออกส่งผลให้เกิดการจับกันของ anti-DIG บนอนุภาคแม่เหล็ก และ Spiky gold แคปซูลที่ปลายแต่ละด้านของโพรบสเต็มลูป ดังนั้นสามารถวัดปริมาณAu^{3+}ด้วยเทคนิค anodic stripping voltammetry (ASV) โดยสามารถวัดโอลิโกนิวคลีโอไทด์เป้าหมายได้ต่ำสุดถึงระดับ 1.84 aM และการประยุกต์ใช้ Spiky gold แคปซูลเพื่อการตรวจวัดจีโนมิกดีเอ็นเอของเชื้อ *E. coil* BL21, ATCC8739 และ O157:H7 ภายใต้สภาวะที่

เหมาะสมในสารละลายตัวอย่าง ซึ่งกรณีศึกษาตัวอย่างใน ณ ที่นี้ได้แก่น้ำนมและน้ำตาลสดพบว่าสามารถตรวจวัดจีโนมิกดีเอ็นเอได้ต่ำสุดที่ระดับ 2-4 CFU mL^{-1} ภายในเวลา 105 นาที

คำสำคัญ : การตรวจวัดจีโนมิกดีเอ็นเอ/ Spiky gold แคปซูล/ สเต็มลูปดีเอ็นเอ/ อนุภาคทองนาโน/ Anodic stripping voltammetry

ACKNOWLEDGEMENTS

I would like to express my profound gratitude and deep regards to my advisor, Assoc. Prof. Dr. Werasak Surareungchai, and co-advisor, Dr. Patsamon Rijiravanich, for their exemplary guidance, invaluable help, monitoring and constant encouragement throughout the course of my Masters degree. In addition, I would like to thank my committee, Asst. Prof. Chamras Promptmas, Dr. Mithran Somasundrum and Dr. Sukanya Oaew, for all of their valuable criticism, suggestions and readiness to serve as members of my thesis committee.

I would also like to take this opportunity to especially express a deep sense of gratitude to Dr. Patsamon Rijiravanich for her cordial support, valuable information and guidance, which helped me in completing this task through various stages.

I am obliged to the staff members of Sensor Technology Laboratory, School of Bioresources and Technology, King Mongkut's University of Technology Thonburi, for the valuable information provided by them in their respective fields. I am grateful for their help, discussions, and friendship during the period of my thesis.

I gratefully acknowledge the financial support from NANOTEC (grant P-110022), Higher Education Research Promotion and National Research University Project of Thailand, Office of the Higher Education Commission and NRCT (grant ภค./2555-กท.53), National Research Council of Thailand for supporting my thesis. I would also like to thank the School of Bioresources and Technology, KMUTT and the Pilot Plant Development and Training Institute, KMUTT for their support and equipment of my study.

Finally, I thank the almighty, my parents, brother and friends for their constant encouragement without which this study would not be possible.

CONTENTS

LIST OF TABLES

LIST OF FIGURES

FIGURE **PAGE**

NOMINATION SYMBOLS

C	concentration	mol L^{-1}
E	potential	V
E_{dep}	deposition potential	V
i_{pa}	anodic stripping current	A
I	electric current density	A cm^2
t	time	s
t_{dep}	deposition time	s
T	temperature	C
v	potential scan rate	V s^{-1}

LIST OF ACRONYMS

Ag/AgCl	silver/silver chloride reference electrode
anti-DIG	anti-digoxigenin
anti-DIG/ML	anti-digoxigenin modified magnetic latex
AP	alkaline phosphatase
APTS	3-aminopropyl triethoxysilane
APTS-MNPL	3-aminopropyl triethoxysilane magnetic nanoparticle
ASV	anodic stripping voltammetry
AuNPs	gold nanoparticles
bp	base pairs
CE	counter (auxiliary) electrode
DIG	digoxigenin
DNA	deoxyribonucleic acid
DPASV	differential pulse anodic stripping voltammetry
DPV	differential pulse voltammetry
FE-SEM	field-emission scanning electron microscopy
GPES	general purpose electrochemical system
HBr/Br_2	hydrobromic acid/ bromine solution
LbL	layer-by-layer
LOD	limited of detection
LNA	locked nucleic acid
MCH	6-mercapto-1-hexanol
PAA	poly(allylamine)
PB	phosphate buffer solution
PBS	phosphate buffer saline
PCR	polymerase chain reaction
PEG	polyethylene glycol
PNA	peptide nucleic acid
*p*NPP	para-nitrophenylphosphate
PSA	polystyrene co-acrylic acid
PSS	poly(sodium 4-styrene) sulfonate
SAMs	self-assembled monolayers
SDS	sodium dodecyl sulfate
SEM	scanning electron microscopy
SL-DNA	stem loop deoxyribonucleic acid
SPCEs	screen-printed carbon electrodes
SPEs	screen-printed electrodes
SSC buffer	saline-sodium citrate buffer
TCEP	tris[2-carboxyethyl] phosphine hydrochloride
TEM	transmission electron microscopy
THF	tetrahydrofuran
UV-vis	ultraviolet-visible
WE	working electrode

CHAPTER 1 INTRODUCTION

1.1 Research background

In recent years, the application of the DNA biosensor has grown rapidly in many areas such as clinical diagnosis [1], food industry [2] and environment [3, 4]. Its application is used for fast, inexpensive and simple detection of DNA of interest while the traditional detection method including the cultural method is unreliable, time consuming and quite laborious [5-7]. Therefore, several DNA biosensor detection methods based on genotypic variables including Southern blot and polymerase chain reaction (PCR) have been used for detection and performance detection in low levels of bacteria. However, PCR often encounters false positivity, long assay times and high assay cost [8], whereas Southern blot technique relies on hazardous radioactive labels [9]. The biobarcode assay based on oligonucleotides is similar to the PCR-free method for quantitative detection of the nucleic acid target and allows for the limit of detection down to the attomolar level [10]. However, the highly sensitive biobarcode assay requires multiple complicated procedures that cause long assay times and the requirement of sophisticated instruments (i.e., microarrays and chip imaging tools) leading to be expensive costs and limited portability. Thus, DNA detection based on electrochemical biosensors is an alternative technique for genomic DNA detection which has been studied in several reports, especially in the genomic detection of foodborne pathogens.

The DNA biosensor is used as an analytical tool based on the nucleic acid recognition process by the hybridization between the complementary single-stranded (ss) DNA probe and the target DNA. The hybridization signal can be measured by several transducers [5] such as optical, electrochemical and micro gravimetric devices. Electrochemical devices, in particular, are widely used as alternative devices for offering the high sensitivity and selectivity of detection by converting the hybridization signal into an electrical signal based on amperometric, potentiometric, and conductometric methods [11]. The target DNA monitoring-based electrochemical DNA biosensor has classified the detection method into label-free and label-based detection [11]. The label-free detection method is a faster and simple technique that achieves its high sensitivity because of a measurable signal in the direct detection [5, 6, 11]. However, its detection results in a high background signal [6]. This detection method overcomes the limitation of enhanced sensitivity of DNA detection. Therefore, the label detection method has been developed to enhance the high sensitivity and selectivity resulting in the use of nanoparticles, enzymes or redox mediators as labels in the detection [6].

Recently, nanoparticles have attracted much attention to apply in a labeling electrochemical biosensor because of its properties in optical and electrical applications [7, 12-14]. Gold nanoparticles (AuNPs) are most commonly used as labels in DNA

detection. Its size and properties not only can be controlled by the preparation condition but it also has the stability function with the biomolecule [12]. The electrochemical DNA biosensor based on the AuNPs label can lead to increasing sensitivity of DNA detection by using the anodic striping voltammetry technique (ASV) for measuring the increasing oxidative AuNPs into metal ions under acid dissolution [15, 16]. The use of AuNPs as electrochemical labels for DNA detection has been developed for streptavidin-biotin specific binding which allows for the detection of low picomolar levels [15, 16]. The improvement of the sensitivity of detection based on the AuNPs label is developed by the silver enhancement method which obtained the detection limit of 1.2 fM [17]. The other enhancement method has efficient amplified signals and allows the detection limits to 600 aM by enhancing with gold [18]. Another method to increase the sensitivity of detection is the increasing amount of AuNPs by using the carrier, particularly in the latex polymer based on layer-by-layer (LbL) technique which can allow the detection down to the aM level [19]. The LbL technique is also used to produce hollow polymer microcapsules for increasing the mass of encapsulated nanoparticles which increase the sensitivity of detection [20]. The hollow polymer microcapsule is also dependent on pH which makes it easier to entrap nanoparticles inside the capsule. However, this technique can encapsulate AgNPs and AuNPs (based on the loading method) and obtain the detection limit to 25 fM [20] and 138 aM [21], respectively.

AuNPs is not the only interesting material for use in DNA detection; the magnetic particle is also used as an analytical tool. Based on several studies, the magnetic particle has been widely used for the detection of nucleic acid, protein and peptides, cells, and other biology [22, 23]. Because of its properties, the magnetic particle can be used for concentration, separation, purification, and identification of the molecule which becomes powerful because it is easy to manipulate and has rapid detection and low cost [24]. Therefore, magnetic particles have been interesting to use in this study to develop the efficiency of the detection platform.

The electrochemical DNA biosensor has been widely used for rapid, sensitive and quantitative genomic DNA detection of foodborne pathogens. *Escherichia coli* (*E. coli*) is one type of foodborne pathogen which is seriously controlled in the food industry because it causes diarrhea and some of its strains can lead to death from anemia or kidney failure. Several genomic DNA detections of *E. coli* that presented the limit of detection in real samples were, 200 CFU mL^{-1} [25], 305 CFU mL^{-1} [26] and 50 CFU mL^{-1} [27] based on real-time PCR, multiplex PCR (mPCR), the electrochemical method and the electrochemical integrated magnetic method, respectively. However, the low infectious dose of *E. coli* which can lead to diarrhea symptoms is 10 CFU mL^{-1}.

The aim of this study is to enhance the sensitivity and selectivity of DNA detection by developing a new approach for the detection of genomic DNA. The spiky gold capsule and anti-DIG modified magnetic (anti-DIG/ML) particles are fabricated and applied to

the developed platform along with the stem loop DNA probe for accurate, rapid detection.

1.2 Objective

The objective of this research is to develop an electrochemical label that can achieve high sensitivity and be applied for genomic DNA detection.

1.3 Scope of work

Construction of spiky gold capsules and anti-DIG modified magnetic latex particles is described and applied into the DNA detection platform based on electrochemicals through the study of efficient genomic DNA of *E. coli* detection in real samples.

1.4 Expected output

The developed genomic DNA detection platform can be applied to detect *E. coli* in real samples and provide high efficiency of detection

CHAPTER 2 LITERATURE REVIEW

This chapter describes the features common to all biosensors including principles of biosensors. DNA electrochemical biosensors are detailed. AuNPs as electrochemical labels, polyelectrolyte microcapsules and the magnetic separation method in DNA detection are reviewed.

2.1 Biosensors

A biosensor is an analytical tool which composes the integration of the specificity of the biorecognition element for direct binding with the target analyte and transducer to a signal generation from the immobilized biorecognition element and target analyte as shown in Figure 2.1.

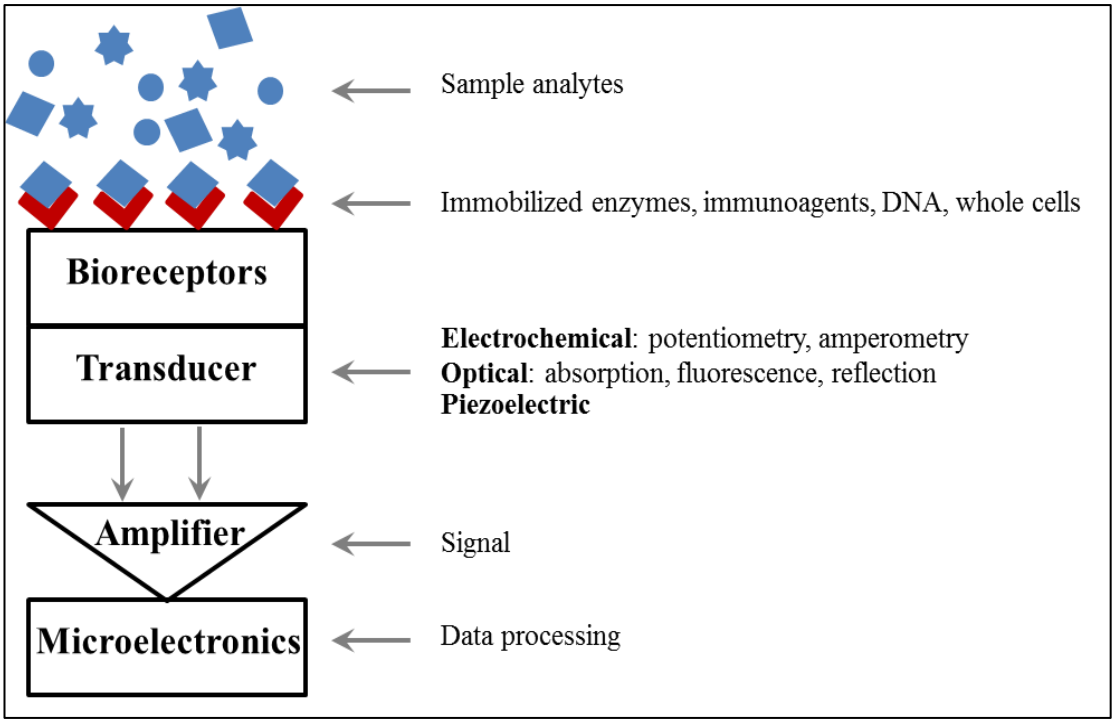

Figure 2.1 The scheme of biosensors [28].

The biorecognition element in the sensor is the biomolecule from living systems which is capable of specific target analyte binding. Normally, the biorecognition element is directly immobilized at the surface of the transducer via method of physical adsorption, surface modification, and deposition of the immobilization layer. The use of the biorecognition elements in the analysis to give selectivity for the target analyte can be classified as an enzyme, antibody, DNA and whole cell [29, 30] which are described briefly here:

a. Enzyme-based biosensor is commonly constructed using enzymes as the biorecognition element in the catalytic process. The catalytic activity of enzymes also allows lower limits of detection compared to common binding techniques. However, the sensor's lifetime is limited by the stability of the enzyme.

b. Antibody-based biosensor is utilized to quantify a specific compound or antigen by using the specific binding affinity of the antibody. However, the antibody has some limitations for detection because of non-specific binding of the polyclonal antibody. Therefore, the monoclonal antibody is used to minimize the non-specific binding but the purification method is very expensive and time-consuming [30].

c. Whole cell-based biosensor is the analyte detection which has living cells as the biorecognition element. This sensor detects the responses of cells after exposure to a sample, which is related to its toxicity. These (toxic) responses can be non-specific, such as DNA damage, heat shock, oxidative stress, metals, organic compounds and compounds with biological importance [30].

d. DNA-based biosensor is an alternative detection using DNA as an affinity recognition element. The recognition detection process is based on the single-stranded DNA to form double-stranded DNA with complementary-target sequence [31].

After the binding between the biorecognition elements and target DNA via enzyme-substrate, the antibody-antigen, DNA-target DNA, and the transducer responded to the biorecognition activity and generated the signal [32]. The result signal from the transducer is changed by their signal transduction mechanism which leads to classification into the following:

a. Piezoelectric material is used as a transducer for a change in mass during the reaction of biorecognition. The quartz crystal microbalance (QCM) is one of the piezoelectric transducers that have been used to measure very small mass changes in the order of pictograms [32]. The QCM has been applied with DNA, protein, lipids and cells for detection [33]. The QCM consists of a thin quartz disk cut using a specific angle from a larger crystal, and by varying the thickness of the crystal; the oscillating frequency from the expansion and contraction can be altered [33, 34].

b. Optical biosensor is a class of analytical techniques which has a changing transduction process in the phase, amplitude, polarization, or frequency of the input light during the biorecognition process. The main components of an optical biosensor are include a light source, optical transmission medium (fiber, waveguide, etc.), immobilized biological recognition element and optical detection system. The optical biosensor can be used in combination with different types of spectroscopic techniques, e.g., absorption, fluorescence, luminescence, bio-optode, surface plasmon resonance (SPR) and fiber grating [35].

c. Electrochemical biosensor is the detection using the electrochemical devices as the transducer. Electrochemical sensors generally can be categorized as conductivity, potentiometric, amperometric and voltammetric sensors [36].

2.2 Electrochemical biosensors

The electrochemical biosensor is the detection using electrochemical devices as transducers. Electrochemical sensors generally can be categorized by transducers as conductivity, potentiometric, amperometric and voltammetric sensors [36].

a. Potentiometric electrochemical biosensor consists of the potentiometric devices as the transducer to measure changing potential in the active species concentration at working electrodes compared with the reference electrodes in an electrochemical cell [37]. The reduction reaction occurs at the surface of the cathode electrode which is described by the Nernst-Donnan equation when under the thermodynamic equilibrium condition which is made under zero current conditions [36].

b. Amperometric electrochemical biosensor is an analyte tool integrated with the amperometric transducer, which detects the species of the oxidation or reduction reaction on the current-potential characteristics. The mass transfer rate of the reaction on the electrode surface is directly affected by the current potential characteristics caused from the an ionic migration as a result of an electric potential gradient, a diffusion under a chemical potential difference or concentration gradient, and a bulk transfer by natural or forced convection. Also, the condition of mass transfer is the total diffusion which can be expressed by Fick’s law of diffusion. The maximum mass transfer rate was led to the limited current potential response [36].

c. Conductometric electrochemical biosensor can measure the change of the electrical conductivity of the cell solution at a potential where no charge transfer process occurs at the electrode surface. However, the effect of the double layer of each electrode surface complicates the conductivity measure interpretation which is related by the Warburg impedance. The effect of both the double layers and the charge transfer process can be minimized by using a high-frequency, low-amplitude alternating current [36].

2.3 Electrochemical DNA biosensors

In recent years, the electrochemical DNA biosensor has become a wildly used device for the detection of analytical compounds which relies on the immobilization of single stranded DNA, the probe sequence, onto the electrochemical transducer surface and on the subsequent recognition of the complementary sequence, the target one, through the specific hybridization process. The DNA electrochemical biosensor plays an important

role in clinical diagnosis and medicine, forensic and environmental analyses, and food safety monitoring, in which high selectivity and sensitivity and rapid and low cost detection is offered [5, 11].

The selectivity of the DNA electrochemical biosensor is based on the nucleic acid recognition process. The nucleotide sequence strand consists of adenine (A), thymine (T), guanine (G), and cytosine (C) bases which resemble each strand by hydrogen bonding between paired bases of A-T and G-C as shown in Figure 2.2.

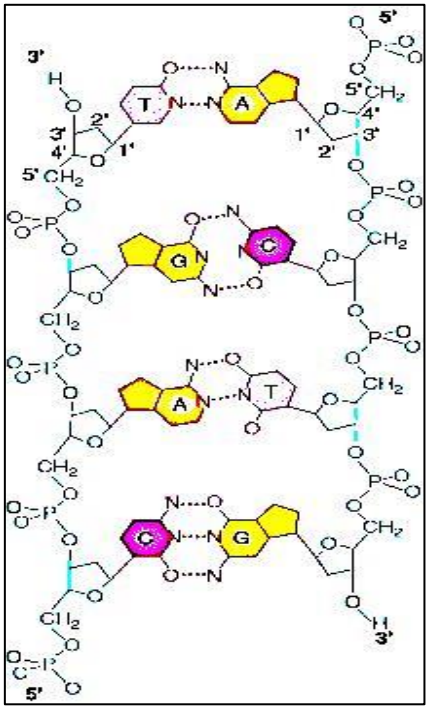

Figure 2.2 The chemical structure of the DNA double helix [38].

The hydrogen bond interaction between the bases paired especially in G-C bonding is significantly associated with stable DNA, thus the GC content percentage is calculated as

$$\frac{\mathrm{G+C}}{A+\mathrm{T+G+C}} \times 100 \qquad (1)$$

whereas A, G, C, and T are the number of occurrences of each oligonucleotide.
The AT/GC ratio is calculated as

$$\frac{\mathrm{A+T}}{\mathrm{G+C}} \qquad (2)$$

The GC content has the relative melting temperature (T_m) which is the temperature at which half the DNA is unwound (Figure 2.3). The higher the G+C content of DNA, the higher the melting point, which is also dependent on the ionic strength of the solution:

the absence of salt, the lower the melting temperature. Because the electrostatic repulsion between the negatively charged phosphate groups in the double strand DNA is suppressed by the positively charged ions of salt solution such as Na^+, the double strand form of DNA is stable [39, 40] under salt solution concentrations.

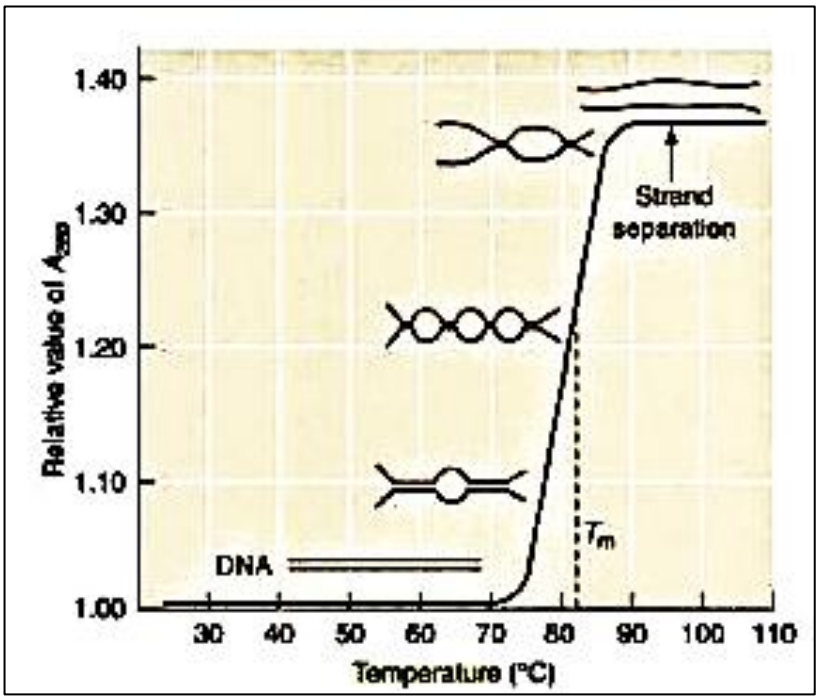

Figure 2.3 The DNA melting curve [39].

The melting temperature (T_m), which relies on equations for double stranded DNA longer than 100 bp [41], can be determined by the following equation:

$$T_m = 81.5℃ + 16.6 \log_{10}[M] + 0.41(\%[G + C]) - 500/n - F \quad (3)$$

whereas, M is the monovalent cation concentration in the buffer (molar), %[G+C] is the GC content, n is length of duplex in the base pair and F is 0.63 ℃ × the percentage of formamide in the solution (℃).

Another calculated equation in which the oligonucleotides are less than 100 nucleotides in length, the cation concentration is less than 0.5 M and the G + C is 30-70% [41] is as follows:

$$T_m = 81.5℃ + 16.6 \log_{10}[Na^+] + 0.41(\%[G + C]) - 675/n \quad (4)$$

However, the acidic or basic condition or chaotropic agents are other factors affected to the stability of the double forms of DNA. Moreover, the linear single stranded DNA can be used as biorecognition molecules, hairpin stem-loop DNA, peptide nucleic acids (PNA) and locked nucleic acid (LNA). The hairpin stem-loop DNA (Figure 2.4) as an

alternative biorecognition molecule can bind to a complementary target DNA sequence using the sequence inside the loop. It is important to use the stem-loop DNA as a probe to increase the specificity of target recognition and reduce the background of the detection as compared with linear DNA probes [42, 43]. The hairpin stem-loop DNA (Figure 2.4) is integrated of the stem and loop structure. The stem structure consists of two short arm complementary sequences binding on either side of the loop during absence of the target. The loop part of the stem-loop DNA consists of the complementary sequence DNA probe that binds with target DNA and changes the stem-loop form into the double helix DNA when the target DNA is present. The melting temperature of SL-DNA plays an important role of the states of the stem loop structure consisting of (1) opened state and (2) closed state. At the melting temperature, the thermal energy is large enough to overcome the binding energy which leads to the open SL-DNA conformation. Conversely, the thermal energy becomes smaller than the binding energy. At temperature conditions lower than the melting temperature, the SL-DNA remains in a closed state [44].

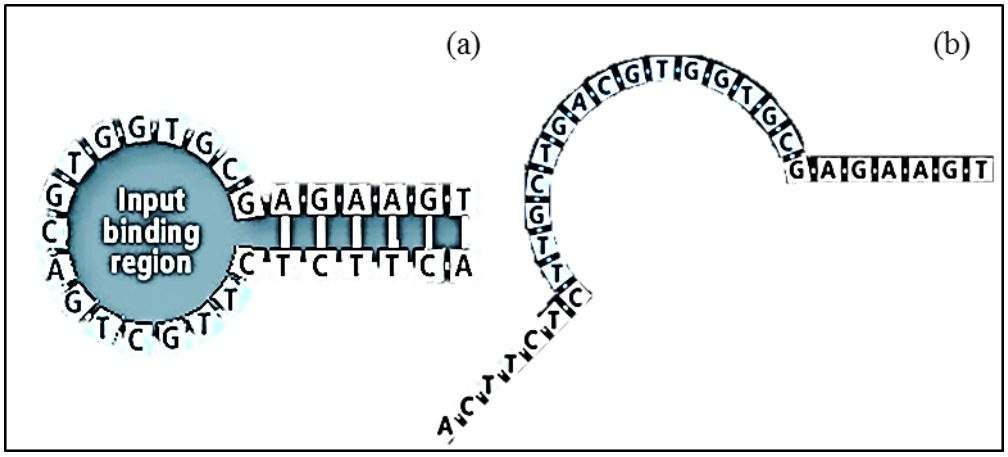

Figure 2.4 The hairpin loop DNA structure consisting of the (a) closed state and (b) opened state [45].

The broad differences of melting temperature range of specific and nonspecific analytes has been interesting for the developed detection probe in the field of electrochemical biosensors based on altering the distances between the electrochemical label and electrode, which results in the change in electron transfer [46, 47]. For example, Fan et al. [48] described the electrochemical DNA detection based on a surface-immobilized DNA hairpin structure as shown in Figure 2.5 which consisted of the ferrocene group as the electrochemical label. Thus, the electron transfer from the ferrocene group through the electrode occurred in the absence of target DNA because of the close distances between the electrochemical label and electrode surface. On the hybridization with target DNA, the redox current result from the electron transfer was largely changed because the ferrocence label was moved away from the electrode surface which had limited detection as low as 10 pM.

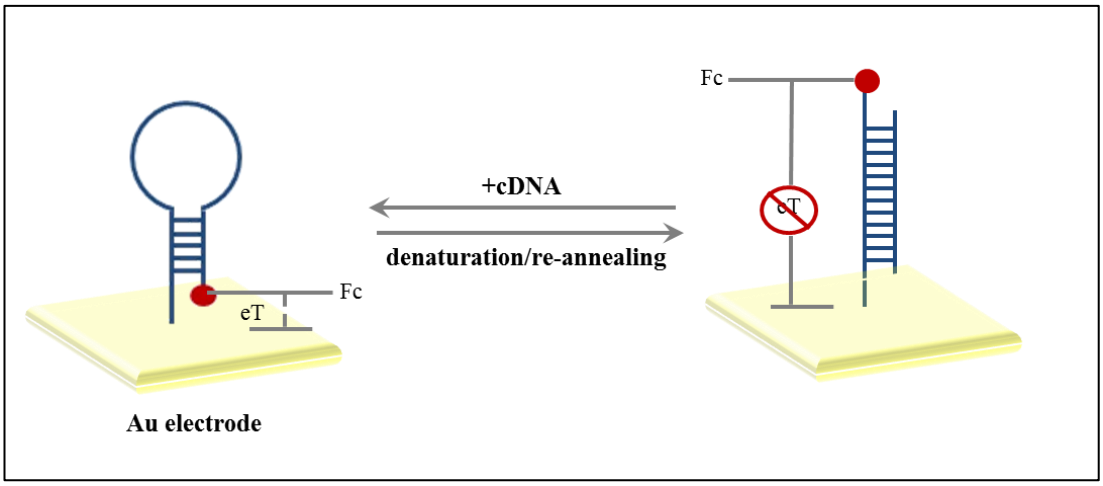

Figure 2.5 Electrochemical DNA detection based on a surface-immobilized DNA hairpin structure [48].

However, the utilized SL-DNA as a probe in the electrochemical biosensor has to immobilize it onto the transducer surface for electron transfer. The immobilization plays an important role process to the sensitivity, detection resolution and the reproducibility [49]. Several DNA immobilization methods onto the electrode surface have been reported:

a. Physical adsorption is the immobilized method based on the forced non-covalent nature which is electrostatic attractive forces between the charged transducer surface and the DNA probe. The positively charged transducer surface is usually modified by chemical agents (polyamidoamine [PAMAM]) because of the negatively charged phosphate group from the phosphate backbone of DNA. However, this method can also induce the nonspecific physical adsorption of target DNA on the immobilized transducer surface. Therefore, blocking agents such as bovine serum albumin (BSA) and succinic anhydride (SA) are commonly used to prevent the nonspecific interactions from being adsorbed on the amine modified surfaces, which leads to the lower background. [50].

b. Entrapment in a gel or polymer is the technical method based on the immobilized physical trapping of the DNA within the three-dimensional matrix of polymeric e.g., polymer gel, polyacrylamide, polypyrolle matrix or sol-gel matrixes. DNA entrapment is more stable than the DNA adsorption method. DNA that was not denatured remained accessible for hybridization [51, 52]. However, the entrapped DNA structure is restricted by the encapsulated material resulting in a loss of hybridization characteristics of the larger nucleic acid and components [51].

c. Cross-linking is a method which entails the linking to itself or co-cross-linking with inert proteins (e.g. BSA) or chemical reagents (such as glutaraldehyde and gloxal) to

combine with the DNA probe. This method is useful to stabilize adsorbed DNA. However, it it difficult to retain the recognition of DNA.

d. Covalent binding is the method using the functional group of DNA to bind with the transducer surface. The common functional groups used for coupling consist of amino, carboxylic, imidazole, thiol, epoxy and hydroxyl groups. The advantages of this method include stability, avoidance of leaching problems, diffusion and aggregation. For the stability of hybridization of DNA, the covalent bond should be linked to the transducer surface via their terminal group. However, several covalently-linked DNA methods are used to rely on the surface of immobilized DNA, based on its simplicity, durability and good layer functionality [51]. The amino-modified DNA is often used for the covalently-immobilized epoxide-, chloromethyl- or aldehyde- modified surfaces directly to the -COOH-modified surface via carbodiimide or –OH-modified surface via cyanobromide. SH-modified DNA can be immobilized to the maleimide-modified surface.

   Moreover, the SH-modified DNA probe has been wildly used to interact with the gold surface. The thiol-gold interaction is covalently adsorbed on the gold surface by creation of a self-assembled monolayer (SAM), leading it to be simply prepared which is highly stable, densely packed and ordered [51]. The thiol group can be generated by selectively reducing disulfide bonds with reagents consisting of dithiothreitol (DTT) and 2-mercaptoethanol (β-mercaptoehanol); nevertheless, the thiol group can reverse the reaction into the disulfide bond after the removal of DTT or 2-mercaptoethanol because of the oxidation by air and aqueous or ethanolic solutions. Hence, the tris-(2-carboxyethyl) phosphine (TCEP) is an alternative reducing agent used to prevent the reformation of disulfide bonds from the oxidation.

   In oligonucleotides longer than 24 bases, the decreasing interaction between the SH group from the DNA strand and gold surface occurred which is treated by a capping agent such as 6-mercapto-1-hexanol (MCH) as shown in Figure 2.6.

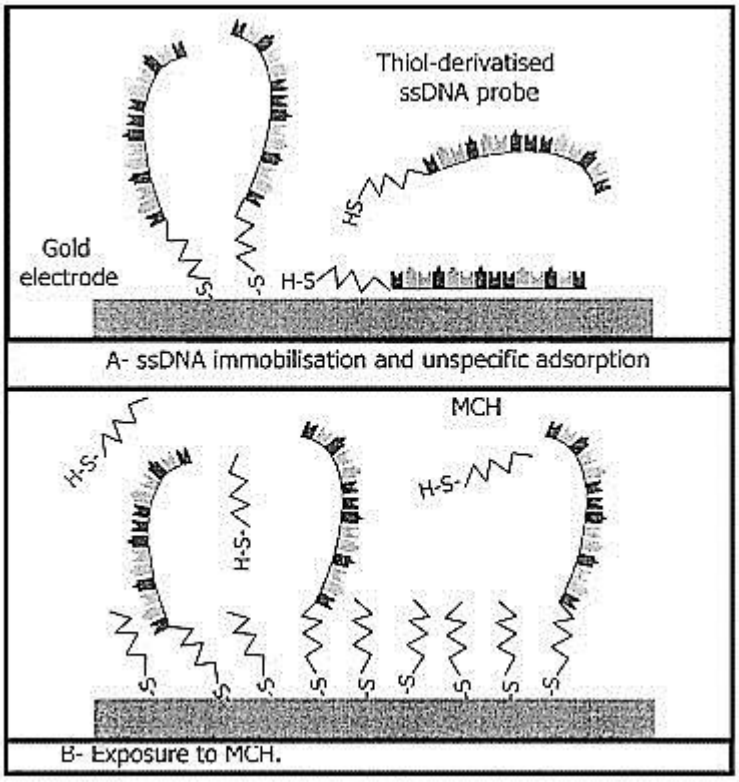

Figure 2.6 Schematic of a thiol immobilized on the gold surface (a) adsorption of single stranded DNA and (b) adsorption of the mixed layer of single stranded DNA and MCH [53].

6-mercapto-1-hexanol (MCH), an alkanethiol reagent concluding the terminal –OH group (Figure 2.7), is widely applied in co-assembled thiol-DNA on the gold surface to reduce the nonspecific adsorption of DNA and increase the hybridization efficiency of DNA detection [54]. MCH has a similar hydrophilic nature to DNA.

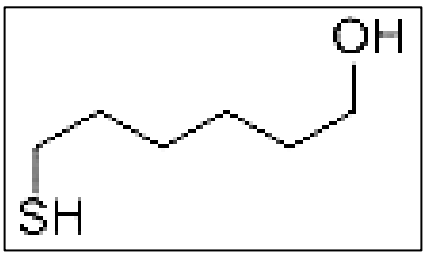

Figure 2.7 6-Mercapto-1-hexanol molecular structures.

e. Affinity interaction is a tool for DNA immobilization consisting of:
   - Streptavidin/avidin-biotin interaction is the most widely used method for rapid detection with high selectivity. Usually, the streptavidin/avidin is immobilized on the surface which has a high affinity to bind covalently with a biotin labeled DNA. Biotin, a small molecule as known as vitamin H, occurs in all living cells

and can be immobilized on DNA-based protein immobilization methods as shown in Figure 2.8.

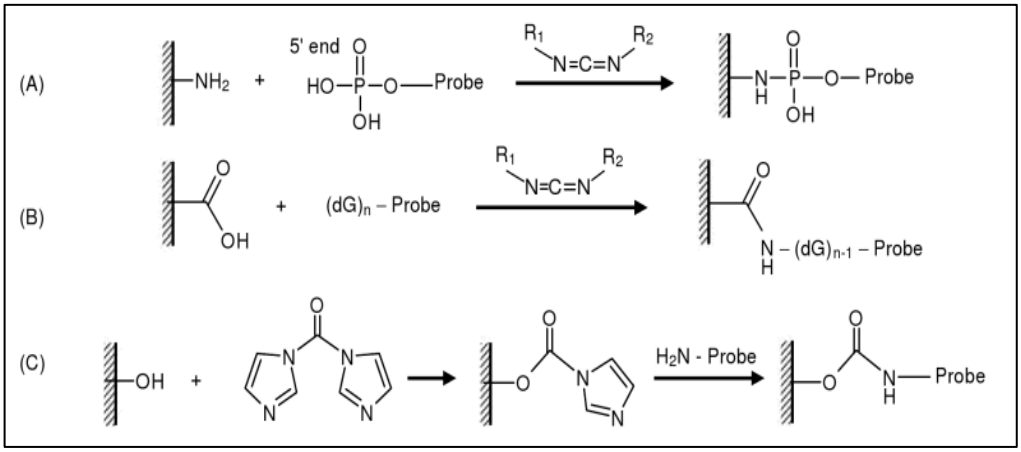

Figure 2.8 Covalent immobilization of the DNA probe to a functionalized support based on the probe (a) coupling to a $–NH_2$ functionalized support, (b) coupling to a carboxyl-modified support and (c) coupling to a hydroxyl-functionalized support [55].

Biotin binding is an extraordinary affinity with avidin or streptavidin proteins. Avidin, a glycoprotein containing carbohydrates isolated from the egg white and tissues of birds, reptiles and amphibians, has a basic isoelectric point (pI) of 10 - 10.5 [56]. The streptavidin molecules are found in Streptomyces avidin which has a pI of 5 - 5.5 [57]. Each subunit binding of streptavidin and avidin have similar affinities for binding up to four biotin molecules. The avidin affinity is stronger than streptavidin because streptavidin is much less soluble in water than avidin. However, avidin has high carbohydrate content which leads to a higher background when the biotin is conjugated.

- The antibody-antigen interaction is a highly specific key-lock non-covalent interaction. DNA is modified with digoxigenin (DIG) which can be directly immobilized with probes for non-radioactive immunoassays, northern/southern blot analysis, and *in situ* hybridization applications which have high specificity of the anti-DIG antibody [58]. DIG is a steroid compound (Figure 2.9) which is extracted from the plants *Digitalis purpurea* and *D. lanata*. The interaction between anti-DIG and DIG is not strong when compared with the biotin/avidin binding [59]. However, it leads to a very low background in DNA assay because this component is not found in animals.

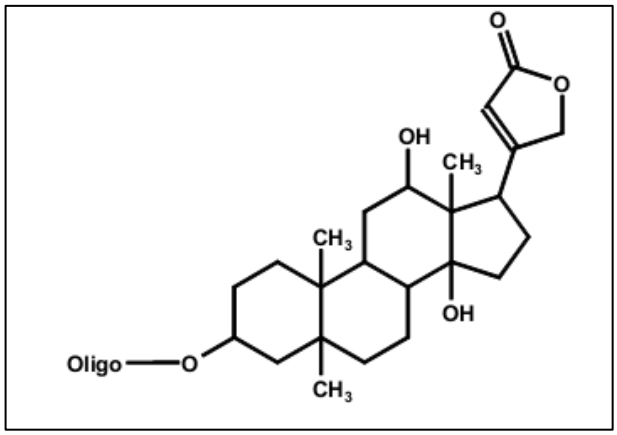

Figure 2.9 The structure of digoxigenin [58].

Electrochemical DNA-based bio-analytical methods have the advantages of high sensitivity, simple operation, low cost, and easy miniaturization, making them an attractive candidate for point-of-care applications. Many electrochemical methods have been developed for the sequence-specific detection of DNA [22-25]. In general, the DNA-based bio-analytical methods using electrochemical means can be categorized into label-free and label-based methods, which will be discussed separately in the following sections.

2.3.1 Label-free electrochemical DNA biosensors

This technique is direct target DNA detection using an immobilized probe directly on the transducer surface. At the present target DNA, the transducer converts the hybridization of the probe-target DNA into a measurable reduction of oxidation base signals (Figure 2.10). The label-free method achieves its high sensitivity in femtomoles of target DNA and seems to be a simple, less time-consuming analysis with unfavorable effects that are inherently quite sensitive [6, 11].

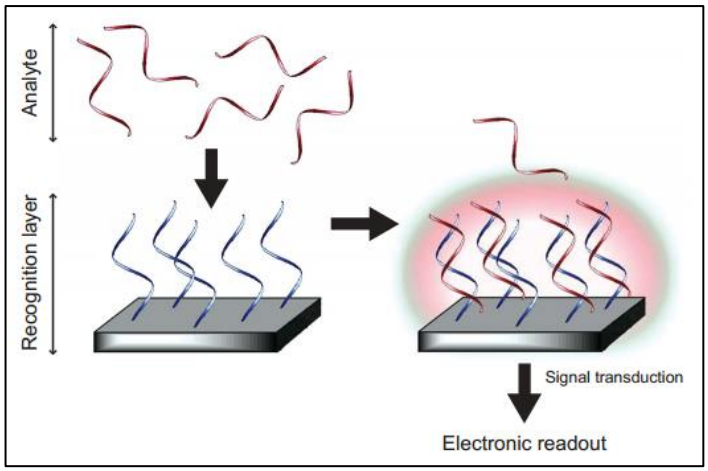

Figure 2.10 Schematic representation of the electrochemical DNA biosensor [6].

The oligonucleotide-based DNA strand including the oxidation of guanine or adenine at the end probe is utilized to directly immobilize on the transducer [60]. The most redox-active base of DNA, found in guanine, has been developed for immobilization as a label-free electrochemical DNA biosensor, which has been shown in the guanine oxidation peak of hybridization of +0.93-1.0 V [61]. Moreover, inosine residues, which are alternative substituted guanine bases, are not electroactive. They hybridize with the cytosine base via hydrogen bond, overcome the limitations of the probe sequence, and also allow the target DNA guanine signal in the detection limit as low as 1.25×10^{-8} M [11]. However, the inosine probe is expensive; thus, the $Ru(bpy)_3$ redox mediator is utilized to greatly amplify the guanine signal. Although other label-free electrochemical DNA detection methodologies have been developed, they still have higher background signals than the labeling method.

2.3.2 Electrochemical-labeled DNA biosensors

An indirect labeling is required to enhance the sensitivity of the electrochemical signal in DNA hybridization detection. Enzyme, redox indicator, and metal complexes can be employed as labels in electrochemical detection [11, 62].

2.3.2.1 Enzyme labels

Enzyme labels have been widely used to generate electrical signals in ultrasensitive electrochemical DNA hybridization detection [5]. The signal amplification based on the electrochemical enzyme label DNA detection is provided by the monitoring of the amplified voltammetric or amperometric signal from the catalytic conversion of a substrate to an electroactive product or redox mediated electrocatalytic transformation (Figure 2.11). Therefore, the various enzymes used as electrochemical labels such as horseradish peroxidase (HRP), alkaline phosphatase (AP), glucose dehydrogenase and glucose oxidase etc. can detect the target DNA as low as the nano-to femtomolar [62].

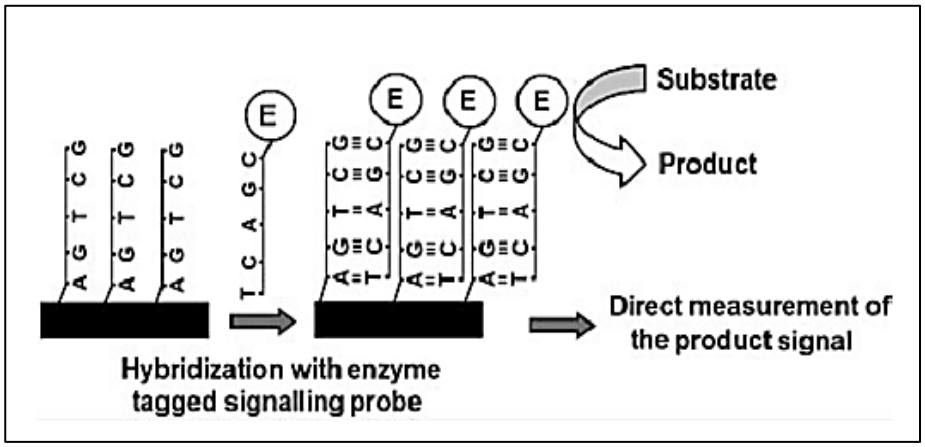

Figure 2.11 Schematic of the enzyme (E) label for electrochemical DNA hybridization detection [63].

2.3.2.2 Redox mediators

The electrochemical DNA hybridization detection based on the redox mediator label is shown in Figure 2.12. The redox signal is measured after hybridization because the redox mediator, which has small compounds, enable forward and reverse electron transfer on the electrode surface by intercalating between double strands of hybridized DNA [63], [64]. The common redox mediators used for electrochemical labels consist of ferrocene, $Ru(bpy)_3^{3+/2+,}$ methylene bule, and ethidium bromide which lead to the limit of target DNA detection as low as famtomoles [6].

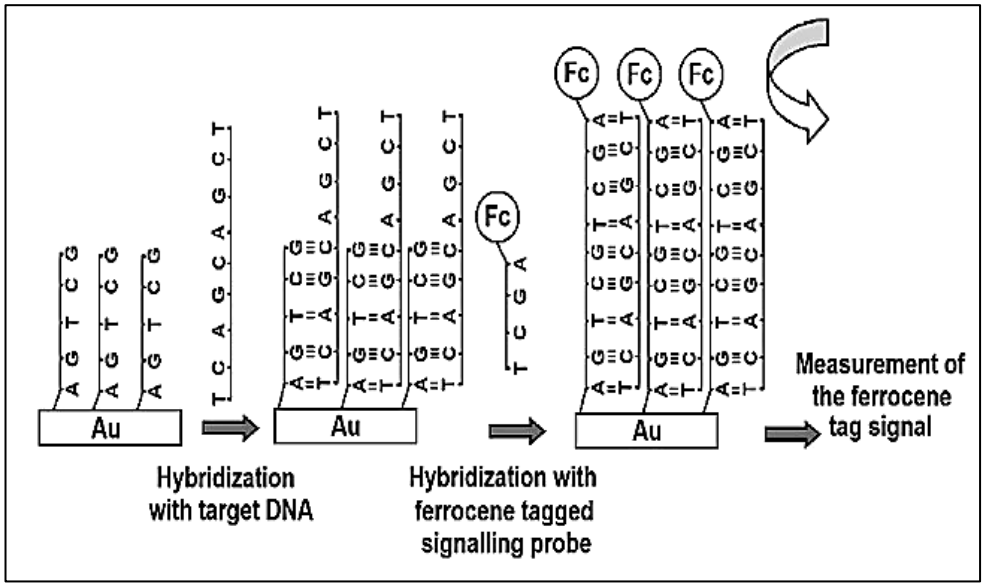

Figure 2.12 Schematic representation of the redox mediator as an electrochemical label for DNA hybridization detection (Fc: ferrocene tag) [63].

2.3.2.3 Metal nanoparticles

The metal nanoparticle labeling technique has been widely used for DNA hybridization detection because of its excellent biocompatibility with biomolecules and its display of unique structural, electronic, magnetic, optical and catalytic properties [65]. The schematic of metal nanoparticle-based electrochemical DNA detection is shown in Figure 2.13 which currently consists of three strategies for detection. The resulting signals of DNA hybridization can be achieved after the hybridization process by directly measuring the electron signal transfer (Figure 2.13 [a]) monitoring the metal ion under acid dissolved conditions (Figure 2.13 [b]), or directly measuring of silver tag signal which is coated on the gold nanoparticle and acid dissolved silver tag (Figure 2.13 [c]) [63].

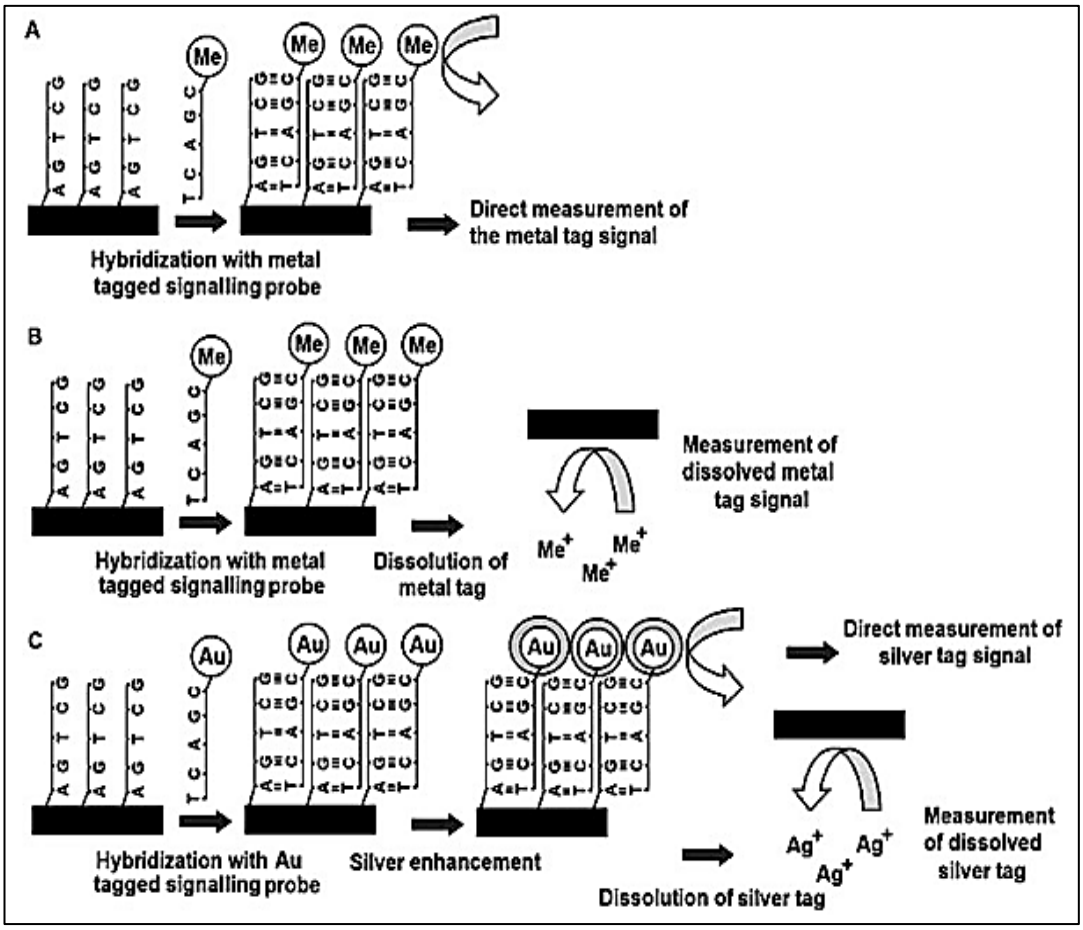

Figure 2.13 Schematic of metal nanoparticles in label-based electrochemical DNA hybridization detection [63].

Gold nanoparticles are generally more chemically stable than Ag nanoparticles when they are dispersed in aqueous solutions [66].

2.4 Au nanoparticles as electrochemical labels

Gold nanoparticles are the most extensively used as functionalized oligonucleotides for highly sensitive and selective DNA recognition schemes by means of electrochemical sensing [12, 65]. Their large specific surface areas and high surface-free energy of gold nanoparticles can lead to DNA adsorption via electrostatic interaction between functional groups of DNA and negatively charged citrate stabilized gold nanoparticles or positively charged gold nanoparticles stabilized with cetyltrimethylammonium bromide (CTAB) or ascorbic acid. Moreover, the thiol functionalized DNA can be strongly covalently adsorbed with gold nanoparticles [12]. The use of gold nanoparticles as electrochemical labels can lead to ultrasensitive DNA detection by anodic stripping voltammetry [15].

The anodic stripping voltammetry of Au^{3+} has been performed based on its reduction to Au^{0} followed by oxidation of the latter. The sensitivity of this method is accumulated in

two processes consisting of the pre-concentration step and stripping step which are described briefly here:

a. The pre-concentration step, which is the accumulation time, is the gold deposited on the surface of the working electrode at a constant potential with the sample solution while being stirred continuously. However, the working condition has to be strictly controlled to achieve reproducible measurement which depends on the accumulation time, accumulation potential, the shape, size and arrangement of the stirrer, the stirring speed (rotation), the sample volume and the surface area of the electrode during the Au deposition step [67].

b. The stripping step is the rest period in which stirring is no longer done in the sample solution. Thus, the cathodic current drops because of the lack of convection. The amounts of deposited gold are small when stirring is stopped at a rest period of 5 s to a maximum of 30 s and the deposited metal is well distributed in the gold drop after several seconds pass. Therefore, the distribution process of gold film on the working electrode surface is complete after only a few seconds. Then the potential scan rate is recorded and the peak current as the measuring signal occurred [67] as shown in Figure 2.14.

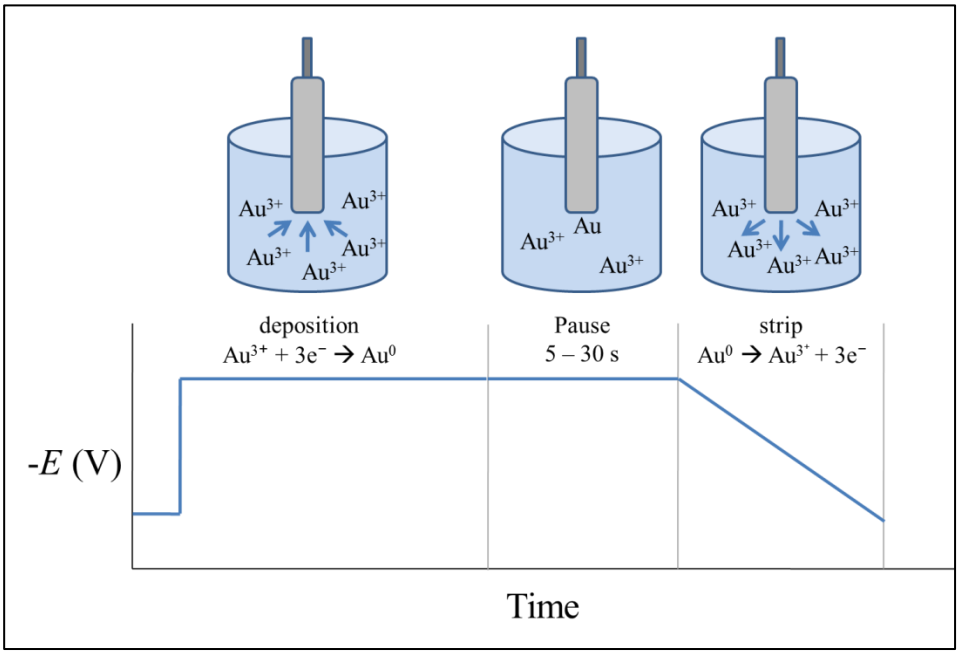

Figure 2.14 The principle of anodic stripping voltammetry of Au^{3+}.

The oligonucleotide probe modified the AuNPs, followed by the release of Au by treatment with a HBr/Br_2 solution and the indirect determination of the Au^{3+} by ASV allows detection as low as 5 pM [16]. The silver enhancement is used to amplify signals and better detection limits have been reported based in the precipitation of silver on AuNPs tags and its dissolution (in HNO_3) and subsequent electrochemical potentiometric stripping detection, [65] which allows detection of target DNA

concentrations as low as 10 nM [68]. Morover, the colloidal gold label can be an alternative silver enhancement. As described by Rochelet-Dequaire [18], the hybridization of the target adsorbed on the bottom of the microwells with an oligonucleotide-modified AuNPs detection probe (pDNA-Au) was monitored by the AVS of the chemical oxidized gold label at a screen-printed microband electrode (SPMBE). However, due to the considerable nonspecific current response of poor reproducibility, it was not possible to significantly improve the analytical conditions. To eliminate the loss of the grown gold label during the post-rinsing step, an aggregating agent consisting of polyethyleneglycol and sodium chloride are led to label aggregation on the bottom of the microwells, which allows detection of DNA targets down to the 600 aM.

To further amplify the signal, AuNPs can be used as a carrier for other AuNPs which can be tagged on polymeric beads via biotin/streptavidin for electrical DNA detection by ultrasensitive electrochemical stripping detection of the dissolved gold tags. This technique allows detection of DNA targets down to the 300 amol level, which offers great promise for ultrasensitive detection of other biorecognition events [69].

Pinijsuwan et al. [19] developed the electrostatic method for fabricating AuNP-coated sub-micrometer-diameter latex spheres for electrochemical labeling by modifying submicrometer-size latex spheres with gold nanoparticles (AuNPs) based on layer-by-layer modification of the latex by polyelectrolytes. This method was successful in detecting the target DNA with a detection limit of 0.5 fM.

Hollow polyelectrolytes can be used instead of latex spheres as carriers of AuNPs by increasing the area in the polyelectrolytes for entrapped gold particles which allows for better limits of target detection of 0.14 fM based on stem loop probes [21].

2.5 Polyelectrolyte microcapsules

Polyelectrolyte microcapsules, which are generally very water-soluble microcapsules, can be prepared by various techniques. The layer-by-layer (LbL) technique is used to prepare polyelectrolyte microcapsules by encapsulating dissolvable templates in the micrometer and nanometer range. The stepwise polyelectrolyte microcapsule based on LbL techniques is performed by consecutively adsorbing oppositely charged polyelectrolytes onto a charged template, which can be either a macroscopic planar surface or the surface of a colloid followed by core dissolution as shown in Figure 2.15. Polyelectrolyte microcapsules have been interesting because of its wide spectrum of potential applications such as corrosion control, biomedical applications, construction of semiconductor nanoparticle materials, release control, etc.

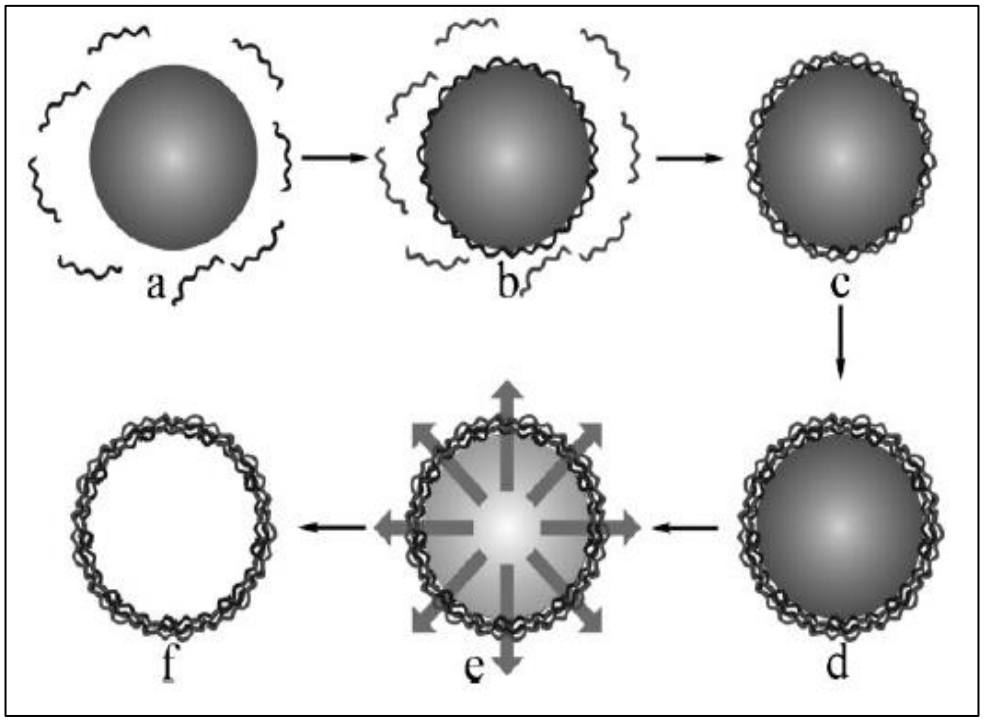

Figure 2.15 Schematic representation of LbL capsules. (a-d) Step-wise addition of oppositely charged macromolecules deposited on a template surface, (e) decomposition of the core and (f) the hollow LbL capsule [70].

Moreover, large surface areas of polyelectrolyte microcapsules have been used to function with DNA, protein, nanoparticle, lipids, viruses, etc. based on the encapsulate or release molecules triggered by changing environmental conditions such as changes in pH, ion concentration, temperature, magnetism, or light.

The application of using polyelectrolyte microcapsules was studied by Rijiravanich et al. [20] which utilized polyelectrolyte microcapsules as carrier labels of AgNPs by loading them into polyelectrolyte microcapsules (as seen in Figure 2.16) for signal amplification in electrochemical DNA biosensors.

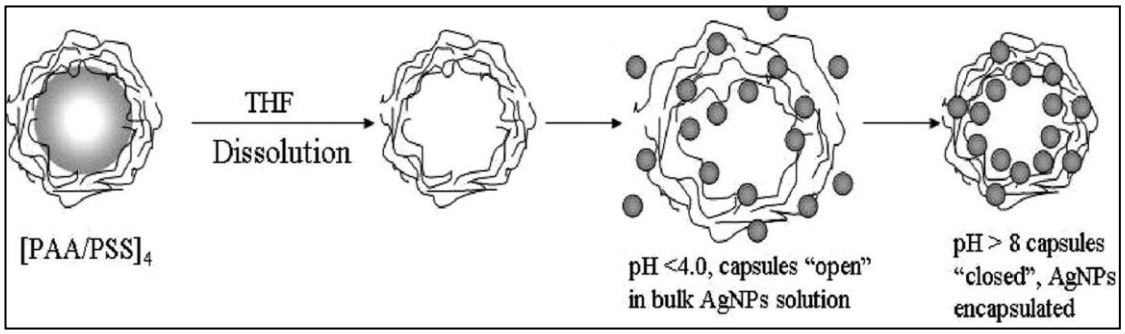

Figure 2.16 Schematic representation of capsule formation and loading with AgNPs by pH control [20].

2.6 Magnetic separation technique

The magnetic separation technique has been developed for isolation of specific viable biomolecules (i.e., whole organisms, antigens, or nucleic acids) by association with biorecogintion elements. The magnetic separation technique is used to replace the centrifugation or filtration steps for target analysis separation from crude samples and interaction with biomolecules [71]. Usually, magnetic particles are immobilized with biorecgoniction elements based on physical adsorption (including hydrophobic, H-bonding, electrostatic intractions) and covalent coupling or chelation association of the chemical function on biomolecules (i.e., amine, thiol, carboxyl, hydroxyl, guanidine, and imidazole, etc.) [72]. Therefore, several biosensor detections have been applied with magnetic particles for rapid and increased selectivity and sensitivity of detection. As described by Zhu et al.[73], in the DNA hybridization assay, the amino silane-coated magnetic nanoparticles were covalently bonded with the phosphate group of DNA probes and had zinc sulfide (ZnS) at the other end for monitoring the target DNA by the ASV technique which presented the detection as low as 0.2 pM L^{-1}. Moreover, the utilized magnetic particles were separated in the DNA detection based on cadmium sulfide nanoparticle (CdS NPs) labels and allowed the limit of detection to 0.08 fM [74].

2.7 Genomic DNA detection

Genomic DNA detection is an alternative method to identify pathogen microorganisms, provide faster detection than traditional methods including the culture and colony counting methods [75], Enzyme linked immunosorbent assays (ELISAs) [76] and polymerase chain reaction (PCR) [77]. These traditional methods are excessively time-consuming and need a technician. However, the detection of pathogens still requires a more rapid, reliable, specific and sensitive method, at low cost in which the biosensor has the potential of detecting pathogens in real-time [78]. Thus, the biosensor has been widely applied in medical diagnostics, food quality control, and environmental monitoring of the defense industry. Figure 2.17 shows the detection of total microbial contamination in the food industry and that the rapid detection can occur in the biosensor detection when compared to the conventional method. Moreover, the microbiological, immunological and molecular biology methods show the detection limit in the range of $10\text{-}10^2$ CFU mL^{-1} [79].

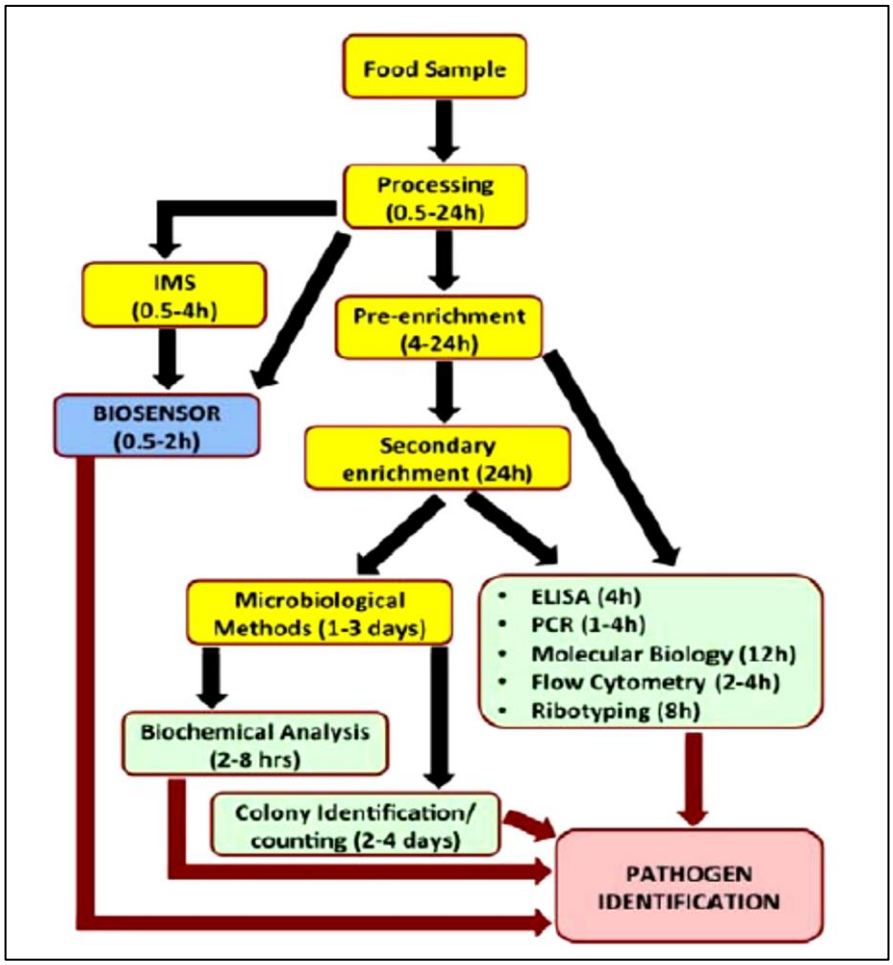

Figure 2.17 A flowchart of the processing steps of food sample analysis by various popular detection methods and relative times taken in pathogen detection [79].

In the food industry, the contaminated pathogens in food are important in order to assess the impact of food safety measures because death or illness from food contamination represents a continuing threat to worldwide public health and socioeconomic development [80]. Hence, foodborne pathogens are utilized as parameters for the food industry and consumers alike by detection of them.

In this study, the requirement of rapid detection and the limit of detection in low levels lead to the development of detection platforms for genomic DNA detection in real samples. Thus, AuNPs and stem loop DNA are applied in the genomic DNA detection platform along with the magnetic separation method. Moreover, this genomic DNA detection platform is used to detect the genomic DNA of *E. coli* as a model in foodborne pathogens.

CHAPTER 3 MATERIALS AND METHODS

3.1 Material and reagents

All the reagents were analytical grade and used without further purification. Poly (allylamine) hydrochloride (PAA, MW~56,000 and MW~ 15,000), poly (sodium 4-styrene) sulfonate (PSS, MW~70,000), tetracholoaurate (III) acid trihydrate ($HAuCl_4 \bullet 3H_2O$), trisodium citrate dehydrate, sodium hydroxide (NaOH), tris [2-carboxyethyl] phosphine hydrochloride (TCEP), 6-mercapto-1-hexanol (MCH), ascorbic acid, ethanol 95%, iron (II, III) oxide (Fe_3O_4), 3-aminopropyl triethoxysilane (APTS), and Tween20 were purchased from Sigma Aldrich (Germany). Sodium borohydrate ($NaBH_4$), sodium chloride (NaCl), sodium dihydrogen phosphate monohydrate ($NaH_2PO_4 \bullet H_2O$), di-sodium hydrogen phosphate dehydrate ($Na_2HPO_4 \bullet 2H_2O$), nitric acid, and nutrient broth media were purchased from Merck (Germany). Polyethylene glycol (PEG, MW~4,000), sulfuric acid (H_2SO4), sodium dodecyl sulfate (SDS), cetyltrimethylammonium bromide (CTAB) were from Bio Basic Inc. Hydrobromic acid was from Ajax Finechem. The bromine was from Panrea. Anti-Digoxigenin-AP, a Fab fragment, was from Roche (Germany). The commercial genomic DNA extraction kit was from the RBC Bioscience Lab (Taiwan). The bovine serum albumin (BSA) was from PAA Laboratories, a cell culture company. The commercial protein assay was from Bio-Rad Laboratories Ltd. Polystyrene-co-acrylic acid (PSA) particles were provided from Pinijsuwan et al. [19]. Sterile Milli-Q water, electric resistance > 18.2 MΩ (KIA, Germany), was used for all of the stock solution. All of the synthetic oligonucleotide sequences used in this study had the following sequences:

1. Thiol-DIG stem-loop DNA (SL-DNA) probe purchase from Gene Link (USA) : SH-$(CH_2)_6$-5'-AAA ggC CgT CTT CCT gAg TAA TAA CTT CCT gAg TgA ATA ACg gCC AAA) -3'-DIG
2. DNA target (*E.coli* K12 44A) Thermo Scientific, Germany : 5'-TAT TCA CTC AGG AAG TTA TTA CTC AGG AAG-3'
3. DNA single mismatch Thermo Scientific, Germany : 5'-TAT TCA CTC AG<u>C</u> AAG TTA TTA CTC AGG AAG-3'
4. DNA triple mismatch Thermo Scientific, Germany : 5'-TAT TCA CTC AG<u>C</u> AA<u>C</u> TTA TTA CTC A<u>C</u>G AAG-3'
5. Non-complementary Bio Basic Inc. (Texas, USA) 5'-AGT AAT GGA ACG GTT GCT CTT TTC ATT TAG CTT TGT TAG CGT TAG GTA TAT -3'

The oligonucleotide stock solutions were prepared in sterile Milli-Q water and kept frozen. The SSC buffer was used for DNA hybridization.

3.2 Apparatuses and electrodes

3.2.1 Apparatuses

Differential pulse anodic striping voltammetry (DPASV) of the dissolved gold label was performed with an Autolab PGSTAT 10 computer-controlled potentiostat (Ecochemic, Netherlands) that was used with the software package "General Purpose Electrochemical System (GPES)". Transmission electron micrographs (TEMs) were obtained with a JEOL model JM-2100, Japan (using an accelerating voltage of 120 kV). Scanning electron microscopy (SEM) and field-emission scanning electron microscopy were carried out using a JEOL model JSM-6300, Japan and a Hitashi model S-4700, Japan, respectively. UV-visible spectroscopic measurement was carried out on a Backman model DU-7000, USA and a microplate reader model Tecan M200. DNA concentration was measured with a Nanodrop spectrophotometer model ND100. A centrifuge model Micro 120 Hettich, Germany was used for sample preparation. Memmert GmbH 8546, Germany, a model of water bath was used for temperature control. NAP-5 column was used for DNA purification.

3.2.2 Electrodes

In the DPASV technique, screen-printed carbon electrodes (SPEs) as working electrodes were combined with reference and counter electrodes which are Ag/AgCl (3M NaCl) and Pt coil counters, respectively. The conductive carbon screen printed electrodes (from Quasense co. Ltd. with product no: Ail120100). The working area at 1.5mm × 4 mm was controlled by pushing insulating tape (polyimide tape) over a portion of the conducting "inks".

3.3 Procedures

3.3.1 Preparation of the hollow shell of the polyelectrolyte microcapsule

0.9 mg of PSA (dissolved in 95% ethanol) was mixed with 150 mL of 1 mg mL^{-1} PAA (dissolved in 0.5 M NaCl) and incubated for 20 min and 20 rpm. This was followed by three centrifugation/redispersion cycles and finally dispersed in sterile Milli-Q water. Then, 150 mL of 1 mg mL^{-1} PSS (dissolved in 0.5 M NaCl) was added for the adsorption of the next layer of polyelectrolyte. After 20 min, three washing steps by centrifugation were performed again. For each polyelectrolyte layer, the adsorption steps were repeated four times. The coated particles (called 4-bilayer [PAA/PSS]) were dispersed in 20 mL of sterile Milli-Q water and kept at room temperature.

900 µL of THF was added to 100 µL of the dispersion 4-bilayer [PAA/PSS] and then mixed. The color of latex disappeared and became turbid. After that, the capsules were

washed three times in each solution (THF, ethanol and sterile Milli-Q water). Finally, the microcapsules were received and kept in 1 mL of sterile Milli-Q water at room temperature.

3.3.2 Preparation of the PAA-capsule

48.44 mL of the 0.5 M NaCl solution (dissolved in H_2SO_4, pH 3) was mixed with 150 mL of 16.00 μg mL^{-1} of microcapsules and then 51 μg of PAA was added and incubated for 30 min at 20 rpm. After that, 100 μg of PAA was added every 30 min until the mass of about 23 mg mL^{-1} of PAA was reached. The pH of the solution was adjusted to 8.0 by using 6 M NaOH for the closed microcapsule. The PAA-capsule was isolated by filtration (cellulose acetate filter, pore size 0.2 μm) to remove unencapsulated PAA. The determination of encapsulated PAA concentration in the PAA-capsule can be calculated by measuring the supernatant absorbance at 210 nm of the UV-vis spectrophotometer. The PAA-capsule was washed three times with sterile Milli-Q water. The PAA-capsule mass could be estimated by the drying and weighting method.

3.3.3 Preparation of the seed decorated PAA-capsule

30 μL of 19.23 mg mL^{-1} of the PAA-capsule was mixed with 70 μL of sterile Milli-Q water, 100 μL of $HAuCl_4$ concentration (the desired concentration: 0.06, 0.07, 0.09, 0.15, 0.25, 0.5, 0.65, 0.75 and 0.85 M) and 20 μL of 1 M NH_4OH and then incubated for 30 min at 20 rpm. 1 mL of sterile Milli-Q water was added before being centrifuged at 14,000 rpm for precipitation of the seed decorated PAA-capsule. The excess amount of $HAuCl_4$ could be measured by the UV-vis spectrophotometer at 294 nm wavelength to estimate the Au^{3+} molecules loaded into the PAA capsule. The seed decorated PAA-capsule was washed three times with sterile Milli-Q water. 1 mL of sterile Milli-Q water was added to the final precipitation. Finally, 200 μL of $NaBH_4$ solution at the same $HAuCl_4$ concentration was added. After 7 hr, the washed Au-Capsule was repeated and kept in 1 mL of sterile Milli-Q water.

3.3.4 Preparation of the spiky gold capsule

100 μL of the seed decorated PAA-capsule was mixed with the solution of 0.1 M CTAB (at these volumes: 1.0, 3.0, 5.0, 7.0 and 10.0 mL), 485 μL of 0.01 M $HAuCl_4$ and 67 μL of 0.1 M ascorbic acid, respectively. The reaction solution was gently mixed for 2 h. Then the pellet from the centrifugation at 14,000 rpm for 10 min was washed and replaced with 100 μL of sterile Milli-Q water. The amount of gold in the spiky gold capsules were directly measured by DPASV techniques (E_{dep} = -0.6 V, t_{dep} = 300 s and scan rate = 30 mV s^{-1}).

3.3.5 Preparation of anti-DIG modified magnetic latex (anti-DIG/ML)

The fabrication of anti-DIG/ML consists of two steps. The brief procedures are shown below:

1. Preparation of APTS coated magnetic nanoparticles (APTS-MNPs)

25 mL of 0.0128 mol L^{-1} of magnetic particles (Fe_3O_4, in 95% ethanol) was mixed with 149 mL of 95% ethanol and 1 mL of sterile Milli-Q water. After being treated with an ultrasonic wave for 30 min, 35 µL of APTS was added and incubated at 37 ˚C and 300 rpm for 7 hr. Then the APTS-MNPs was washed 5 times with ethanol and finally dried in an oven at 60 °C.

2. Preparation of anti-DIG/ML

50 µL of the PSA solution (100 mg mL^{-1} in 95% ethanol) was incubated with 1 mL of APTS-MNPs solution (5 mg mL^{-1} in 95% ethanol). After 30 min, the magnetic latex was filtrated by a cellulose acetate filter, pore size 0.45µm, and then the resuspension was washed three times with 1 mL of 95% ethanol and kept in 1 mL of 0.01M phosphate buffer (PB, pH 7.0).

To conjugate the magnetic latex and anti-DIG, 300 µL of magnetic latex, 10 µL of 1 mU anti-DIG, 90 µL of 2% BSA solution (in sterile Milli-Q water) and 100 µL of PB pH 7.0 were mixed and incubated for 2 hr. Then, the anti-DIG/ML was collected by using the magnetic field and washed three times with 1 mL of 0.02% Tween20 PB for the removal of excess BSA and anti-DIG. After that, 1 mL of PB was added and kept at 4 ˚C.

3.3.6 DNA hybridization detection by using the spiky gold capsule label

80 µL of 1 nM SL-DNA probe, 50 µL of 1pM target DNA and 40 µL of 1x SSC buffer (consisting of 0.150 M NaCl and 0.015 M sodium citrate, pH 7.0) were mixed and incubated at 40 ˚C for 40 min. Then, 80 µL of anti-DIG/ML was added into the solution reaction and incubated for 20 min. After that, the DIG-SL probe and anti-DIG/ML interaction were collected under the magnetic field, followed by washing twice with 1% SDS in SSC buffer and three times in SSC buffer at 4 ˚C. For the blocking conformation, the temperature was controlled at 4 ˚C until detection was finished. 200 µL of 0.5% PEG was incubated for 10 min and then washed twice with 1% SDS in sterile Milli-Q water and three times with sterile Milli-Q water. Then 8 µL of 0.1µM TCEP, 50 µL of spiky gold capsules and 80 µL of 105 µM 6-mercapto-1-hexanol was added and incubated for 30 hr, washed twice with 1% SDS in sterile Milli-Q water and

three times with sterile Milli-Q water and finally, redispersed in 50 µL of sterile Milli-Q water.

The electrochemical DNA hybridization was monitored by ASV analysis using the method of Au^{+} enhancement. The SPCE was used as a working electrode, an Ag/AgCl reference electrode and a platinum counter electrode in an electrochemical cell. The SPCE was rinsed with deionized water. After being dried under nitrogen gas, the SPCE was immersed into 800 µL of a plating solution consisting of 1 M HBr/0.1 M Br_2 and 5 µL of the hybridized DNA. The potential step at -0.60 V, scan rate 30 mV s^{-1} and the voltammograms from 0 V to 0.8 V were applied for a fixed time (300s). This step was done under stirring for 270s with time to rest for 30s.

The incubation time of DIG/anti-DIG interaction, self-assembly between the thiol group of the SL-DNA probe and the spiky gold capsule, DNA hybridization time and temperature and the SL-DNA probe concentration have been studied and optimized. Moreover, the selectivity and quantification of DNA hybridization, the extracted genomic DNA and the *E. coli* detection in real samples was investigated under optimized conditions.

3.3.7 Preparation of bacteria cells

10% (vol/vol) stock cell culture of selected *E. coli* BL21, ATCC8739, O157:H7 and *S. enterica serovar* Typhimurium were transferred to 150 mL of nutrient broth (NB) and incubated at 37 ˚C and 200 rpm for 14 hr. After that, cells were collected by centrifuging at 13,000 rmp for 10 min, resuspended three times with 0.01 M phosphate buffer saline (PBS, pH 7.4) and finally kept in PBS.

The number of cultural cells was directly counted on the surface area of the plate by the spread plate method. 0.1 mL of 10-fold serial dilution of the cell solution was spread over an agar surface. After incubating at 37 ˚C for 24 hr, the viable cells were counted and reported as the number of colony forming units per milliliter (CFU mL^{-1}).

3.3.8 Genomic DNA extraction method

To obtain the genomic DNA for platform detection, the cultured cells from procedure 3.37 were used for genomic DNA extraction following these methods.

3.3.8.1 Heat shock

1 mL of cultured cells was centrifuged at 13,000 rpm for 1 min, followed by washing with SCC buffer and replacing the supernatant with 65 µL of SSC buffer and 35 µL of 10% SDS in SSC buffer in the tube. The cultured cells in the tube were incubated at 100

˚C for 10 min and then immediately moved to ice. After that, the genomic DNA was collected by keeping the supernatant from centrifugation at 13,000 rpm for 1 min.

3.3.8.2 Commercial genomic DNA extraction kit

The commercial genomic DNA extraction kit of RBC Bioscience Lab was used to extract the genomic DNA of cultured cells by following its protocol. Briefly, 1 mL of cultured cells was centrifuged at 13,000 rpm for 1 min, the supernatant was discarded and then 200 µL of GT buffer was added, followed by mixture and incubation at room temperature for 5 min. After that, 200 µL of GB buffer was added into the tube, mixed and incubated at 70 ˚C for 10 min. Then, 200 µL of 95% ethanol was added into the tube and the solution was moved into a GD column in a 2 mL collection tube. Next, the flowed supernatant was discarded after being centrifuged at 13,000 rpm for 2 min. 400 µL of W1 buffer was added into the column, centrifuged at the same rpm for 30 s and then the flow-through was discarded. Then 600 µL of wash buffer was added into the column and centrifuged for 30 s. Only the GD column was centrifuged for 3 min to dry the column. Finally, 100 µL of preheated elution buffer (70 ˚C) was added and then centrifuged for 1 min to collect the supernatant as the genomic DNA of cultured cells. The extracted genomic DNA were incubated at 100 ˚C for 10 min and then immediately moved to ice.

3.3.9 Preparation of food samples

In this study, the commercial UHT plain milk and fermented palm juiced were used as the sample matrix for spiking *E. coli* cells to study the possibility of genomic DNA detection in real samples. The volume ratio of cultured cells and sample milk on fermented palm juice was 1:9. The cultured cells were diluted as the assigned co-concentration. Then 1 mL of spiked cells in the sample was centrifuged at 13,000 rpm for 1 min to discard the supernatant solution and displaced with 200 µL of GT buffer. Finally, the genomic DNA in the real sample was derived after being extracted, following the precedence in 3.3.8 based on the commercial extraction kit.

CHAPTER 4 RESULTS AND DISCUSSION

The increasing sensitivity and selectivity of DNA hybridization detection was developed by a new platform design integrating spiky gold capsules as an electrochemical label for signal enhancement, stem loop DNA (SL-DNA) as a highly selective biorecognition probe and anti-digoxigenin modified magnetic latex (anti-DIG/ML) particles for rapid separation in detection. Therefore, the fabrication of the spiky gold capsule and anti-DIG/ML at optimized platform detection including the incubation time of DIG/anti-DIG interaction, self-assembly time between the thiol group of SL-DNA probe and the spiky gold capsule, DNA hybridization time and temperature and SL-DNA probe concentrations were investigated. Then the sensitivity and selectivity for oligonucleotide and genomic DNA detection were characterized. Finally, the application detection of bacteria in real samples was studied. Results and discussion are described in this chapter.

4.1 Characterization of spiky gold capsule labels

In this study, the spiky gold capsule was fabricated for using as an electrochemical label in DNA detection. There are 4 main steps for preparation of the spiky gold capsule including (1) the hollow shell of the multilayer polyelectrolyte, (2) encapsulation of the polyelectrolyte, (3) seed mediated growth of the gold nanoparticle in the polyelectrolyte capsule and (4) synthesis of the spiky gold capsule. Overall schematics of spiky gold capsule fabrication are shown in Figure 4.1. The multilayer polyelectrolyte coated on poly styrene-co-acrylic acid (PSA) particles are fabricated by the layer-by-layer self-assembly method. The PSA latex particle was used as a template which represents the negative charges from the carboxylic group at the surface of the particle. The positive charges from the amine group (NH_4^+) of polyallylamine (PAA) are self-assembled on the surface of PSA and represent positive charges on the surface of the latex particle. Continuously, the negative charges from the sulfonate group (SO_3^-) of polystyrene sulfonate (PSS) were coated on the outmost layer, hence, the 1 bilayer PAA/PSS had been coated on the PSA particles. These sequential depositions of oppositely charged PAA/PSS polyelectrolytes were performed to be the 8^{th} layer (4 bilayers PAA/PSS) on the PSA particle. Then the PSA core was dissolved using THF to provide the hollow shell of the multilayer polyelectrolyte. Since the inside of the hollow shells are vacant, the short polyallylamine was chosen to encapsulate the inside of the hollow shell and was also coated at the outer layer. The method of encapsulation is based on changes in the pH and ionic strength in the solution. At a pH lower than 4, PAA as a weak polymer will be fully protonated of amino groups and created a local excess of positive charges which results in the opened capsule by their electrostatic repulsion [81]. When the pH is higher than 8, the amino groups are almost completely deprotonated which results in the capsule closing and encapsulation of species within the hollow shell of the multilayer polyelectrolyte (called PAA-capsule).

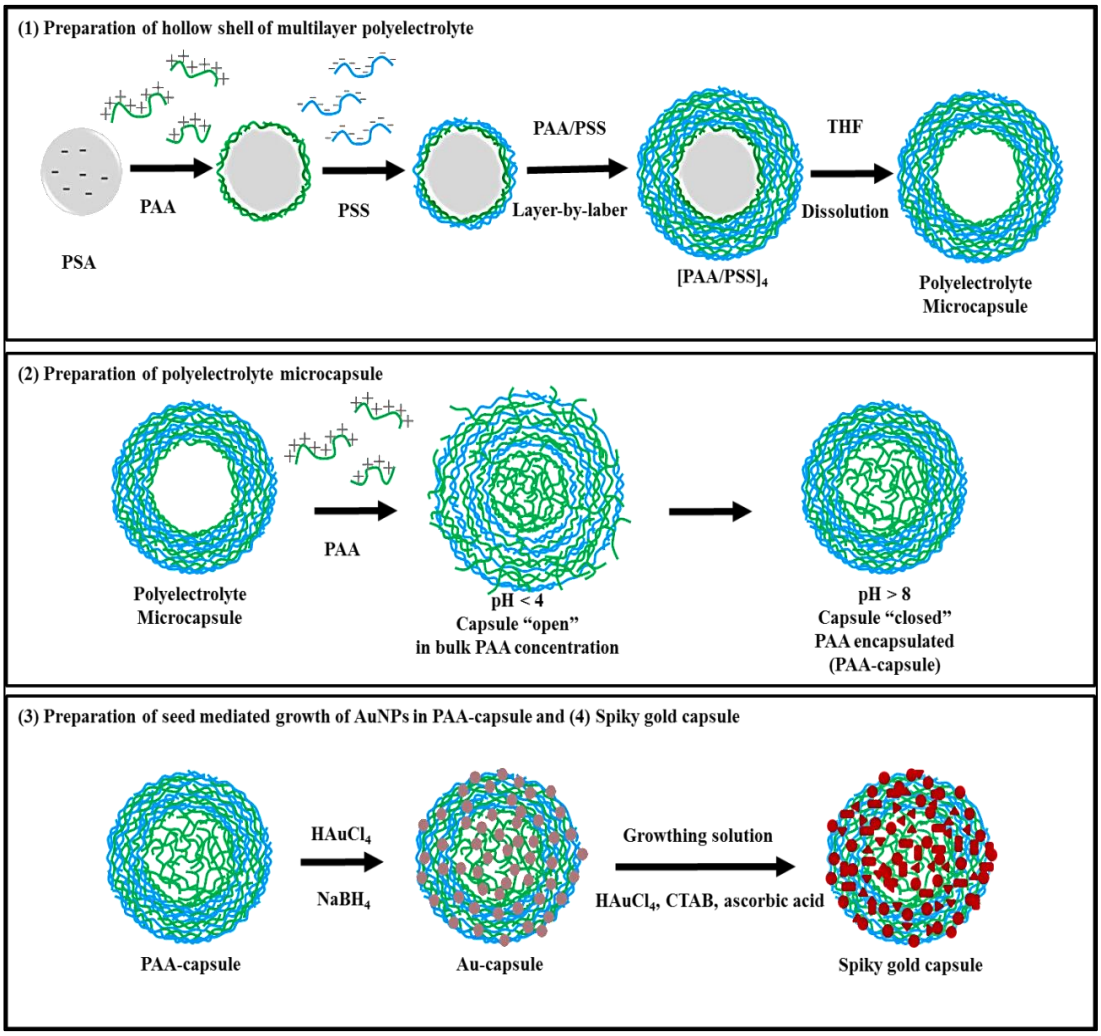

Figure 4.1 Schematic of spiky gold capsule fabrications.

The morphology of the PSA particle, 4 bilayer PAA/PSS particle, hollow shell of multilayer polyelectrolyte and PAA-capsule were studied by using TEM in which their images are shown in Figure 4.2 (a - d). The PSA particle shows a spherical shape with a diameter of about 441.13 ± 5.6 nm (n = 42). This particle is well dispersed in an aqueous solution, similar to a milky solution. The diameter of the 4 bilayer PAA/PSS particle (with a diameter of 464.6 ± 7.4 nm: n = 42) shows that it is bigger than the PSA diameter by 23.4 ± 9.3 nm, which means that the multilayer polyelectrolyte can coat onto the surface of PSA. Moreover, a slightly rough surface of the 4 bilayer PAA/PSS particle is observed (as shown in Figure 4.2 [b]). After dissolution of the PSA template using THF, the hollow shell of the multilayer polyelectrolyte was obtained. The TEM image (Figure 4.2 [c]) shows the oval shape of the hollow shell because the dried stage of the shell can perform the shrinkage of the hollow shell. The diameter of the hollow shell polyelectrolyte was estimated to be about 425.19 ± 11.73 nm (n = 5) with a shell thickness of 48.04 ± 3.92 nm. This also has the advantage of the multilayer polyelectrolyte wall which can be controlled by the variation of the pH value [20]. After The pH solution of the swollen multilayer wall was adjusted to 8 or more than 8with

NaOH to diffuse the molecule of the short polyallylamine into the hollow shell. Then the closed state was achieved by adjusting the pH to encapsulate the PAA inside the capsule to be the PAA-capsule in which the size of the PAA-capsule is swollen with a diameter of 426.84 ± 4.96 nm (n =5) and a thickness of 48.5 ± 2.33 nm.

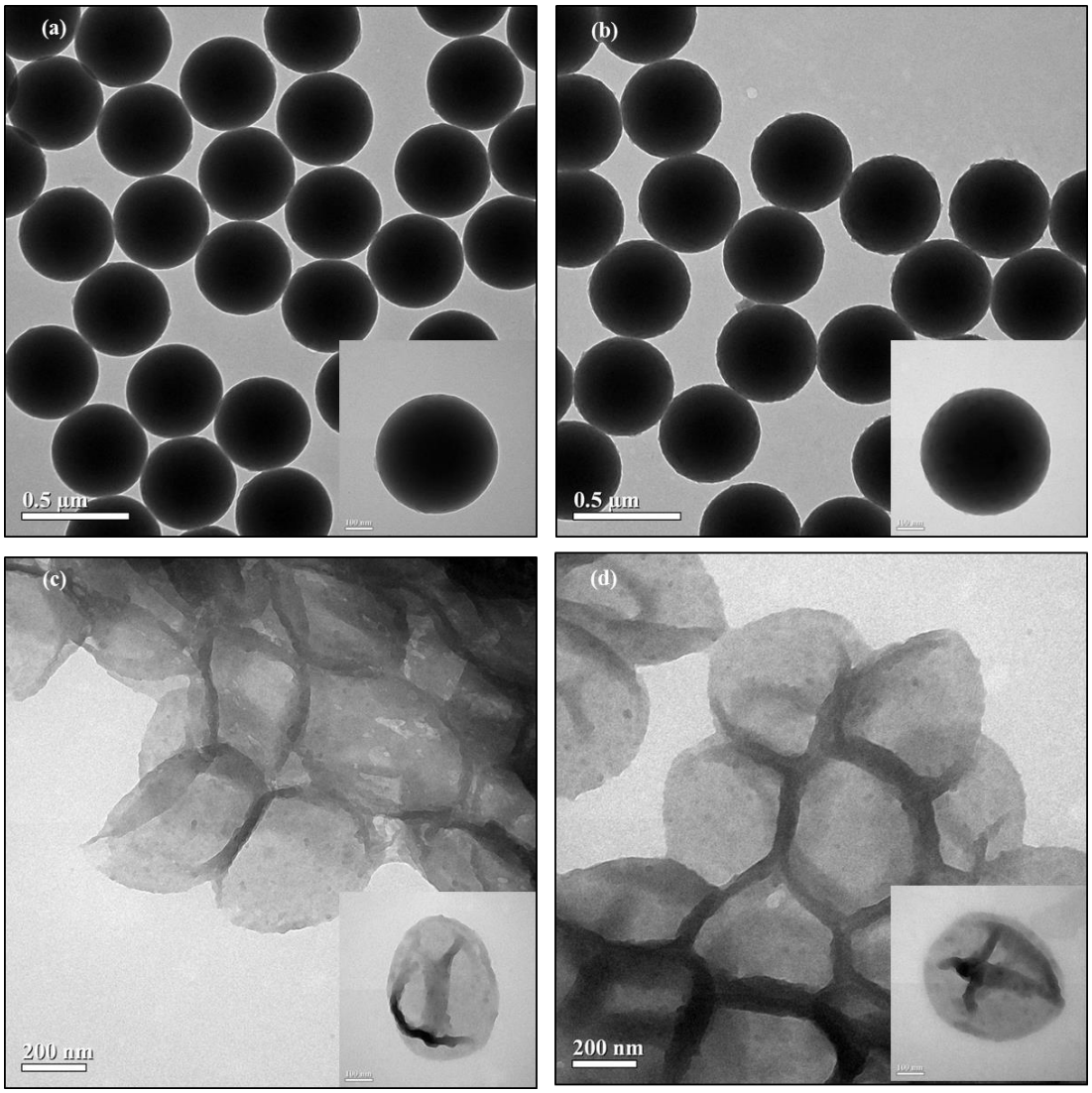

Figure 4.2 TEM images of (a) PSA particles (scale bar = 0.5 µm and 100 nm), (b) 4 bilayer PAA/PSS particles (scale bar = 0.5 µm and 100 nm), (c) hollow shell of multilayer polyelectrolyte (scale bar = 200 nm and 100 nm) and (d) PAA-capsule (scale bar = 200 nm and 100 nm).

The amount of PAA encapsulated was estimated by measuring the UV absorbance of excess polyallylamine solution at 210 nm wavelength. The linear curve of the polyelectrolyte between the absorbance at a wavelength of 210 nm and the concentration of polyallyamine in the range of 0.1 to 10 µg μL^{-1} (as shown in Figure 4.3) is Abs = 0.4675 c – 0.0003 and r^2 = 0.999, in which c is the PAA concentration (µg μL^{-1}). The amount of PAA encapsulated in the hollow shell of the multilayer polyelectrolyte particle was about 0.137 g of PAA encapsulated per g of hollow shell.

Finally, a PAA-capsule mass can be quantified as 1.54×10^{-13} µg P^{-1} (supporting appendix A).

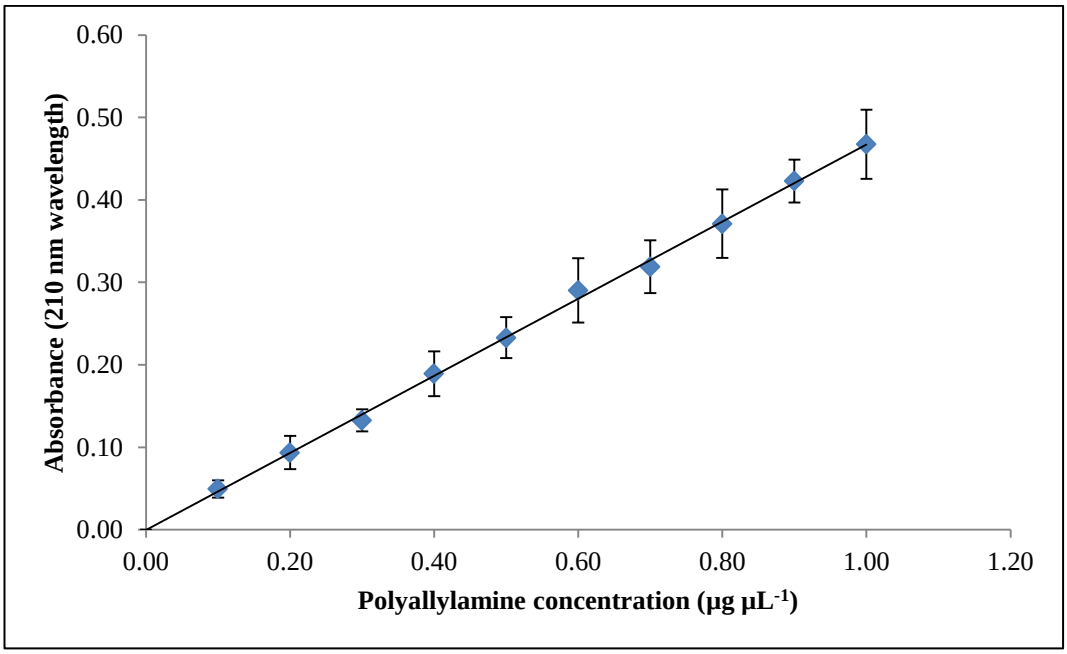

Figure 4.3 Linear calibration curve of UV absorbance of polyallylamine concentration at the wavelength of 210 nm. Error bars show ± 1 standard deviation (n = 3).

The spiky gold capsules were synthesized using the PAA-capsule in which the preparation methods were adapted from Sanchez-Gaytan et al [82]. The small seed particles of gold (nm) were first synthesized in PAA-capsules by reducing $[AuCl_4]^-$ adsorbed in the PAA-capsule with $NaBH_4$. To grow spiky gold capsules, the seed decorated PAA-capsules were placed in a growth solution containing Au^+ and CTAB. After 2 h of the reaction, the spiky gold capsules were precipitated by centrifugation and redispersed in water. The molecules of Au^{3+} ion loaded in the PAA-capsule were determined by using UV-vis spectrophotometric and electrochemical methods. The seed decorated PAA-capsules were synthesized and optimized by varying the concentration of $HAuCl_4$ between 0.06 and 0.85 M.

Based on the UV-vis spectrophotometry, the excess amount of $[AuCl_4]^-$ could be detected at the wavelength of 294 nm (spectra peak of $HAuCl_4$ as shown in the inset Figure 4.4). The linear calibration curve of $HAuCl_4$ between the UV absorbance and concentration of $HAuCl_4$ (Figure 4.4) shows the linear equation as Abs = 4.0326 *c* - 0.1363, r^2 = 0.9994 (where c is concentration of $HAuCl_4$ [mM]). The presumable amount of Au^{3+} ion encapsulated in the seed decorated PAA-capsule was calculated from the subtraction of ions before and after synthesis. Figure 4.5 shows the increase of Au^{3+} ion encapsulated in the seed-decorated PAA-capsule with the concentration of $HAuCl_4$ used in the reaction.

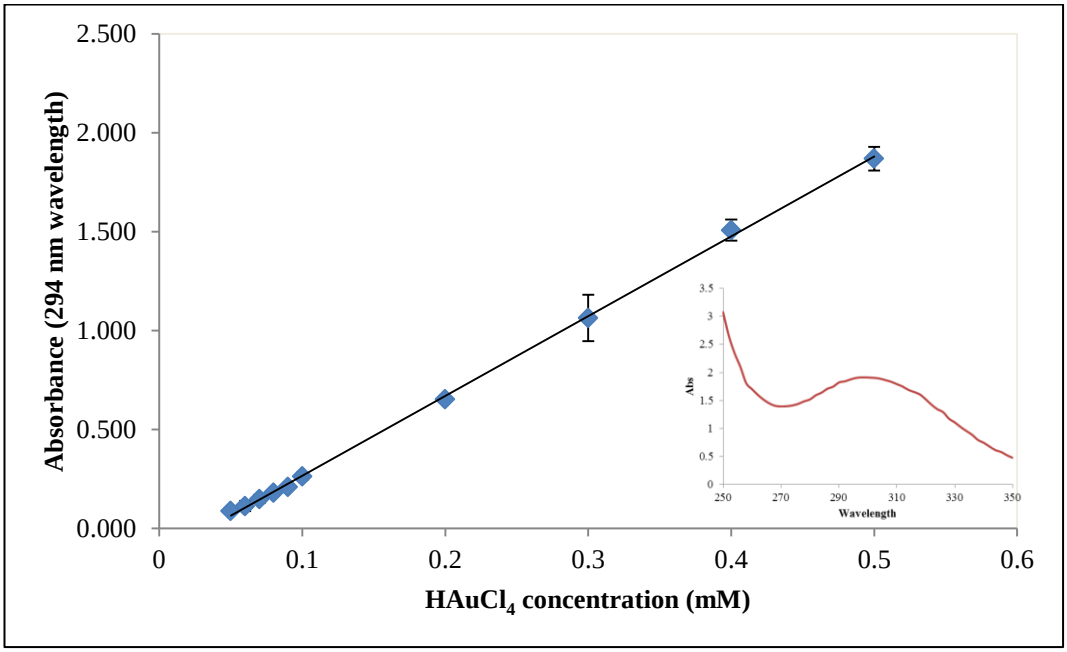

Figure 4.4 Linear calibration curve of $HAuCl_4$ concentration and UV absorbance at the wavelength of 294 nm. Error bars show ± 1 standard deviation (n = 3). (Inset figure shows the UV spectrum of 0.5 mM $HAuCl_4$).

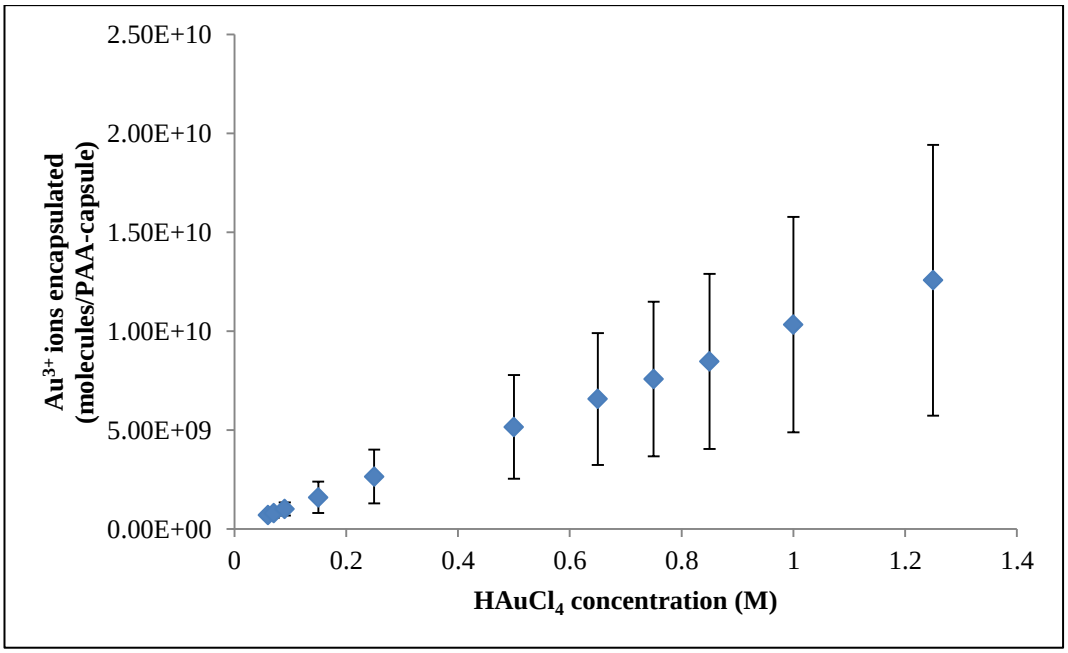

Figure 4.5 The capability of Au^{3+} encapsulation in the seed decorated PAA-capsule based on measured UV absorbance at the wavelength of 294 nm. Error bars show ± 1 stanard deviation (n = 3).

Nevertheless, this increase is unlimited, in which this indirect measurement is not proper to optimize. Therefore, the direct measurement was alternatively detected by using the differential pulse anodic stripping voltammetry (DPASV) method. In this method, the seed decorated PAA-capsule was directly used to detect. The seed gold particles could be dissolved in acid bromine solution to release Au^{3+}, and then Au^{3+} ions can be deposited on carbon SPE for pre-concentration and stripping Au^{0} out by the differential pulse voltammetry technique. Figure 4.6 shows the voltammogram of 1 µM $HAuCl_4$ compared with the seed decorated PAA-capsule, in which their peak potentials are 3.67×10^{-6} and 4.27×10^{-6} mV, respectively.

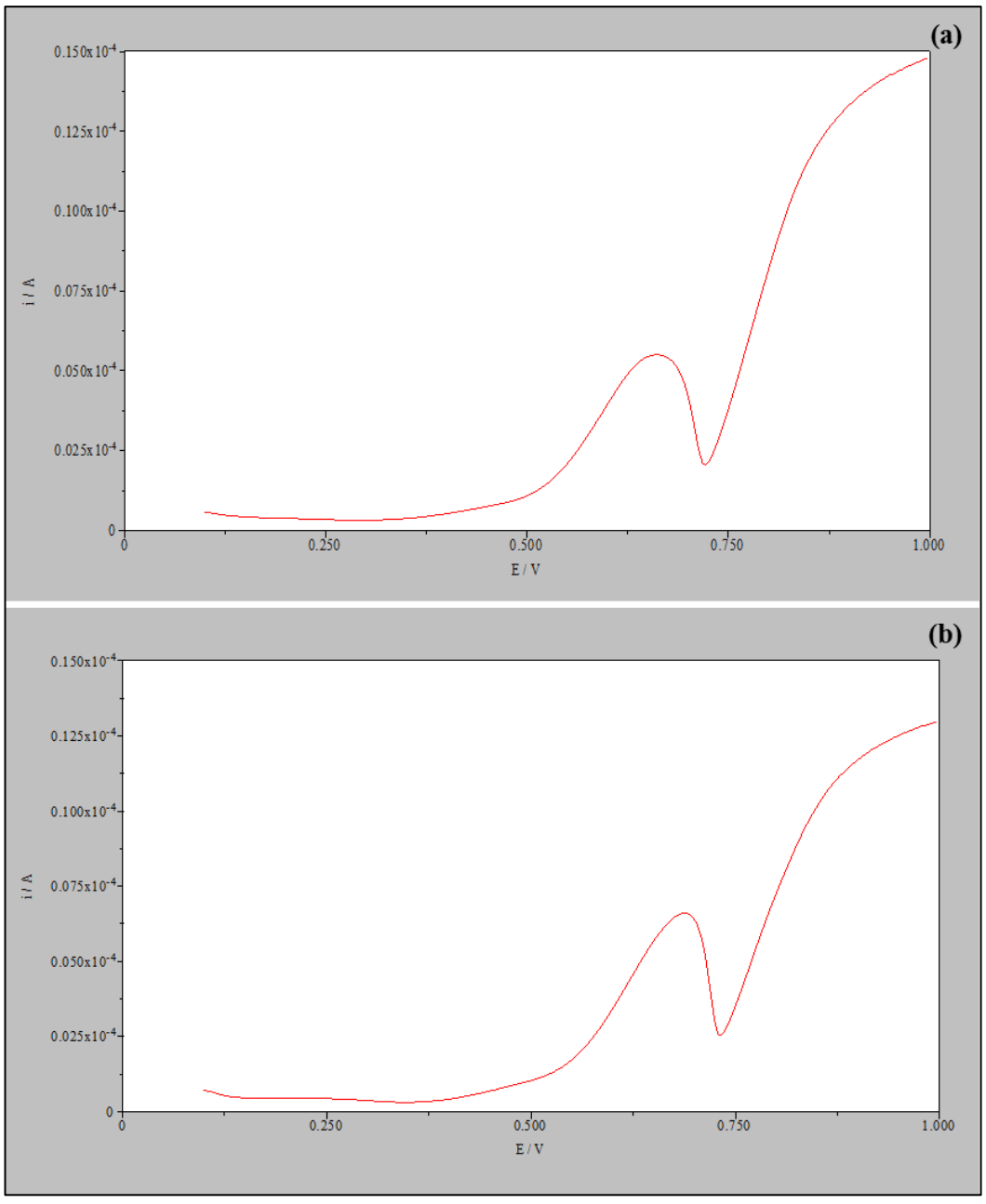

Figure 4.6 Voltammogram of (a) 1 µM $HAuCl_4$ and (b) seed decorated PAA-capsule (DVASV conditions are E_{dep} = -0.6 V, t_{dep} = 300s and scan rate = 30 mV s^{-1}).

To estimate the amount of Au^{3+} molecules in the seed decorated PAA-capsule, the linear calibration curve of $HAuCl_4$ was performed as shown in Figure 4.7. The linear range between 0.62 µM and 3.11 µM shows the linear equation to be $i_{pa} = (1.0 \times 10^{-6})\ c - (3 \times 10^{-7})$ and $r^2 = 0.9952$ (where c is the $HAuCl_4$ concentration in the bulk solution and i_{pa} is the anodic peak current of $HAuCl_4$). Hence, the amount of Au^{3+} molecules loaded in a PAA-capsule could be calculated (supporting appendix A).

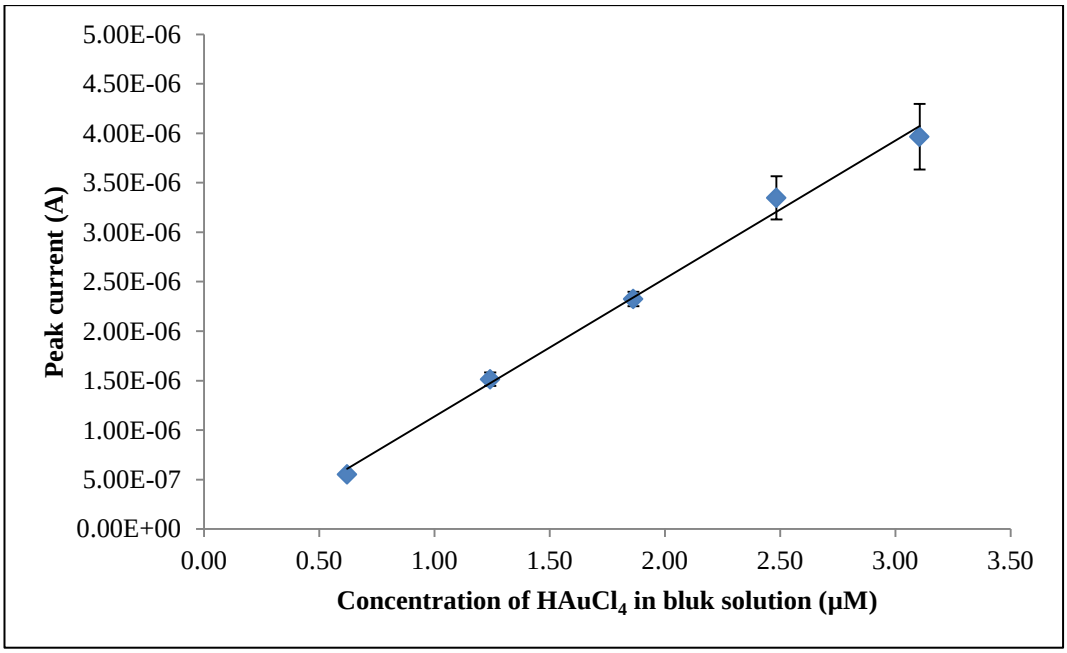

Figure 4.7 Linear calibration curve of $HAuCl_4$ concentration at SPCE by DPASV. Error bars show ± 1 standard deviation (n = 5).

Figure 4.8 shows the capability of Au^{3+} molecules in the seed decorated PAA-capsule at various concentrations of $HAuCl_4$ in the synthesis reaction, in which the highest Au^{3+} molecules loaded were observed at 0.15 M $HAuCl_4$. At this concentration, the Au^{3+} molecules per PAA-capsule were about 1.34 $\times 10^8$ per capsule. Additionally, the Au^{3+} molecules increased with the concentration of $HAuCl_4$ at 0.06 to 0.15 M, with a slight decrease and saturation at a $HAuCl_4$ concentration higher than 0.5 M. The results from the direct and indirect detection methods are not associated which shows that indirect detection probably detected the 1st supernatant of excess $HAuCl_4$. The unadsorped $HAuCl_4$ in the hollow capsule may diffuse out after the washing step before catalyzing with $NaBH_4$. However, this amount of Au^{3+} molecules is lower than the previous work [19-21], as shown in Table 4.1.

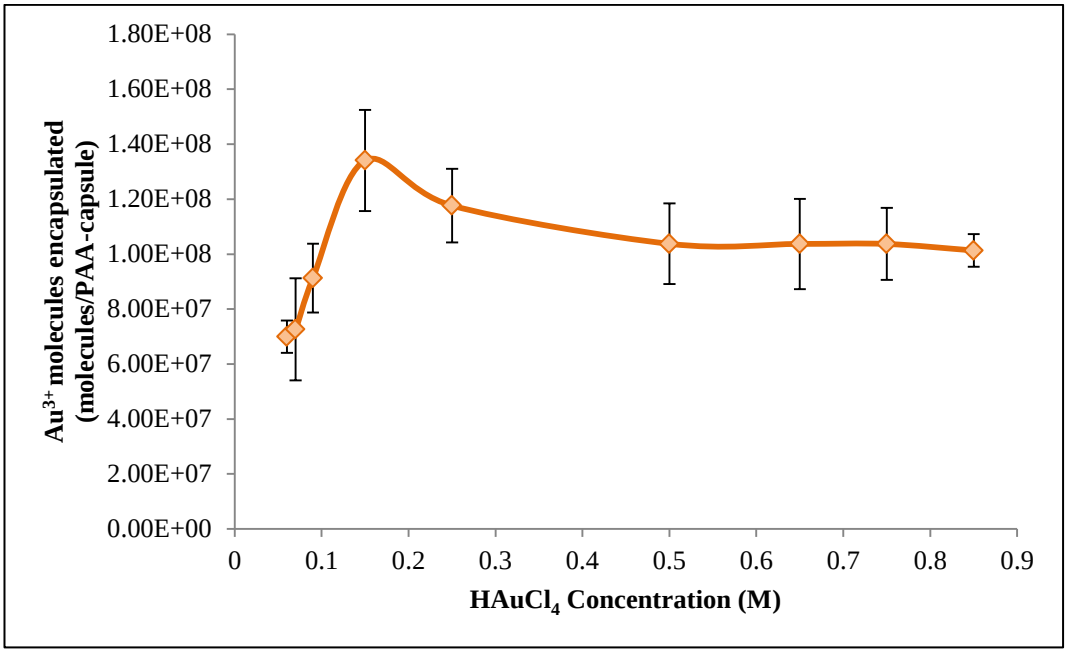

Figure 4.8 The capability of Au^{3+} molecule encapsulation in the seed decorated PAA-capsule based on the ASV method. Error bars show ± 1 standard deviation (n = 5).

Table 4.1 Amount of ion molecules per particle by different electrochemical labels.

Research	Electrochemical label	The amount of molecule ions per particle
Pinijsuwan, et al, [19]	Au-Latex	$7.4 \pm 2.4 \times 10^{7}$ Au^{3+}
Rijiravanich, et al,[20]	Ag-Capsule	7.00×10^{8} Ag^{+}
Fatimah, et al, [21]	Au-Capsule	6.39×10^{8} Au^{3+}
This Work	Au-Capsule: seed mediated growth method	1.34×10^{8} Au^{3+}

The spiky gold capsules were synthesized by using the seed decorated PAA-capsule as the nucleation center for growing gold particles in the presence of CTAB, the cationic surfactant used as a stabilizer and capping agent. The weak reducing agent of ascorbic acid reduced Au^{3+} into Au^{+} which can be bound more strongly to the cationic CTAB micelles on the seed decorated PAA-capsule that were derived by variations in the volumes of growth solutions (1.0 to 10.0 mL). Figure 4.9 shows the TEM images of (a) the seed decorated PAA-capsule and (b-f) the spiky gold capsule derived at various growth solution volumes (1.0 – 10.0 mL). The TEM images show that the size of Au particles is bigger when the volume of growth solution increases; though, the broken capsules are observed at volumes of growth solution higher than 7.0 mL. At high volumes of growth solution, the Au^{+} ions are highly reduced on the capsule surface, leading to a bigger size of gold nanoparticles. This can possible block the diffusion of the growth solution, which causes a difference in osmotic pressure between outside and inside the capsule, resulting in deformation and broken capsules [83].

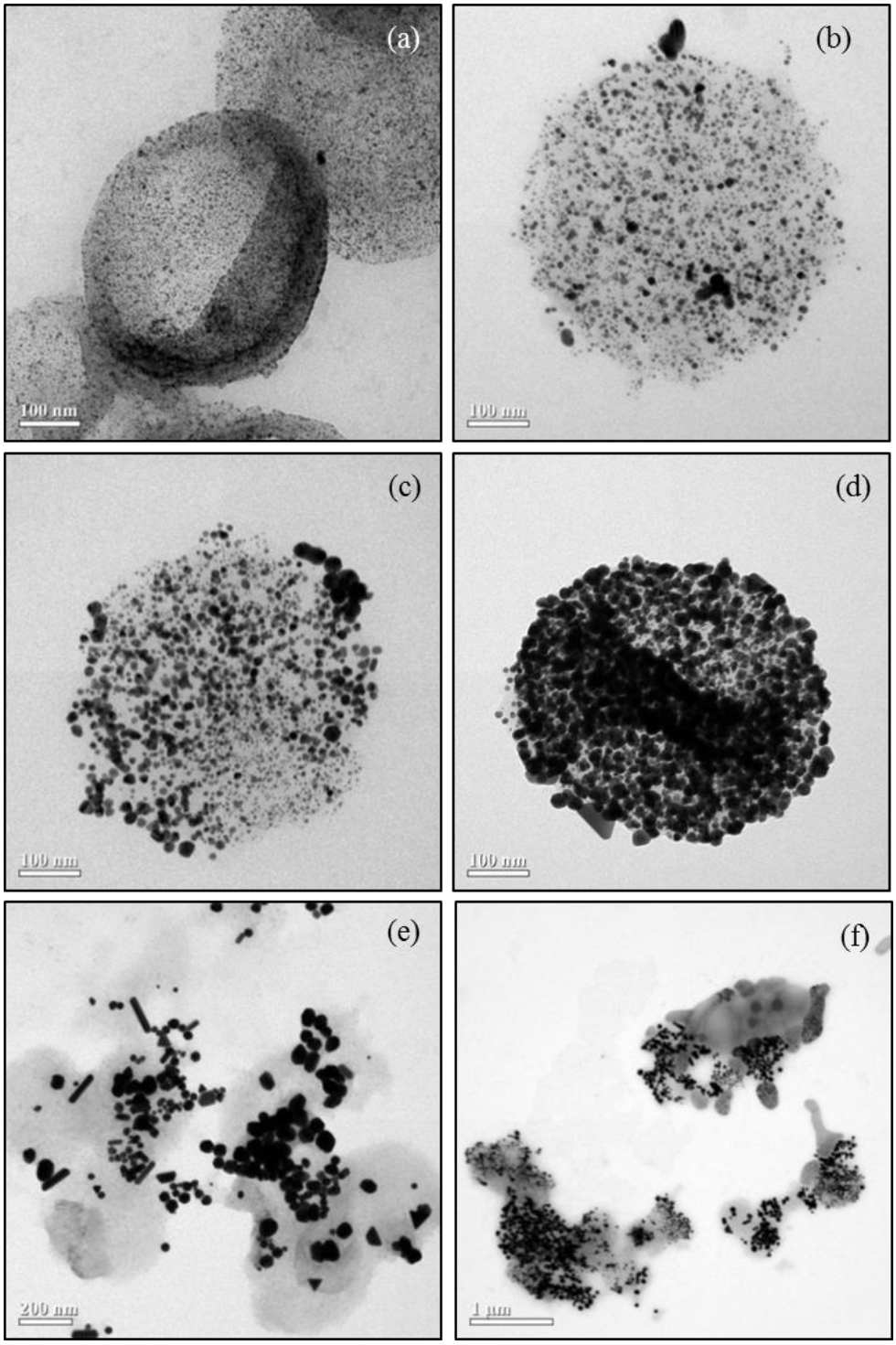

Figure 4.9 TEM images of the spiky gold capsule (a) seed decorated PAA-capsule and (b-f) spiky gold capsules at various growth solution volumes for (b) 1 mL, (c) 3 mL, (d) 5 mL, (e) 7 mL and (f) 10 mL (scale bar: [b-d] = 100 nm, [e] = 200 nm and [f] = 1 µm).

The amount of Au^{3+} molecules in the spiky gold capsule were also directly detected by using the DPASV method and calculated from the linear equation derived from Figure 4.7. The amount of Au^{3+} molecules increased with the large volumes of growth solution that were obtained as shown in Figure 4.10. Therefore, the optimized spiky gold capsule

was derived by using the growth solution at 5.0 mL which provides the Au^{3+} molecule as 1.02 $\times 10^{11}$ molecule per capsule. The cross-section of the PAA-capsule and spiky gold capsule were done after molding the capsule in epoxy resin and cutting. Such TEM images were taken, as illustrated in Figure 4.11 (supporting appendix A). These images should confirm that the morphology of the capsule is spherical. The blank image dots in Figure 4.11(b) represent Au nanoparticles which bind on the polyelectrolyte shell and also on the short polyallylamine which probably leak out.

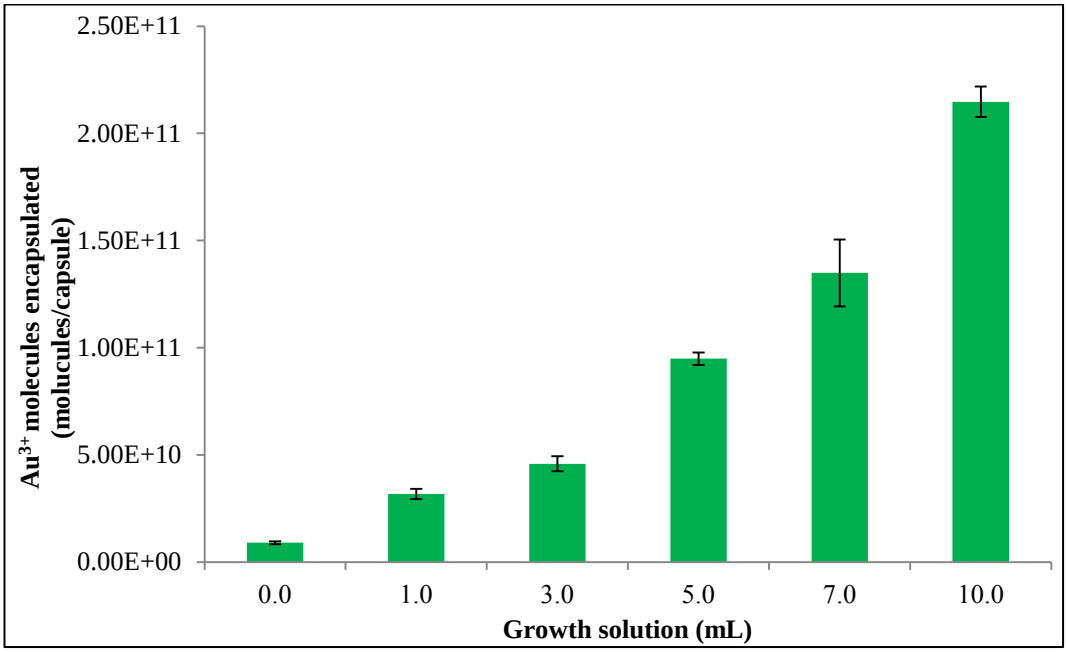

Figure 4.10 The capability of Au^{3+} molecules in spiky gold capsule particles at various growth solution volumes based on the DPASV method. Error bars show ± 1 standard deviation (n = 5).

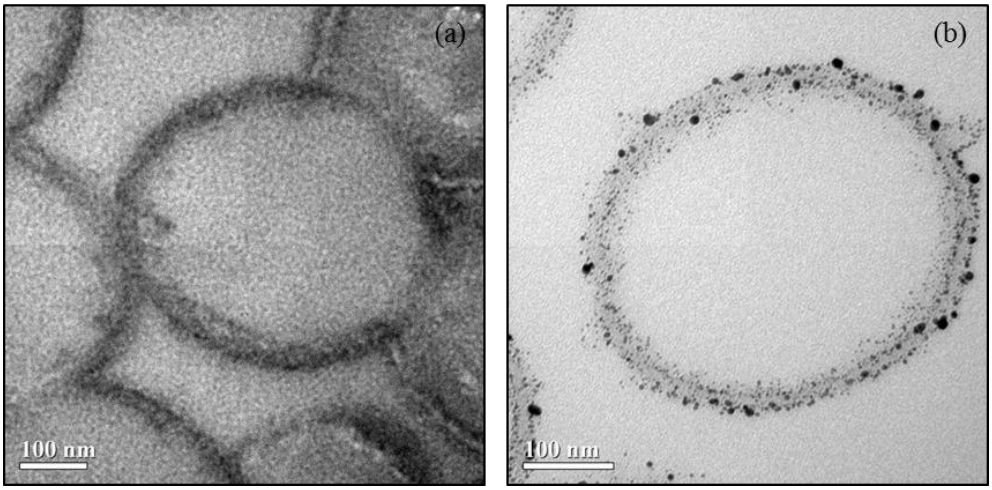

Figure 4.11 Cross-section TEM images of (a) PAA capsule and (b) spiky gold capsule (scale bar = 100 nm).

4.3 Characterization of anti-DIG/magnetic latex

In this study, anti-digoxigenin modified magnetic latex (anti-DIG/ML) particles were fabricated, as shown in the schematic of Figure 4.12 for using in the DNA hybridization detection platform. An external magnetic field was also applied for the target separation form sample matrixes. Anti-DIG as an antibody was carried on the surface of the magnetic latex to make for an easier interaction and a faster separation of the target antigen, digoxigenin (DIG). Therefore, the DNA probe tagged with DIG will be used for further experiments of DNA hybridization detection.

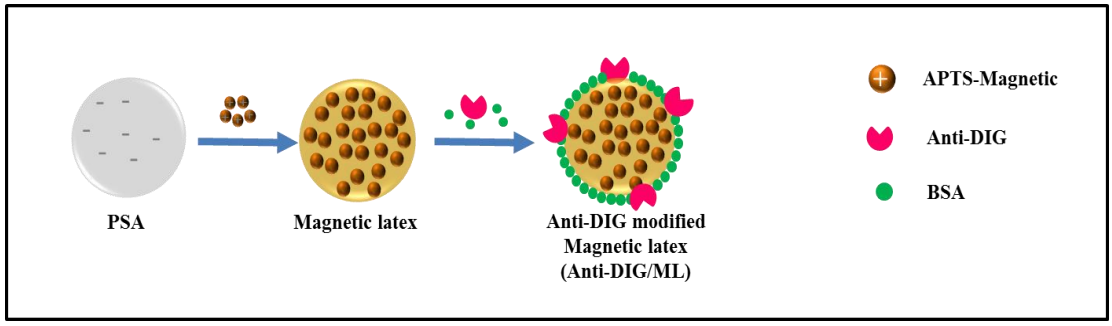

Figure 4.12 Fabrication of magnetic label particles.

The magnetic latex particles were prepared with coated 3-aminopropyl triethoxysilane (APTS) modified Fe_3O_4 nanoparticles (APTS-MN) on a PSA microsphere via electrostatic interaction between positive charges of the amino group from APTS and negative charges on the surface of PSA. The advantages of using PSA as a template for magnetic latex fabrication are its variable size [84] and its easily controlled precipitation [85]. Otherwise, APTS is a silane coupling agent which can be reacted with the metal oxide surface directly (as shown in Figure 4.13) for the advantages of biomolecules conjugated by providing the amino group [86]. Therefore, the anti-DIG-AP were modified on the magnetic latex via electrostatic interaction between the negative charges of alkaline phosphatase (pI = 4.5 [87]) and the amino group of APTS on magnetic latex particles. Finally, anti-DIG/ML particles were derived. Figure 4.14 shows the successful anti-DIG/ML particles preparation by the assay kit (from Sigma Aldrich, Germany). The kit uses *p*-nitrophenyl phosphate (*p*NPP) as a phosphatase substrate which turns yellow when dephosphorylation occurs by alkaline phosphatase modified anti-DIG. They show that only the color of anti-DIG/ML changes to yellow; otherwise, the color of magnetic latex solution did not change. Moreover, the amounts of anti-DIG on magnetic latex were estimated by using the Bradford technique (based on BSA standard curve) to be 3.45×10^5 molecules per magnetic latex particle.

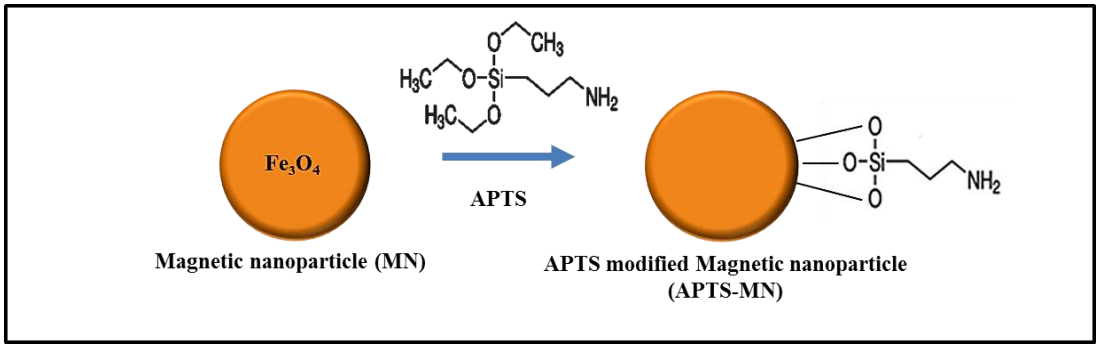

Figure 4.13 Schematic of the functionalized amine group on the surface of magnetic particles.

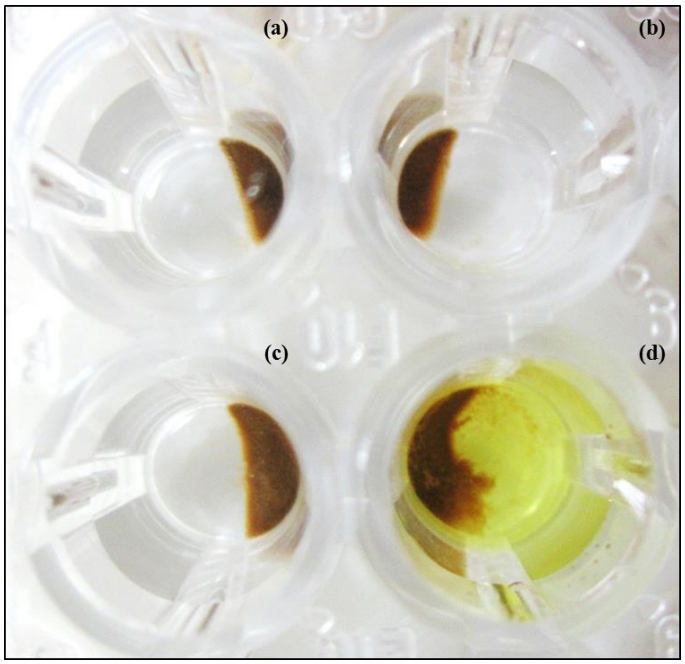

Figure 4.14 Image of the changing colorimetrics of the solution (a) magnetic latex in PBS, (b) anti-DIG/ML in PBS, (c) magnetic latex in *p*-nitrophenyl phosphate (*p*NPP) and (d) anti-DIG/ML in *p*NPP (*p*NPP is the substrate of alkaline phosphatase).

The morphology of PSA latex and anti-DIG/ML particles were observed by Fe-SEM images in Figure 4.15 (a) and 4.15 (b), in which anti-DIG/ML shows a rougher surface and bigger size of magnetic beads and anti-DIG on the PSA latex. The results from UV-spectrophotometry and FE-SEM images indicate that the magnetic particles and anti-DIG was completely covered on the latex particle surface. This was applied to separate the analyzed biomolecule based on the interaction of anti-DIG and DIG for detecting DNA hybridization based on spiky gold capsule labeling.

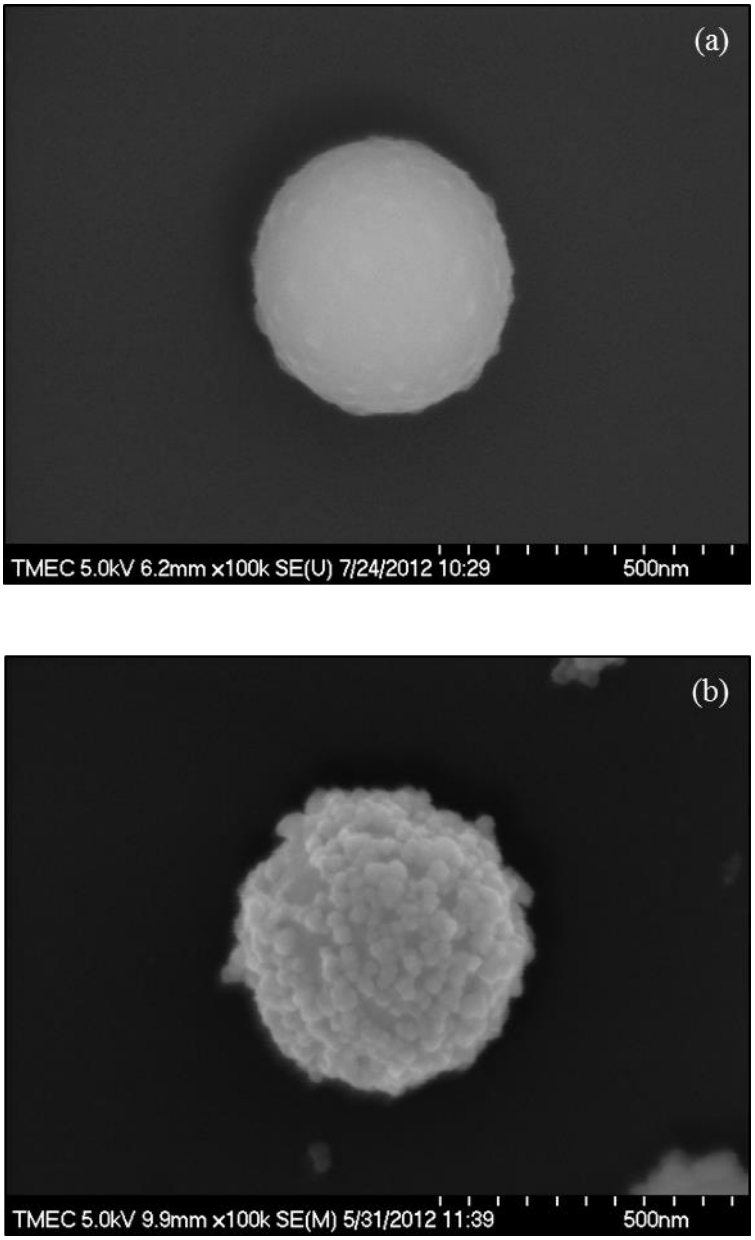

Figure 4.15 Fe-SEM images of (a) a PSA latex particle and (b) an anti-DIG/ML particle (scale bar = 500 nm).

4.3. Electrochemical DNA hybridization detection

In this part, the huge amount of gold particles on spiky gold capsule labeling had the effect of increasing the current signal in the sensitivity of DNA hybridization detection. The stem loop DNA (SL-DNA) was used as a single probe in which the thiolated group and DIG were modified at each end of the strand probe with the sequence of SH-(CH2)6-5'-AAA ggC CgT CTT CCT gAg TAA TAA CTT CCT gAg TgA ATA ACg gCC AAA) -3'-DIG (its structure is shown in Figure 4.16). The thiolated group will self-assemble to Au nanoparticles on the spiky gold capsule. By the way, di-sulfide bonding (S=S) is easily formed by itself. Therefore, TCEP was used as a strong reducing agent to reduce the disulfide bonds into the SH group which has more stable, effective and complete reactions without the need for removal other than reducing agents such as β-mercaptoethanol, mercaptoethylamine and dithiothreitol (DTT) [88, 89]. Moreover, MCH was used as a competitor DNA probe to prevent the non-specific DNA adsorption and also prevent flat orientation of the DNA probe. This occurs by repuls on between the negatively charged carboxyl group of MCH and phosphate groups of DNA probe [90]. At the other end, DIG was used for specific interacting with anti-DIG as the alternative to bind anti-DIG/DIG which was covered on the anti-DIG/ML from the result in Section 4.2. DIG is the small molecule which was extracted from the plant. It does not occur in other biological materials [91], which means that the unspecific background signal in DNA detection can be reduced [92]. One of the important properties of SL-DNA is the temperature dependent loop formation which can be induced to the linear formation based on the melting temperature (T_m) of the stem part sequence [93, 94]. The stem loop structure is present when the temperature condition is lower than the T_m value; nevertheless, the linear formation was also observed at a higher T_m value. Thus, the SL-DNA was used to study the enhanced specificity of the probe-target interaction [94, 95], the same as in this study. For the experiment, the sequence DNA of *E. coli* type K12-44 as a conserved region of several *E. coli*, 5'-TAT TCA CTC AGG AAG TTA TTA CTC AGG AAG-3', was firstly used as complementary target DNA for proofing the DNA detection platform. Therefore, the detection platform of DNA hybridization based on the spiky gold capsule label was described as following in Sections (4.3.1 and 4.3.2).

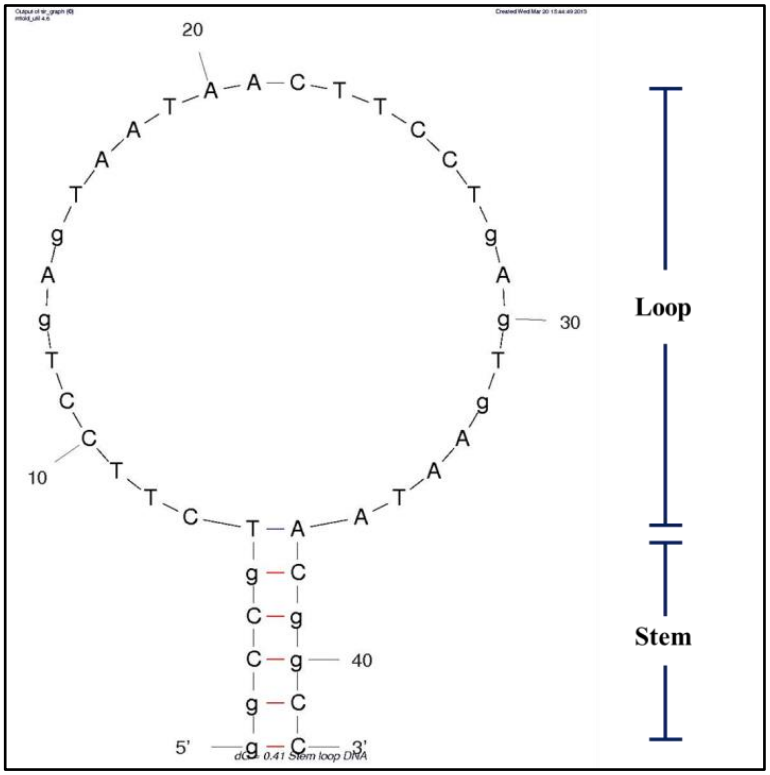

Figure 4.16 The structure of the stem loop DNA probe of this experiment predicted by the Mfold web server [96].

4.3.1 Biosensor platform design I

The DNA sensor platform I was developed by using a single SL-probe in which one end of the probe loop was tagged with the spiky gold capsule label and the other end of the loop was tagged with DIG. The process of detection is shown in Figure 4.17 in which DIG, initially, could not bind to anti-DIG/ML because of steric hindrance from the spiky gold capsule. Otherwise, the probe hybridized with target DNA that straightened out the loop, enabling linking to an anti-DIG modified magnetic separation. Hence, the magnetic separation could select the label in which the oxidative gold metal dissolved in an acidic bromine-bromide solution and DPASV detection of the release Au^{3+} ion was performed at an SPCE (E_{dep} = -0.6 V, t_{dep} = 300 s, and scan rate = 30 mV s^{-1}). By the way, the current signal derived from the detection DNA at 0 M and 1 pM are not significantly different (Figure 4.18) [as the t-test analysis shows a 99.5% confidence level (supporting Table B.1) with and without target DNA]. These results show that this platform is not sensitive and specific enough to detect DNA in which it is probably from the precipitation of labeling while the hybridization process is under SSC buffer and shaking conditions (Figure 4.19). This precipitation of the label had an effect on the washing step and background current response. Therefore, the new platform detection was designed by using pre-hybridization between target DNA and the SL-DNA probe before adding labeling as described in Section 4.3.2.

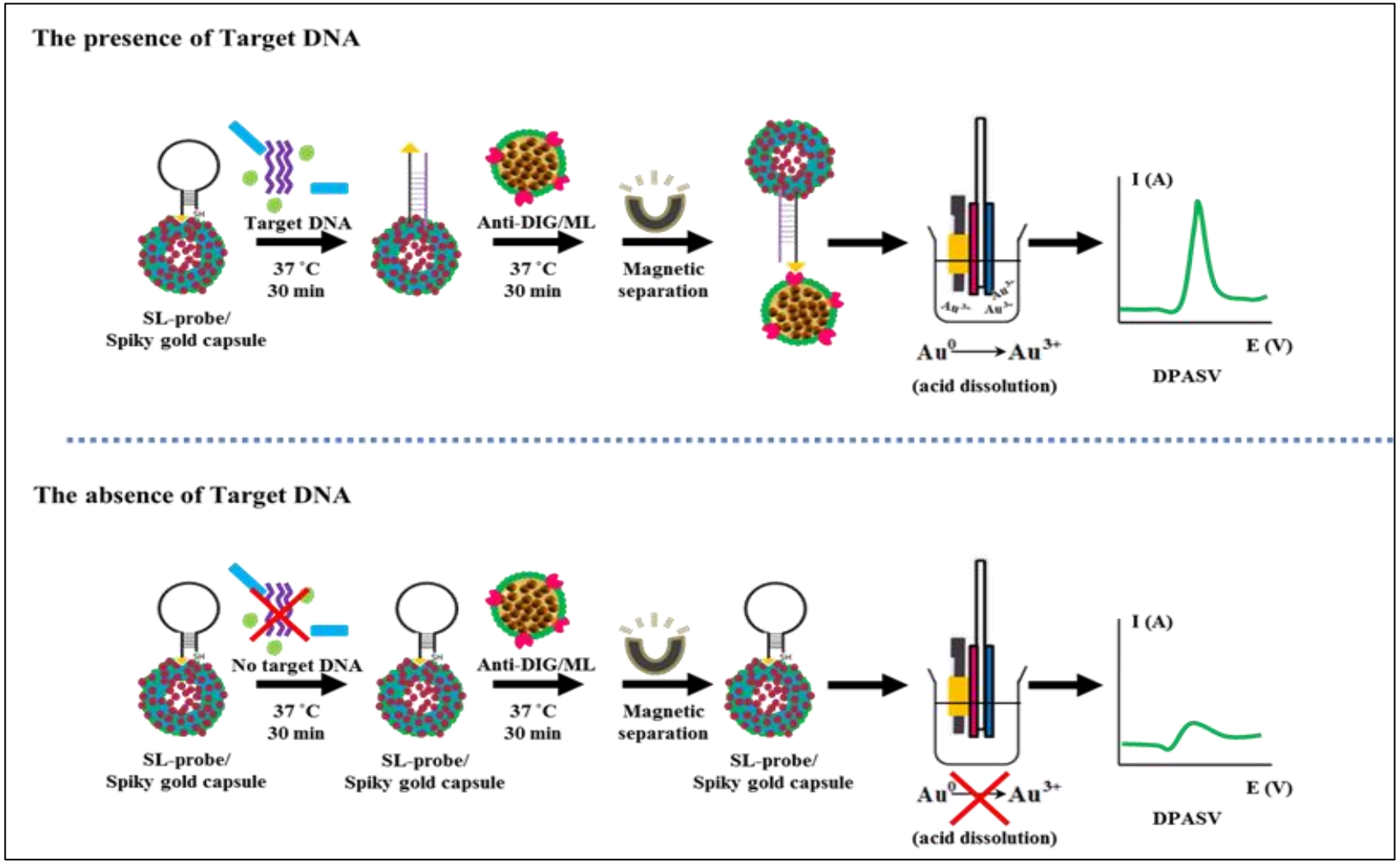

Figure 4.17 The biosensor platform I schematic of DNA detection using spiky gold capsule label.

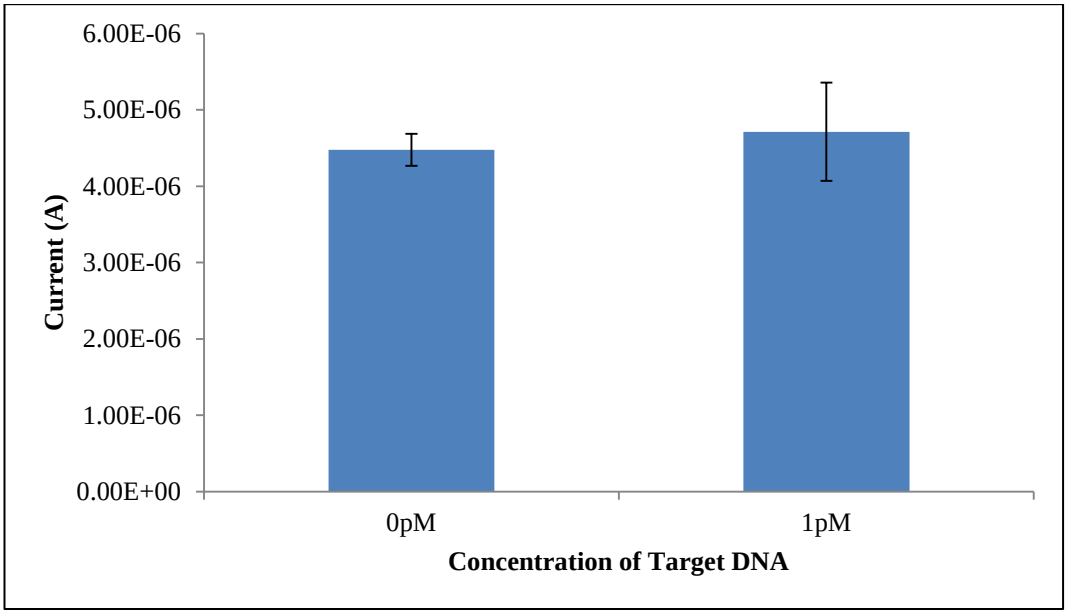

Figure 4.18 The current response of the DNA hybridization platform I at non-target DNA and 1pM of target DNA. Error bars show ± 1 standard deviation (n = 5).

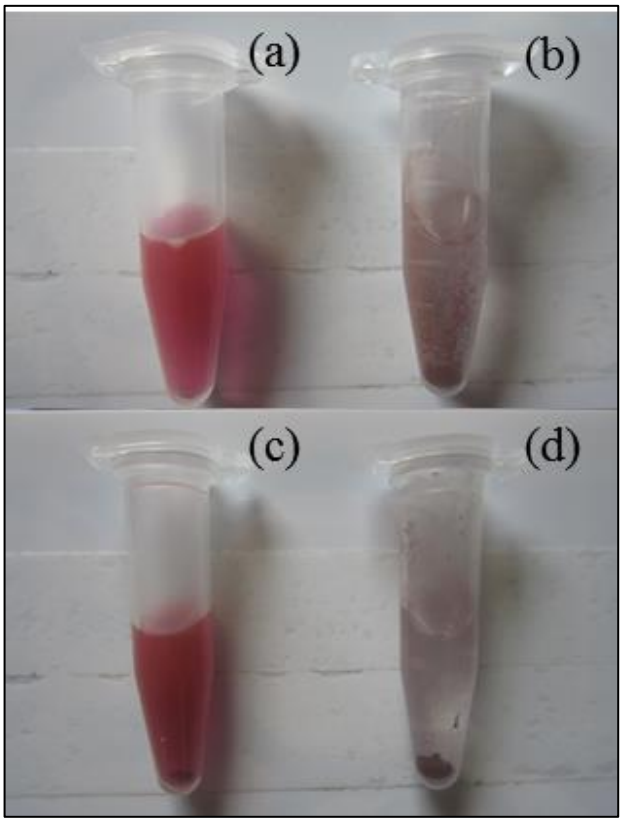

Figure 4.19 Spiky gold capsule dispersion in (a) sterile Milli-Q water under non-shaking conditions, (b) SSC buffer under non-shaking conditions, (c) sterile Milli-Q water under shaking and (d) SSC buffer under shaking conditions (shaking conditions: speed = 500 rpm and temperature = 25˚C).

4.3.2 Biosensor platform design II

To solve the precipitation of labeling, the biosensor platform design II was used, as shown in Figure 4.20. Firstly, the hybridization between the SL-probe and target DNA were performed before being separated by a magnetic field via the interaction of DIG and anti-DIG. After that, the condition temperature was controlled at 4℃ to change the conformation of SL-DNA. Loops were added for self-assembly with free thiol groups on the other end of the hybridized SL-DNA. The DNA hybridization can be monitored by measuring the oxidative gold metal dissolution in an acid bromine-bromide solution and DPASV detection of the released Au^{3+} ion at SPCE. On the other hand, in the absent target DNA, the spiky gold capsule label could not bind with thiol on SL-DNA because of the steric hindrance of anti-DIG/ML. The current signal of DNA hybridization detection using the platform II process was shown in Figure 4.21, in which the significant impact on the DNA detection at $p<0.05$ based on t-test analysis (supporting Table B.2) and the different standard deviation of the current signal with target DNA and without target DNA. Hence, this method analysis could be used for target DNA detection in higher efficiency than platform I with a higher ratio and lower standard deviation as shown in Figure 4.22. Moreover, this platform could be used for detection because the Fe-SEM image (Figure 4.23) was confirmed as the morphological spiky gold capsule. The magnetic labels were conjugated together based on the Au-thiol DNA probe linkage and magnetic-anti DIG-DIG DNA probe via antigen-antibody interaction. The platform was optimized in terms of the incubation time of the DIG/anti-DIG interaction, self-assembly between the thiol group of SL-DNA probe and the spiky gold capsule, DNA hybridization time and temperature and SL-DNA probe concentration. After the selectivity and quantification on DNA hybridization with optimized conditions was studied, the extracted genomic DNA was also done for *E. coli* detection.

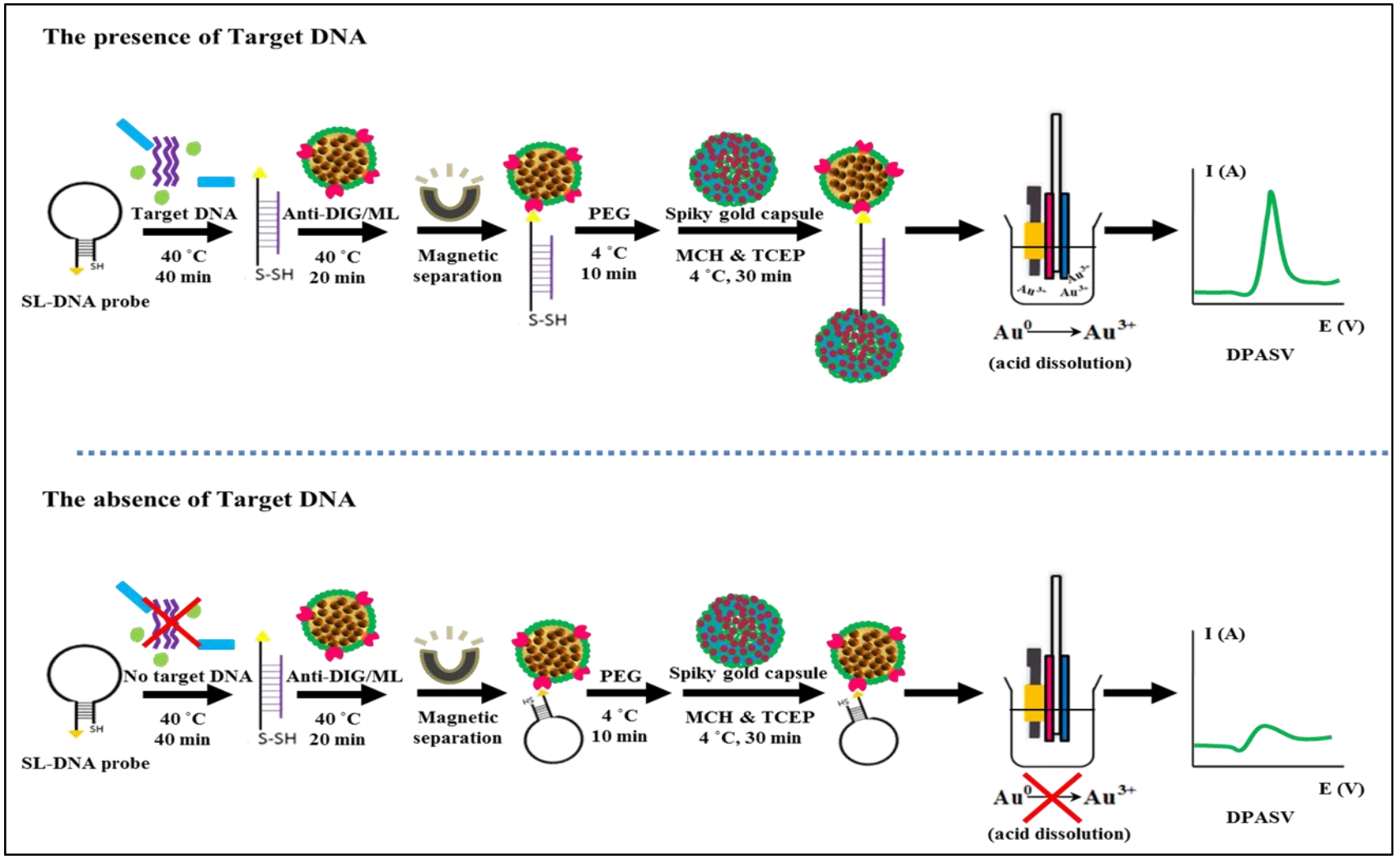

Figure 4.20 Schematic DNA hybridization platform II based on pre-hybridization.

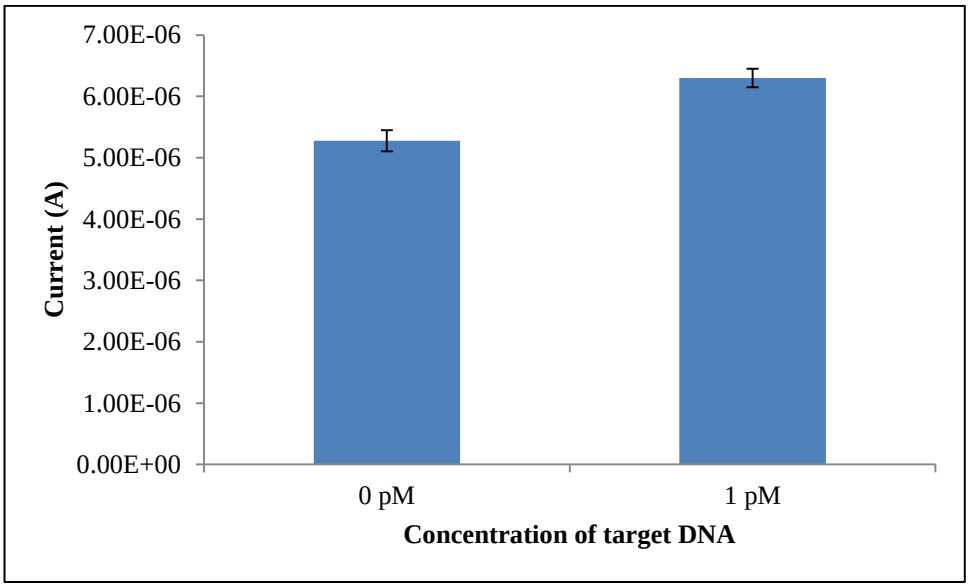

Figure 4.21 The current response of DNA hybridization detection based on platform II between non-target DNA and 1pM of target DNA. Error bars show ± 1 standard deviation (n = 5).

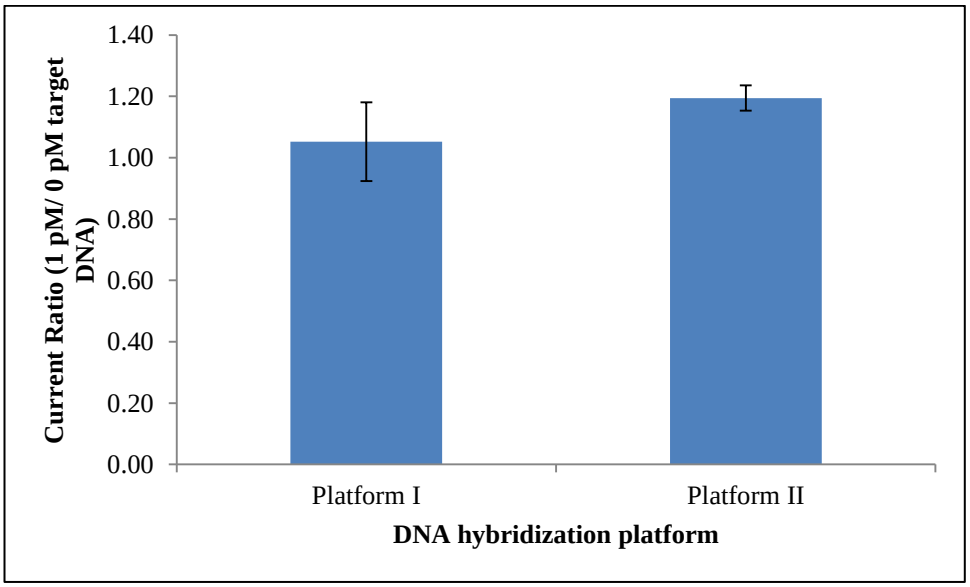

Figure 4.22 The current ratio of DNA hybridization with 1 pM and without target DNA based on platform I and II. Error bars show ± 1 standard deviation (n = 5).

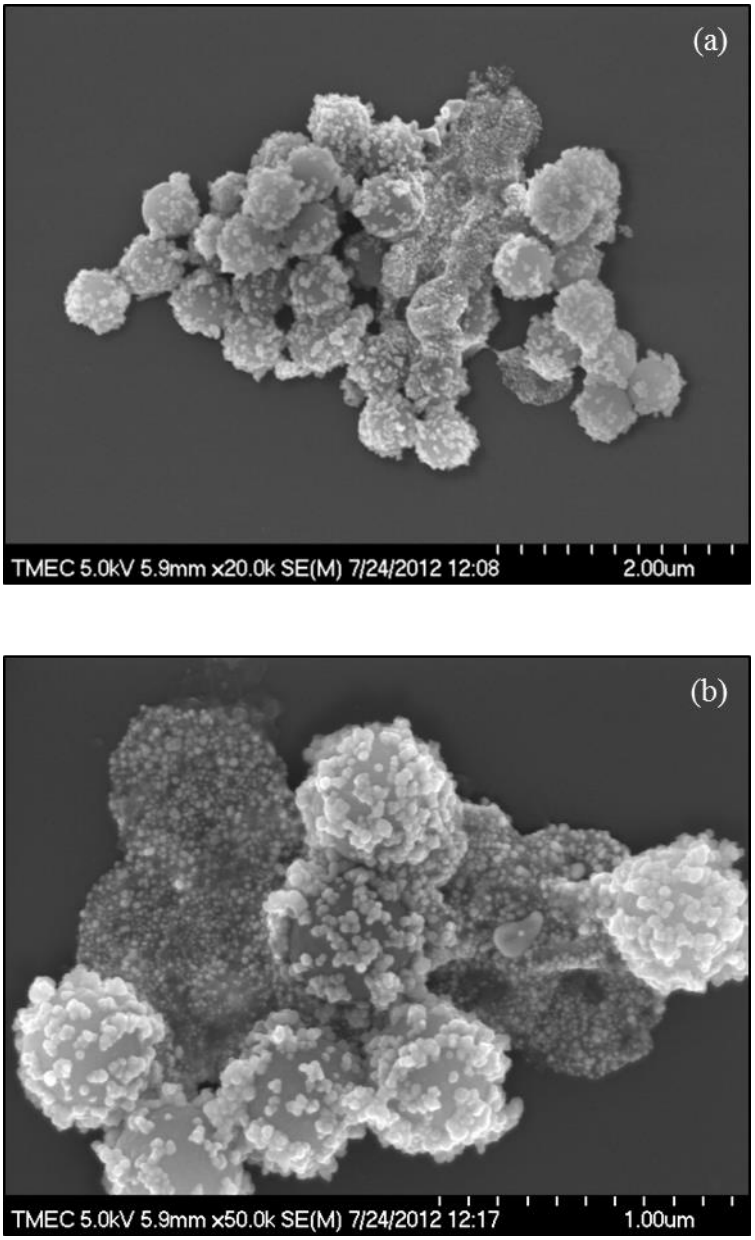

Figure 4.23 FeSEM images of conjugated spiky gold capsules and anti-DIG/ML under the hybridization detection of 1 pM target DNA based on platform II ([a] scale bar = 2.00 μm and [b] scale bar = 1.00 μm).

4.5 Optimization conditions for DNA hybridization detection

4.4.1 Effect of incubation time between anti-DIG/ML and DIG tagged SL-DNA probe

After hybridization between the SL-DNA probe and target DNA for 30 min at 37 ˚C, the complex of hybridization had been bound with anti-DIG/ML via DIG/anti-DIG interaction in which the DNA complex could be separated and selected by using the magnetic field. The anti-DIG as a functional antibody presented on magnetic latex can be specific in binding with DIG molecule. The incubation time parameter had several reports which had impacted the strength of the antigen-antibody reaction [97]. Therefore, the anti-DIG and DIG incubation time had been optimized to favor the maximal binding by varying the incubation times at 10, 20, 30, and 40 minutes. The results are shown in Figure 4.24 and 4.25 in which the current signals increased with the incubation time until the current ratios were saturated at 20 min. By prolonging the incubation up to 40 min, the current signals were not statistically significant. Based on the study by Yusoff et al. [98], there were also no significant differences for the incubation time of the antibody and antigen because the antigen and antibody was bound immediately after the reaction mixture. Therefore, the incubation time for 20 min was chosen for further experiments.

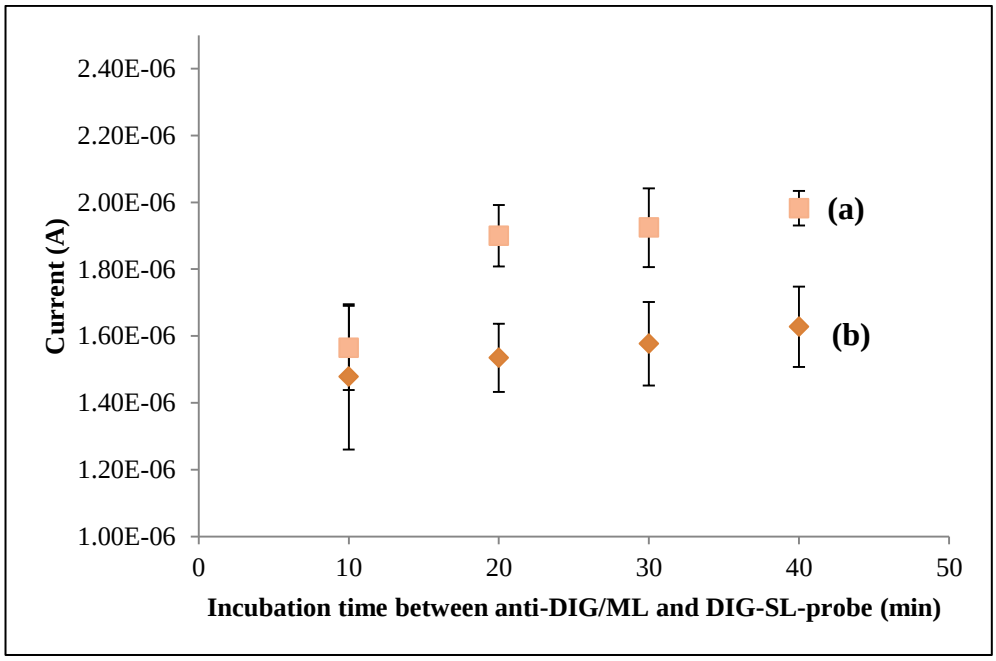

Figure 4.24 Effect of anti-DIG magnetic binding time on the current response of the (a) 1pM target DNA and (b) 0 pM target. Error bars show ± 1 standard deviation (n = 5).

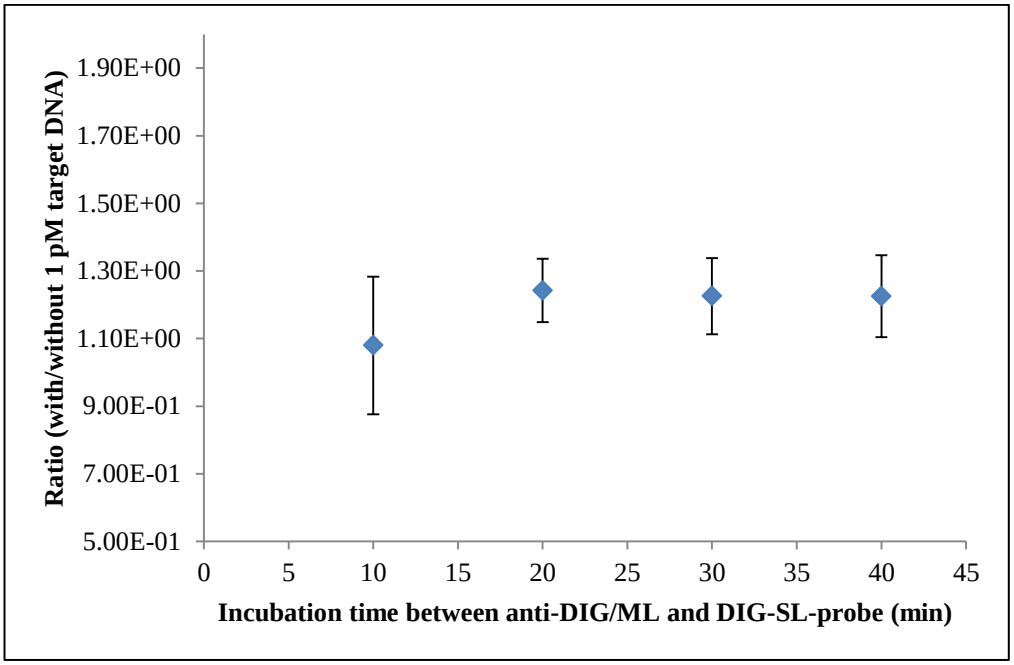

Figure 4.25 Effect of anti-DIG magnetic binding time on the current ratio. Error bars show ± 1 standard deviation (n = 5).

4.4.2 Effect of DNA hybridization time optimization

The DNA hybridization time was an important parameter which impacted hybridization efficiency. Thus, the incubation time of hybridization has to be optimized [99]. The optimization was studied by controlling the hybridization temperature at 37 ˚C and varying the hybridization times at 10, 20, 30, 40, 50, and 70 minutes. Figure 4.26 and 4.27 shows the signal current result for 1 pM target detection increasing from 10 to 40 min then decreasing a bit. The current ratio with and without 1 pM target DNA (Figure 4) shows that the maximum hybridization time is at 40 min. According to the data, the hybridization time at 40 min was chosen for further experiments.

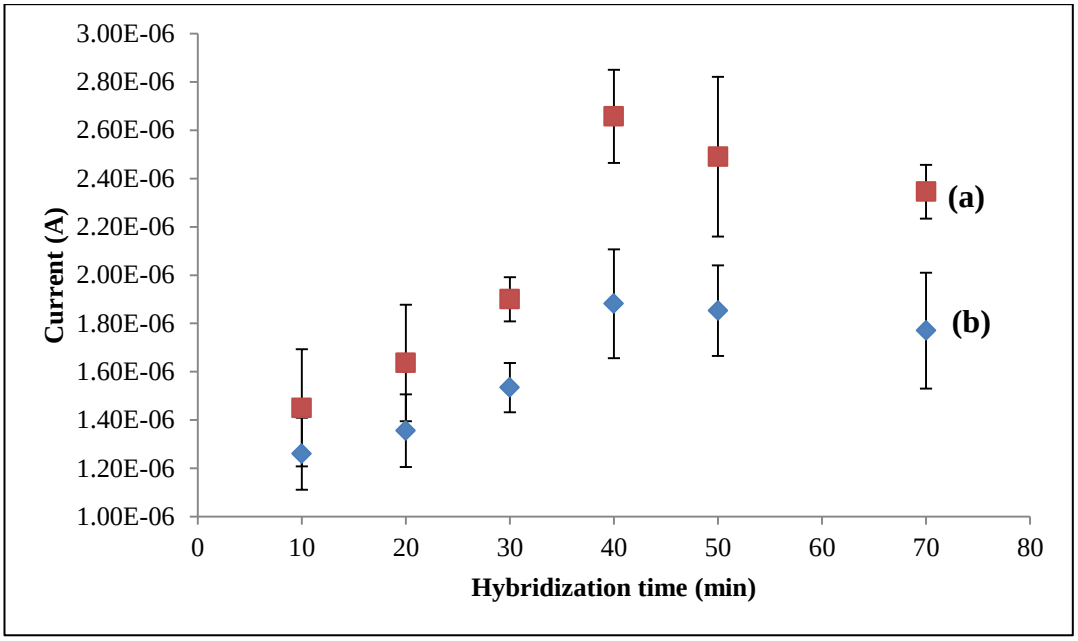

Figure 4.26 Effect of DNA hybridization time on the current response of the (a) 1pM target DNA and (b) 0 pM target. Error bars show ± 1 standard deviation (n = 5).

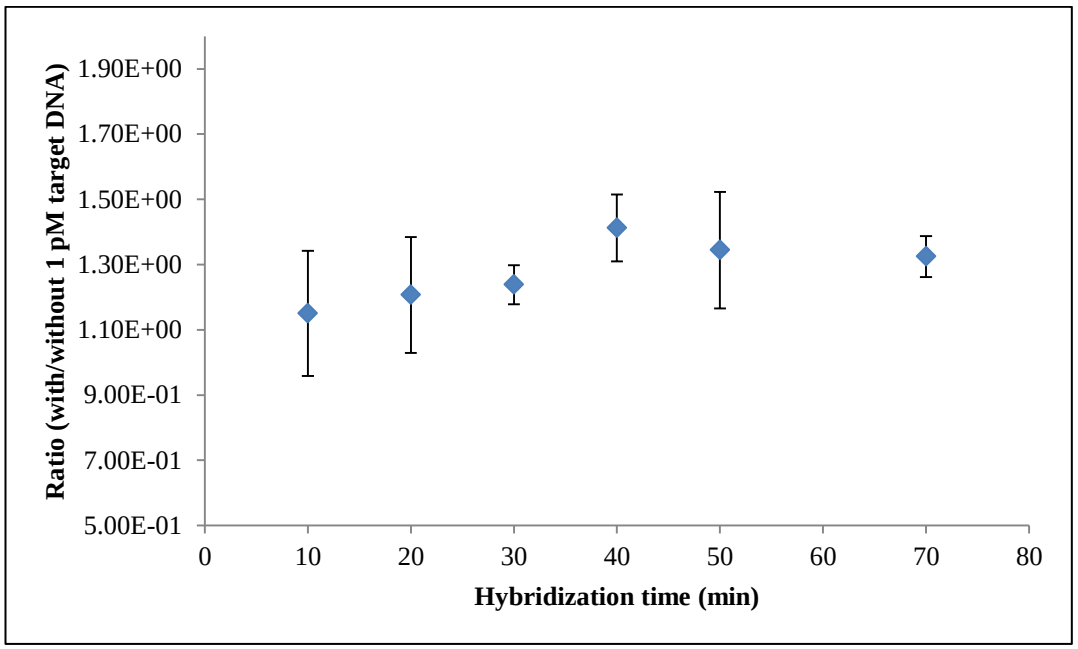

Figure 4.27 Effect of DNA hybridization time on the current ratio. Error bars show ± 1 standard deviation (n = 5).

4.4.3 Effect of self-assembly time of Au-S bonding

The linkage step between the thiol-hybridization complex and spiky gold capsule was conducted by using TCEP as a reducing agent which reduced the disulfide bonds into the SH group, and then covalently attached to the Au nanoparticle surface of the spiky gold capsule. The result of the reaction was a function of self-assembly times which were determined to establish the optimal time of incubation at 10, 20, 30, 40, and 60 minutes. The current increased in the range of 10 to 30 min and after that the responses were stable despite increasing incubation times (Figure 4.28). However, the current ratios with and without target DNA (shown Figure 4.29) were not significantly different, which could be affected from the concentration of TCEP. Mery et al. [100] mentioned that at 1:1 ratio of TCEP to disulfides, the complete reaction required nearly one hour. In this experiment, the ratio of TCEP to disulfides was 10:1; thus, the complete reaction should be less than one hour. At the high concentration of TCEP (30 µM), the reaction was complete within 40 seconds at pH 1.5 to 8.5 [101]. Therefore, the Au-SH bonding of the probe reaction could be finished within 10 minutes as the result shows in Figure 4.29. Nevertheless, the optimum time was 30 min since it performs the stable current.

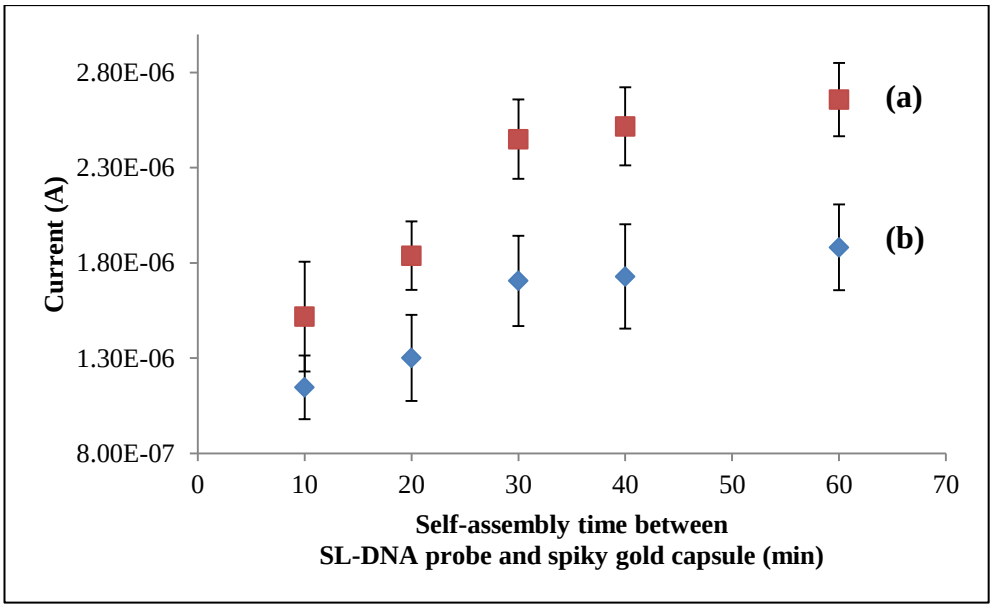

Figure 4.28 Effect of thiol-DNA linkage time on the current response of the (a) 1 pM target DNA and (b) 0 pM target. Error bars show ± 1 standard deviation (n = 5).

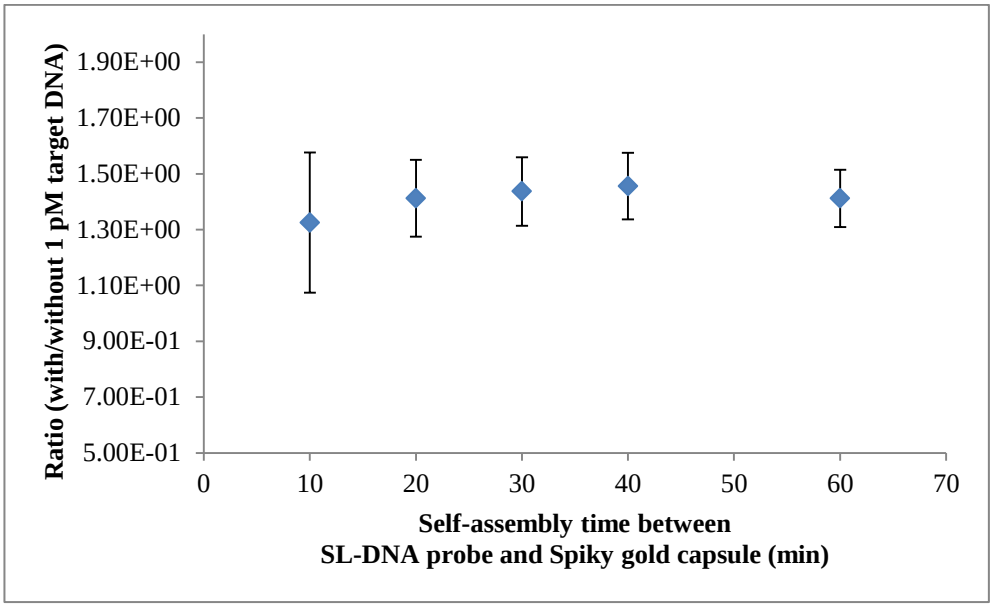

Figure 4.29 Effect of thiol-DNA linkage time on the current ratio. Error bars show ± 1 standard deviation (n = 5).

4.4.4 Effect of hybridization temperature

Temperature is the other important parameter which can affect DNA hybridizations, especially for the SL-DNA probe. Its structural appearance (as shown in Figure 4.16) depends on the melting temperature [44]. At a lower melting temperature, the thermal energy is not enough to overcome the binding energy; thus, the SL-DNA formation still remains. Conversely, the thermal energy is higher than the binding energy at the higher melting temperature which changes it into a linear conformation [44]. In this experiment, the temperature was optimized by varying the temperature in the ranges of 20, 30, 37, 40, and 60 ˚C. Experimental results from Figure 4.30 and 4.31 indicate that the best current signal was obtained from the hybridization temperature carried out at 40℃. The typical reaction temperatures are usually considerably lower than T_m [102]. It gives the temperature at which half of all probes form a duplex with their target although the other half are unbound. A decrease in the current signal was observed at temperatures higher than 40 ˚C since they are near the 58 ˚C melting temperatures of SL-DNA, which was calculated by the Biomath program. From the other study, it has been reported that the Na^+ ion concentration could also be significantly affected as the melting temperature [103, 104]. However, a conjugated antibody and antigen via avidin-biotin or anti-DIG-DIG was also affected by temperature in which the protein interactions decreased at temperatures higher than 40 ˚C [105]. Because the antigen-antibody binding was reversible based on the basic thermodynamic principle, temperature could be the important parameter affecting affinity constants [106, 107]. At the high temperature condition, there was a low affinity constant which had a weak affection and tended to dissociate readily of the antigen-antibody interaction [106]. Hence, 40 ˚C was selected as the optimum hybridization temperature.

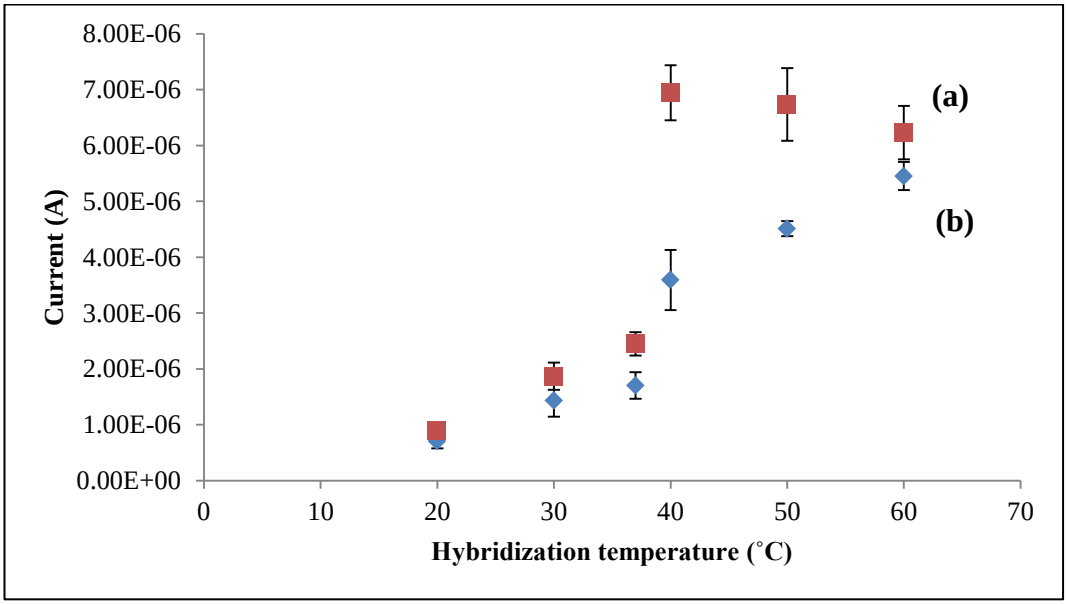

Figure 4.30 Effect of hybridization temperature on the current response of the (a) 1pM target DNA and (b) 0 pM target. Error bars show ± 1 standard deviation (n = 5).

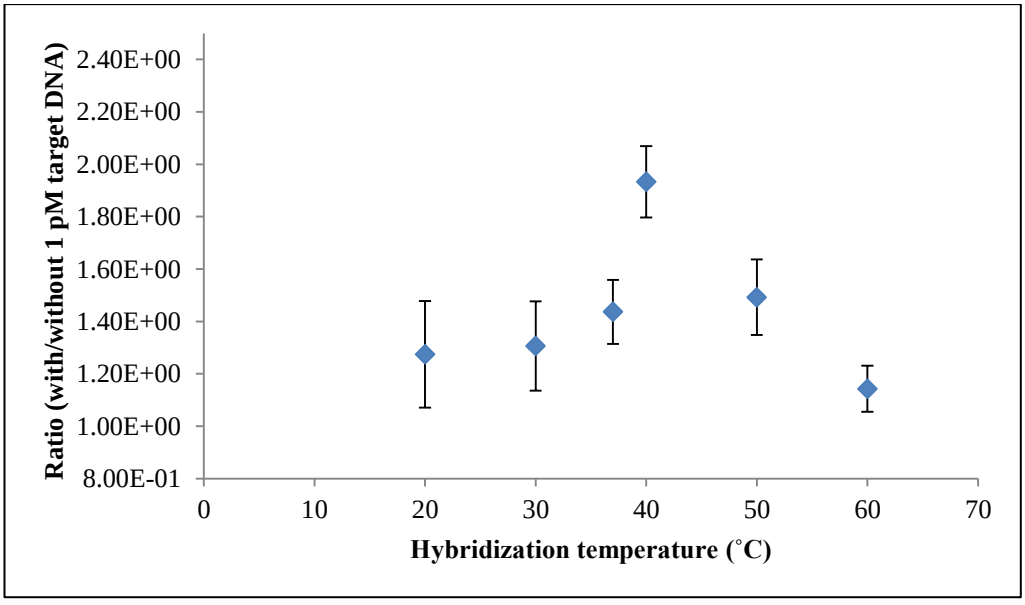

Figure 4.31 Effect of hybridization temperature on the current ratio. Error bars show ± 1 standard deviation (n = 5).

4.4.5 Effect of SL-DNA probe concentration

The SL-DNA probe concentration was a key promoter for improving the signal to the noise ratio of DNA detection. This was done by reducing nonspecific deposits and background signaled problems as a result of too high probe concentrations. The following SL-DNA probe concentrations were used: 1 µM, 100 nM, 10 nM, 1 nM, 100 pM, and 1 pM. Results summarize in Figure 4.32 and 4.33 indicating that increasing the SL-DNA probe concentration higher than 10 nM had no significant effect on the hybridization signal strength ($p<0.05$, supporting Table B.3). In fact, increasing the probe concentration only increased the sensitivity of detection, but it also increased the background [108]. Therefore the optimum SL-probe concentration should be 1 nM to obtain the maximum signal to noise ratio. However, the SL-probe concentration at 10 nM was chosen because of the lower standard deviation when compared with 1 nM of the SL-probe concentration.

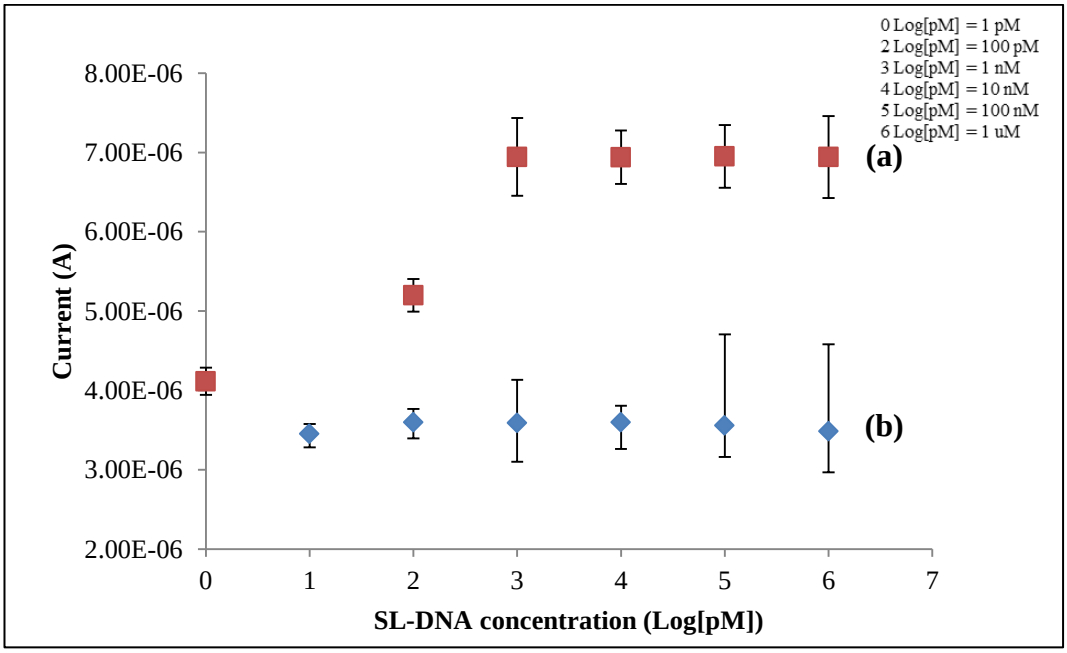

Figure 4.32 Effect of SL-DNA concentrations on the current response of the (a) 1pM target DNA and (b) 0 pM target. Error bars show ± 1 standard deviation (n = 5).

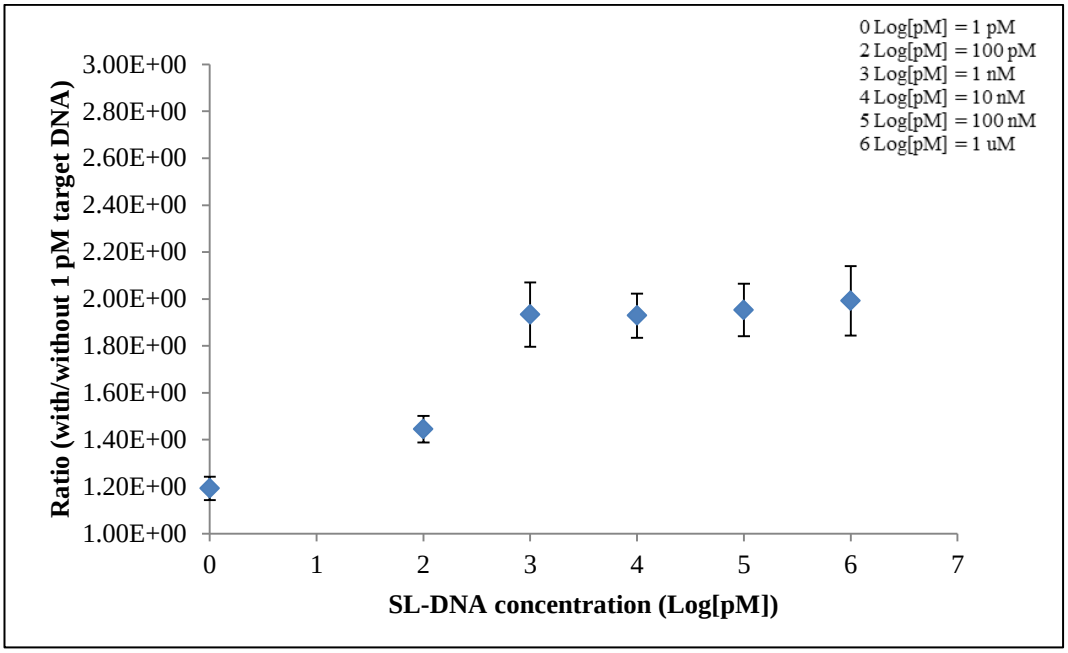

Figure 4.33 Effect of SL-DNA concentrations on the current ratio. Error bars show ± 1 standard deviation (n = 5).

The study of optimization conditions are used to detect the DNA hybridization based on the platform design which are described briefly here: the hybridization between the SL-probe and target DNA was incubated at 40 ˚C for 40 min. After that, the anti-DIG/ML was added and incubated for 20 min and separated the DNA hybridization when under the magnetic field at 4 ˚C. Then, unbinding of the target DNA was removed by washing with 0.1% SDS in SSC buffer for two times and SSC buffer for three times. The PEG used as formation blocking was incubated for 10 min at 4 ˚C and then the excess PEG was washed two times with 0.1% SDS in sterile Milli-Q water and three times in sterilied Milli-Q water. 0.1 µM of TCEP and 6-Mercapto-1-hexanol and spiky gold capsules were mixed with the PEG-blocked DNA hybridization, incubated for 30 min at 4 ˚C, followed by sterile Milli-Q water washing and finally kept in 50 µL of sterile MQ-water. These optimized conditions were used to study the sensitivity and selectivity of this platform detection through the genomic DNA detection in real samples.

4.4.6 Sensitivity

The quantification of DNA hybridization detection based on platform II was studied for the investigation of the capability of DNA sensors to target DNA using different concentrations of the target oligonucleotides in the ranges of 0.1 aM to 100 pM. Figure 4.34 shows that the current signal depended on the concentration of target DNA, in which the linear regression equation for the range of 0.1aM to 100 pM target DNA concentration was calculated as $y = 4.08 \times 10^{-7} c + 3.30 \times 10^{-6}$ ($r^2 = 0.939$), where, c is the log concentration of the target DNA (zM) and y is the peak current responses (A). The detection limit of this platform detection was 1.84 aM which was calculated based

on this equation: limit detection of peak current value (i) = $\mu_b + 3\sigma_b$, where μ_b is the peak current response mean of non-complementary target DNA and σ_b is the standard deviation of the peak current of non-complementary target DNA (as 3.94×10^{-6} and 2.29×10^{-7}, respectively). Previously, the electrochemical DNA hybridization detection method based on AuNP was summarized in Table 4.2. The limit of detection was lower when using other materials with AuNP such as deposited Ag [68], latex polymer [19], and hollow polyelectrolytes [20, 21]. However, this DNA detection method not only used hollow polyelectrolytes, but the magnetic particles were also applied to detect target DNA. This method shows the lower detection than the other method with highly sensitive DNA hybridization platform, thus the genomic DNA detections from cultured cell bacteria (*E. coli* were used as a model) had been applied.

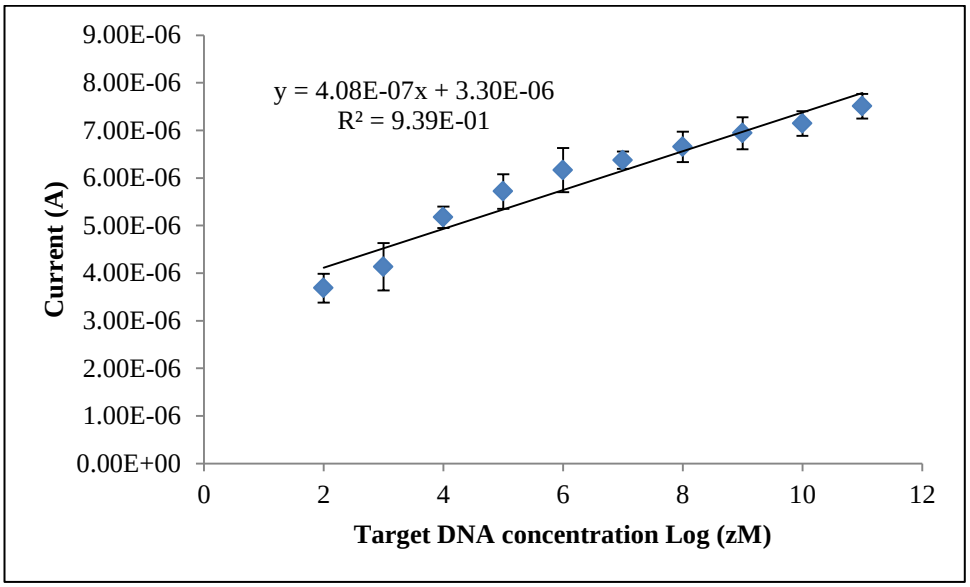

Figure 4.34 Calibration curve of the target DNA concentration. Error bars show ± 1 standard deviation (n = 5).

Table 4.2 Comparison for the DNA hybridization detection method using AuNPs.

Modification	Method of Detection	Limit of Detection	Ref
AuNP label on DNA probe	ASV/LSV	5 pM	[16]
AuNP label on DNA probe/Ag dep.	Ag oxn (ASV)	10 nM	[68]
AuNP label on DNA probe/Au dep.	ASV/CV	0.6 fM	[18]
Au latex label on DNA probe (Avidin/biotin)	ASV/DPV	0.5 fM	[109]
Au capsule label on SL-DNA probe (Avidin/biotin)	ASV/DPV	0.14 fM	[21]
Spiky gold capsule label on SL-DNA probe (DIG/anti-DIG)	ASV/DPV	1.84 aM	This work

4.4.7 Selectivity

The ability of the DNA sensor to recognize a particular sequence of DNA was investigated by exposing it to three kinds of DNA sequences, including a perfect complementary target, a single-base mismatched oligonucleotide, a three-base of mismatched oligonucleotide and a non-complementary target DNA at the same concentration (100 fM). Figure 4.35 shows the experimental results of the specificity test which had normalized current with each type of oligonucleotide. The highest normalized current of the complementary target was observed, whereas the normalized current of the non-complementary target DNA was very poor. The normalized currents of three-base mismatched and single-base mismatched DNA were achieved with low significance with the 16.31% and 28.91% hybridization event, respectively. Thus, this DNA biosensor exhibited good and high performance for selectivity and specificity. The SL-DNA probe had more specific recognition of target DNA than linear DNA probes [110]. Its conformation was affected by its specificity which was important to the low background signal and improved selectivity [111]. Moreover, the melting temperature of the loop portion was higher than the stem portion; thus, there was lower stability of mismatched SL-probe duplexes which caused the mismatched target to not form hybridization [93, 111].

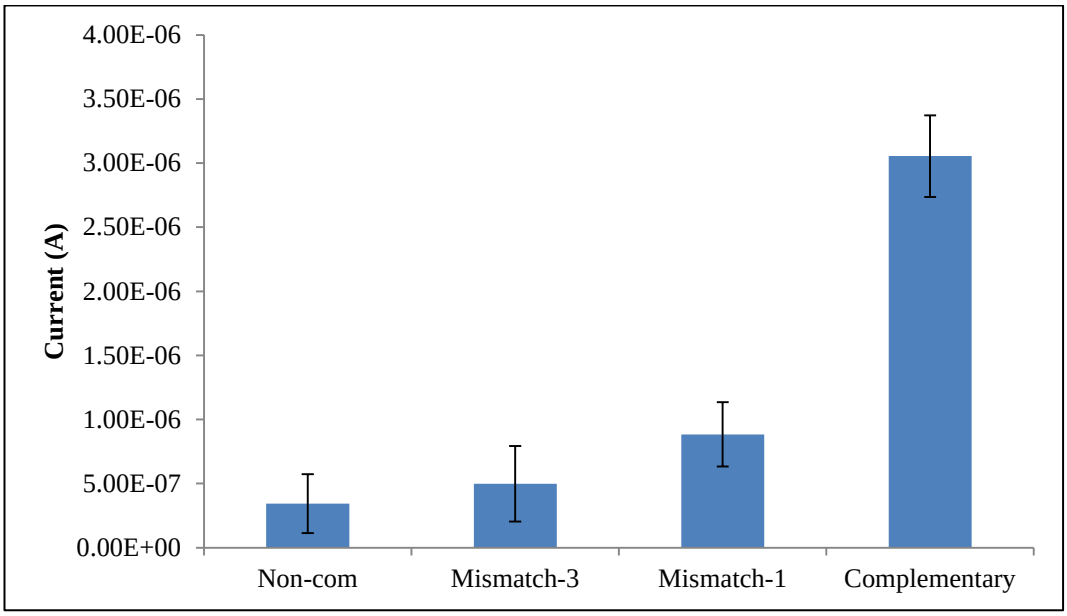

Figure 4.35 Corresponding histogram between the types of oligonucleotides to the peak current responses. Error bars show ± 1 standard deviation (n = 5).

4.5 Genomic DNA hybridization detection

Direct detection of genomic DNA without requiring polymerase chain reaction (PCR) mediated target DNA amplification was observed by this ultrasensitive detection platform. The genomic DNA from *E. coli* was extracted by using the heat shock method and commercial genomic DNA extraction kit to study hybridization efficiency to genomic DNA. Then, the proper extraction method was used to extract and measure the series of genomic DNA dilutions for *E. coli* and *Salmonella*. Finally, the spiked cultured bacteria in real samples were also applied to detect the amount of genomic DNA in real samples.

4.5.1 Genomic DNA extraction method

In this study, the *E. coli* strains BL21 and ATCC8730 were extracted by using the heat shock method and commercial genomic DNA kit method. The heat shock method was done by heating at 100 ˚C for 10 min to break the cell and then the genomic DNA in the supernatant will be collected in SSC buffer containing 10% SDS. Figure 4.36 shows the current response derived from genomic DNA of *E. coli* BL21 and ATCC8739 extracted by the heat shock method and commercial genomic DNA extraction kit method. The extraction methods were significantly different at $p<0.05$ (supporting Table B.4). Therefore, the commercial genomic DNA extraction kit had higher performance for genomic DNA detection than the heat shock method. Because the commercial test kit has a genomic DNA separation step which results in the extracted genomic DNA sample from the commercial test kit having higher purity than genomic DNA from the heat shock method. Hence, the commercial kit was used in further experiments.

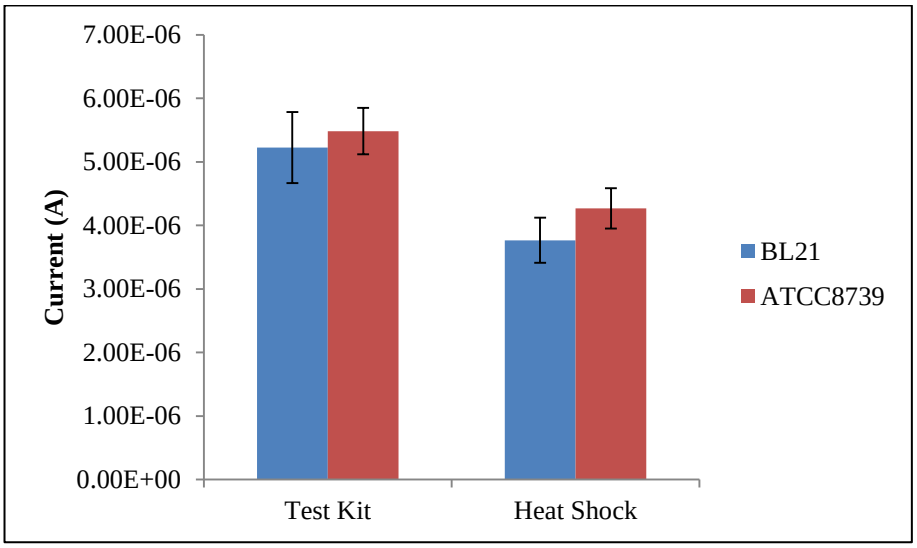

Figure 4.36 The current response of DNA hybridization based on different genomic DNA extraction methods: (a) Test kit and (b) Heat shock (*E. coli* BL21 = 3.2×10^5 CFU mL^{-1} and *E. coli* ATCC8739 = 4.48×10^5 CFU mL^{-1}). Error bars show ± 1 standard deviation (n = 5).

4.5.2 Characterization of genomic DNA detection

Based on the commercial genomic DNA extraction kit, genomic DNA of *E. coli* consisting of BL21, ATCC8739 and O157:H7 were used as the complementary targets. Since the used sequences of probes are in the tandem repeats of the conserved region of *E. coli* (i.e., non-pathogenic, uropathogenic and enterohemorrhagic), cell strains BL21, ATCC8739 and O157:H7 were cultured and extracted to investigate the genomic DNA detection. *Salmonella* bacteria were also extracted from genomic DNA to study the selectivity of the detection platform. The linear current response of genomic *E. coli* BL21, ATCC8739 and O157:H7 are shown in Figure 4.37 (a - c), in which the increase in current was the same as the increase in genomic concentration.

The linear calibration range, equation and r^2 derived from the detection of genomic DNA of *E. coli* strains BL21, ATCC8739 and O157:H7 are summarized in Table 4.2. The sensitivities (see the slope of equation) of genomic detection were BL21 > ATCC8739 > O157:H7, in which they relate to the amount of nucleotides on the genomic DNA from the NCBI database (BL21 = 4,570,938 bp, ATCC8739 = 4,746,218 bp and O157:H7 = 5,572,075 bp). The genomic size of *E. coli* O157:H7 was the biggest since it has the sequence range for specific only pathogenic bacteria, which are not found in non-pathogenic *E. coli*. With the bigger genomic size, the possibility of SL-DNA probe hybridization with genomic DNA is more difficult which affects the current response and sensitivity. The signal response to *Salmonella* was the lowest although the size of genomic was 4,857,432 bp.

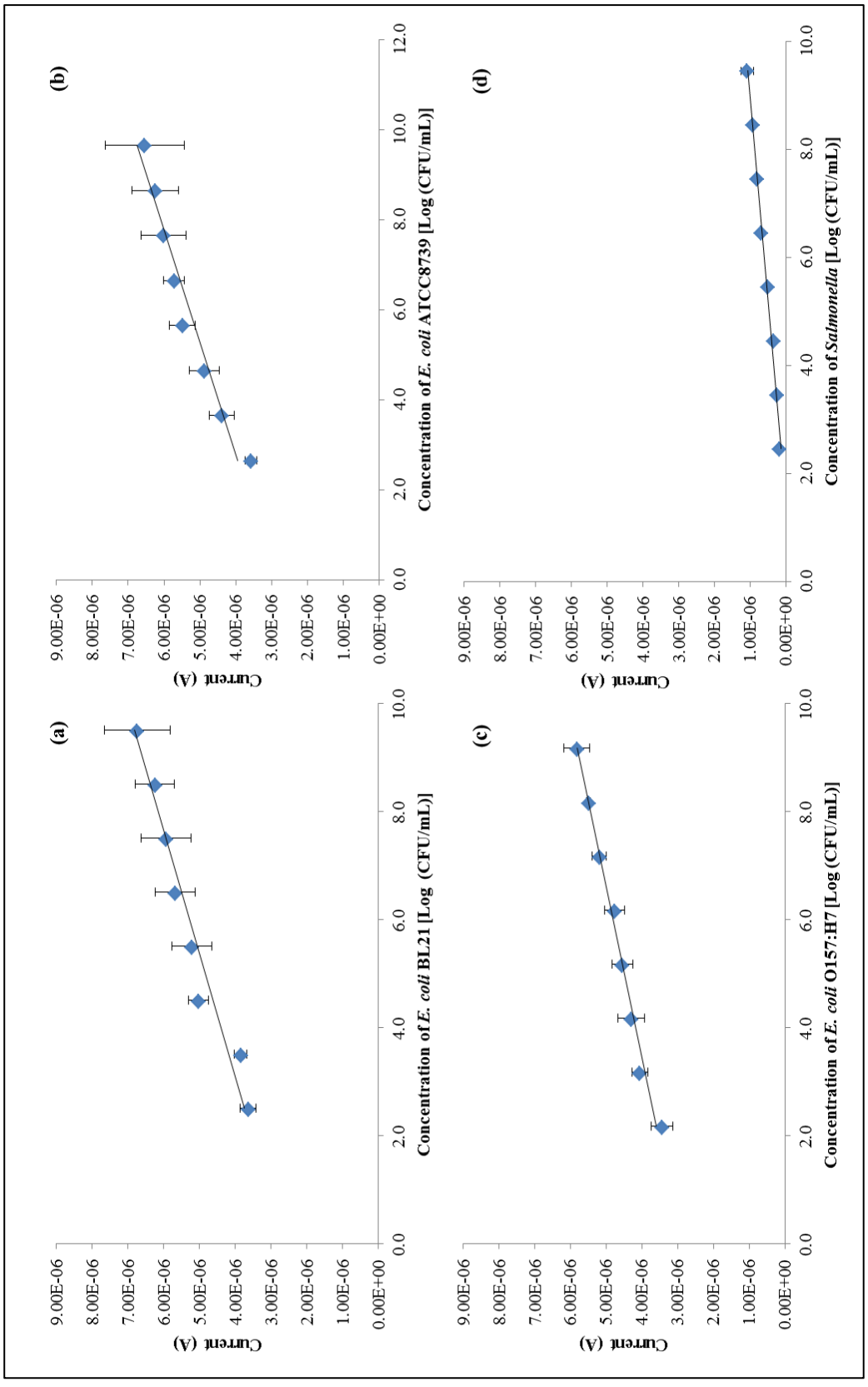
(a)
(b)
(c)
(d)
Current (A)
Concentration of E. coli BL21 [Log (CFU/mL)]
Concentration of E. coli ATCC8739 [Log (CFU/mL)]
Concentration of E. coli O157:H7 [Log (CFU/mL)]
Concentration of Salmonella [Log (CFU/mL)]
9.00E-06
8.00E-06
7.00E-06
6.00E-06
5.00E-06
4.00E-06
3.00E-06
2.00E-06
1.00E-06
0.00E+00
0.0
2.0
4.0
6.0
8.0
10.0
12.0

Table 4.3 Representation of the linear calibration range, equation and r^2 obtained from the genomic DNA detection of *E. coli* and *Salmonella*.

Bacteria	Linear range (CFU mL^{-1})	Linear equation	r^2
E. coli BL21	3.20×10^2 - 3.20×10^9	$y = 4.39 \times 10^{-7} c + 2.65 \times 10^{-6}$	0.957
E. coli ATCC8739	4.48×10^2 - 4.48×10^9	$y = 4.01 \times 10^{-7} c + 2.88 \times 10^{-6}$	0.950
E. coli O157:H7	1.48×10^2 - 1.48×10^9	$y = 3.18 \times 10^{-7} c + 2.90 \times 10^{-6}$	0.986
Salmonella	2.83×10^2 - 2.83×10^9	$y = 1.34 \times 10^{-7} c + 1.95 \times 10^{-7}$	0.991

c is the *E. coli* concentration (CFU mL^{-1}) and y is the peak current response (A).

Therefore, the detection platform based on pre-hybridization on the SL-DNA probe and spiky gold capsule label performed good selectivity. Thus, the genomic DNA of *Salmonella* bacteria were used to determine the detection limit based on the equation of $(i) = \mu_b + 3\sigma_b$, where μ_b is the peak current response mean of 10^9 CFU mL^{-1} of *Salmonella* and σ_b is the standard deviation of peak current of 10^9 CFU mL^{-1} of *Salmonella* in which $\mu_b = 1.16 \times 10^{-6}$ and $\sigma_b = 9.28 \times 10^{-8}$.

Hence, the high sensitivity on the genomic DNA of *E. coli* BL21, ATCC8739 and O157:H7 were derived with the detection limits as 4.18×10^{-6}, 6.65×10^{-7} and 8.52×10^{-8} CFU mL^{-1}, respectively. These LODs are lower than 0, in which the genomic DNA extraction used for this detection was not the only viable cell by the plate count method because cell death could occur during cell generation [112]. Based on the kinetics of biological processes, the rate of death was negligible at the log phase while the growth rate was the maximum constant [112]. In this experiment, *E. coli* cells were also harvested at log phases, thus, the LOD of this detection could be possible for the genomic DNA detection of cell death. Nevertheless, it could be excellent for enterohemorrhagic *E. coli* (EHEC) which has strains capable of producing Shiga toxin including *E. coli* O157:H7 because its toxin was released during growth [113].

4.6 Application in real samples

In recent years, the developed genomic DNA detection has been studied for high accuracy genomic DNA analysis through use in real sample detection. However, real samples such as soil, food, etc. have several components (i.e., carbohydrates, lipid, protein, other organic or inorganic components, etc.) which reduce its sensitivity and specificity. The sample preparation is a major step to remove the non-selective components before detection. However, this platform detection was designed to separate the DNA hybridization from the reaction solution when under the magnetic field. Thus, the genomic DNA detection in real samples was investigated.

4.6.1 Plain milk samples

UHT milk was used for an illustrating sample matrix (i.e., protein and lipids) for the detection of *E. coli*. The *E. coli* cultured cells were spiked into UHT milk and then the genomic DNA of *E. coli* was extracted using the commercial genomic DNA extraction kit for detection under the optimized procedure. The equation of the linear response in Table 4.3 was used to determine the limit of detection with the μ_b and $3\sigma_b$ values of milk (unspiked cells) which were 1.83×10^{-6} and 6.31×10^{-7}, respectively (n = 15). The LOD for *E. coli* strains is shown in Table 4.4 in which they are about 2 CFU mL^{-1}. Figure 4.38 shows a significant relationship between calculated concentrations and real spiked concentrations of *E. coli* BL21 (Figure 4.38 [a]), ATCC8739 (Figure 4.38 [b]) and O157:H7 (Figure 4.38 [c]) at $p<0.05$ based on ANOVA analysis (supporting Table B.5). However, high standard deviations of genomic DNA detection in milk sample were observed. The length of SL-DNA probe is 48 bp (approx. 16.32 nm) of which the target binding part is 30 bp. Since the extracted genomic DNA is much longer than this, different kinds of partial binding can occur.

Table 4.4 Limit of detection of *E. coli* in a milk base on platform II detection.

Strains of *E. coli*	LOD (CFU mL^{-1})
E. coli BL21	2.45
E. coli ATCC8739	2.11
E. coli O157:H7	2.60

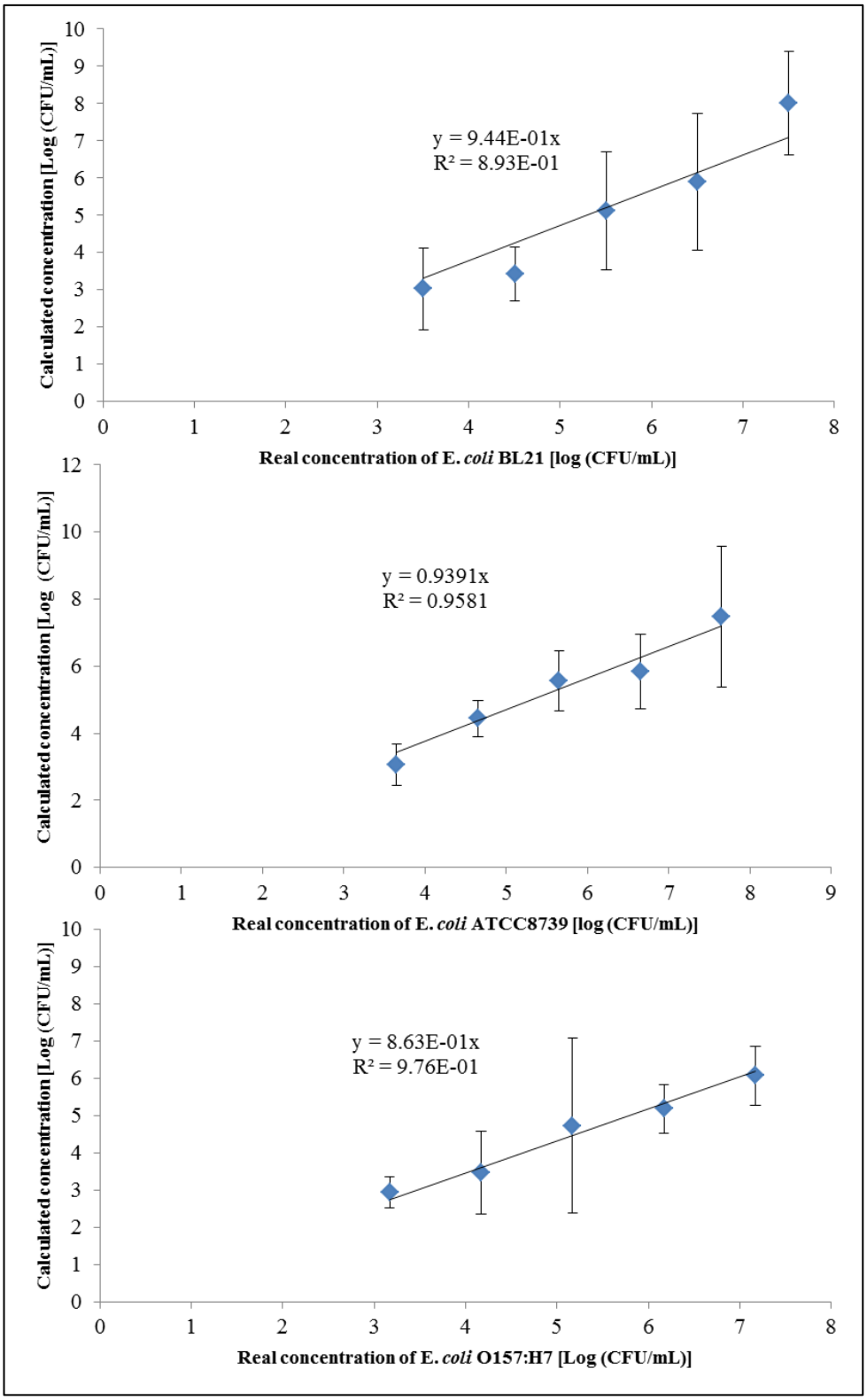

Figure 4.38 The relationships between calculated and real concentrations of *E. coli* BL21, ATCC8739, O157:H7 in milk samples. Error bars show ± 1 standard deviation (n = 3).

4.6.2 Fermented palm juice

Fermented palm juice is produced from palm sap or palm juice containing carbohydrates (110-130 g L^{-1}), protein (150-190 mg L^{-1}), fat (0.4-0.8 g L^{-1}), various minerals (Na, K, Ca, Fe), polyphenols and ascorbic acid (30-40 mg L^{-1}) [114]. Therefore, palm juice has been a rich medium capable of supporting the growth of various types of microorganisms (i.e., aerobic mesophilic bacteria, lactic acid bacteria and yeast.) Moreover, coliform bacteria including *E. coli* are also found in palm juice with the range of 3 to 6.78 log CFU mL^{-1} which could be contaminated from the environment and equipment used for tapping and from birds sheltering in the palm tree [115]. Hence, the detection of genomic DNA of *E. coli* was investigated on sterilized palm juice fermentation by spiking the *E. coli* into the sample for genomic DNA detection with the same procedure. The LOD results are shown in Table 4.5 using the regressive equation from Table 4.3 with the μ_b and $3\sigma_b$ values of unspiked cells in fermented palm juice as 2.09×10^{-6} and 6.59×10^{-7}, respectively (n = 15). The efficiencies of genomic DNA detection in fermented palm juice were also associated with a significant relationship between the real cell concentration and calculated cell concentration at $p<0.05$ (ANOVA test, supporting Table B.6) as shown in Figure 4.39. The standard deviations of the genomic DNA detection in fermented palm juice also showed high values which could be possibly because by the length of SL-DNA probe relative to the extracted genomic DNA as explained in 4.6.1.

Table 4.5 Limit of detection of *E. coli* in fermented palm juice based on platform II detection.

Strains of *E. coli*	LOD (CFU mL^{-1})
E. coli BL21	3.23
E. coli ATCC8739	2.97
E. coli O157:H7	3.68

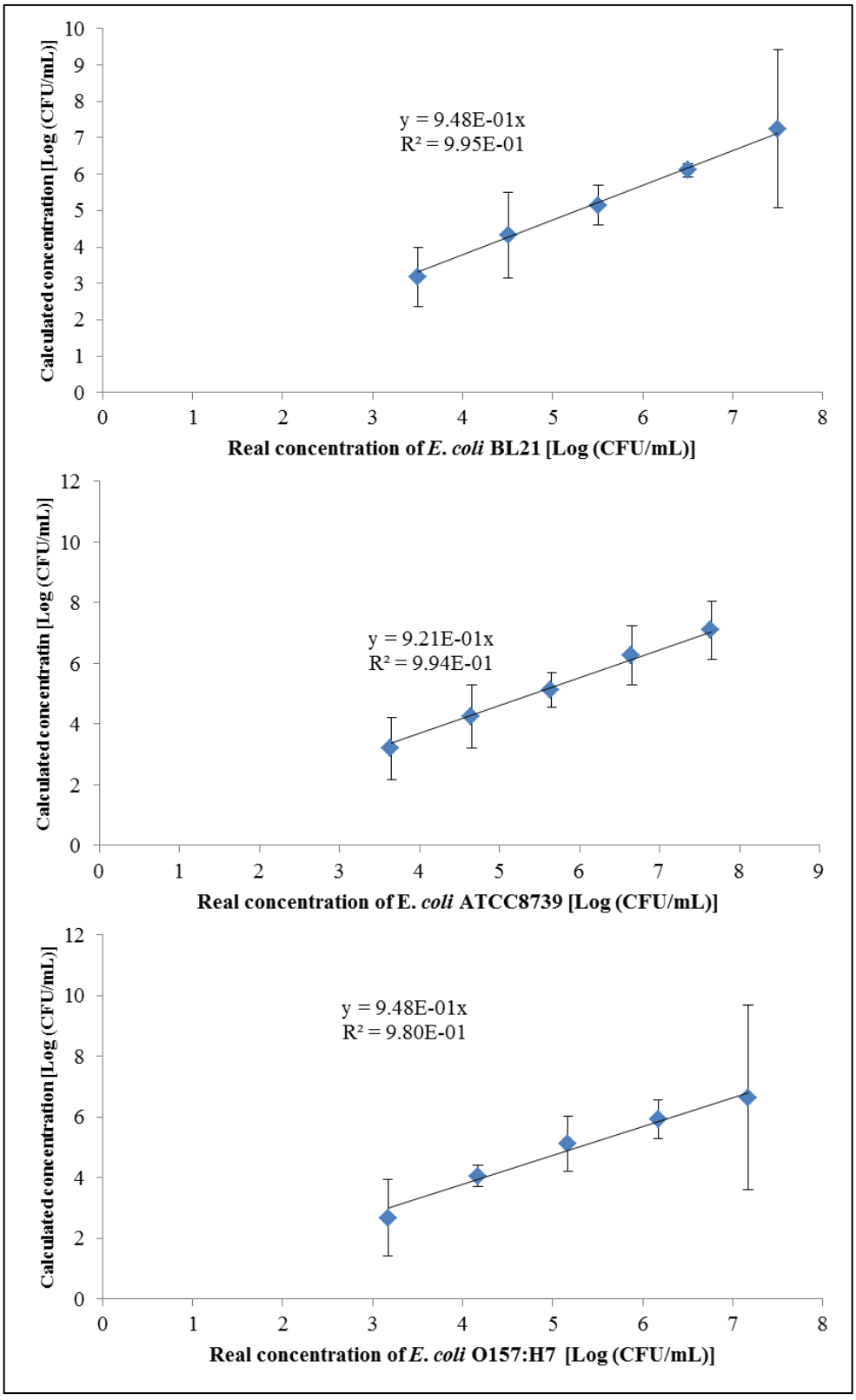

Figure 4.39 The relationships between calculated and real concentrations of *E. coli* BL21, ATCC8739, O157:H7 in fermented palm juice samples. Error bars show ± 1 standard deviation (n = 3).

The platform detections based on pre-hybridization with the SL-DNA probe and spiky gold capsule label were successfully applied to detect the genomic DNA of *E. coli* in real samples (such as milk and fermented palm juice). This platform showed greater LOD than the other genomic DNA detection methods which are shown in Table 4.6. The time assays after the extraction method occurred in this study within 105 min with the limited detection in the range of 2 - 4 CFU mL^{-1}.

Table 4.6 Comparison of genomic DNA detections of *E. coli* in real samples based on electrochemical DNA biosensor.

Detection Method[a]	Measurement	Sample	Time assay	LOD (CFU mL^{-1})	Ref.
DPV	α-naphthyl phosphate	Milk	3.5h	305	[26]
CV	5 methyl-phenazinium methyl sulfate	Seawater	3-5h	200	[25]
DPV	Daunomycin	Water	2h	50	[27]
ASV	Au^{3+} ions	Milk	105 min	2-3	This work
		Fermented palm juice		3-4	
[a] ASV, anodic stripping voltammetry; DPV, differential pulse voltammetry; CV, cyclic voltammetry.					

CHAPTER 5 CONCLUSIONS AND RECOMMENDATIONS

A highly sensitive and selective genomic DNA detection platform was successfully demonstrated by using electrochemical spiky gold capsule labels. Approx. 1.02×10^{11} Au^{3+} molecules were loaded per capsule of spiky gold capsule. The SL-DNA probes contained a DIG and thiol group at either end to allow interaction with anti-DIG-magnetic and spiky gold nanoparticles, respectively. The SL-DNA probe was hybridized with target DNA before separation by magnetic field via the interaction of DIG and anti-DIG-magnetic latex under the optimized conditions. The separated hybridization complex was tagged with spiky gold capsules and then Au^{3+} ions were detected by differential pulse anodic stripping voltammetry (DPASV). The platform had a limit of detection of 1.84 aM, the lowest quantity of target oligonucleotides. Genomic DNA of *E. coli* BL21, ATCC8739, and O157:H7 were detected in a concentration range of approx. 10^2 - 10^9 CFUmL^{-1} with detection limits of 4.75×10^{-9}, 3.97×10^{-10} and 7.34×10^{-12} CFU mL^{-1}, respectively. There are < 1 CFU because they include the detection of DNA from dead cells. The detection of dead cells is useful in the case of enterohemorrhagic *E. coli* strains such as *E. coli* O157:H7, as the toxins they produce will be present after cell death [113]. The platform was also used to detect *E. coli* BL21, ATCC8739, and O157:H7 in real samples with detection limits of 2.45, 2.11and 2.60 CFU mL^{-1} from milk samples and 3.23, 2.97 and 3.68 CFU mL^{-1} in fermented palm juice, respectively, with a 105 min assay time.

Future research on the length of extraction genomic DNA should be reduced by the catalytic of restriction enzyme. The detection in real samples should investigate the interference from compounds such as lipids, proteins, carbohydrates or phenolic compounds. This detection platform could be applied to detect other food pathogens in food samples by changing the nucleotide sequence of the SL-DNA probe. Hence, this platform could possibly be adapted to multiplex detection or a microfluidic system.

References

1. Malhotra, B.D. and Chaubey, A., 2003, "Biosensors for Clinical Diagnostics Industry", **Sensors and Actuators B: Chemical**, Vol. 91, No. 1–3, pp. 117-127.

2. Velusamy, V., Arshak, K., Korostynska, O., Oliwa, K., and Adley, C., 2010, "An Overview of Foodborne Pathogen Detection: In the Perspective of Biosensors", **Biotechnology Advances**, Vol. 28, No. 2, pp. 232-254.

3. Bagni, G., Osella, D., Sturchio, E., and Mascini, M., 2006, "Deoxyribonucleic Acid (DNA) Biosensors for Environmental Risk Assessment and Drug Studies", **Analytica Chimica Acta**, Vol. 573–574, pp. 81-89.

4. Wang, J., Rivas, G., Cai, X., Palecek, E., Nielsen, P., Shiraishi, H., Dontha, N., Luo, D., Parrado, C., Chicharro, M., Farias, P.A.M., Valera, F.S., Grant, D.H., Ozsoz, M., and Flair, M.N., 1997, "DNA Electrochemical Biosensors for Environmental Monitoring. A Review", **Analytica Chimica Acta**, Vol. 347, No. 1–2, pp. 1-8.

5. Wang, J., 2002, "Electrochemical Nucleic Acid Biosensors", **Analytica Chimica Acta**, Vol. 469, No. 1, pp. 63-71.

6. Drummond, T.G., Hill, M.G., and Barton, J.K., 2003, "Electrochemical DNA Sensors", **Nature Biotechnology**, Vol. 21, No. 10, pp. 1192-1199.

7. Cai, H., Wang, Y., He, P., and Fang, Y., 2002, "Electrochemical Detection of DNA Hybridization Based on Silver-Enhanced Gold Nanoparticle Label", **Analytica Chimica Acta**, Vol. 469, No. 2, pp. 165-172.

8. Oaks, J.L., 2007, "Laboratory Diagnosis of Viral Infections", In **Equine Infectious Diseases**. Debra, C.S., et al., W.B. Saunders, Saint Louis, USA, pp. 116-124.

9. Knowles, D.M., 2000, **Neoplastic Hematopathology**, 2nd ed., Lippincott Williams & Wilkins, Philadelphia, USA, pp. 316.

10. Nam, J.-M., Stoeva, S.I., and Mirkin, C.A., 2004, "Bio-Bar-Code-Based DNA Detection with PCR-Like Sensitivity", **Journal of the American Chemical Society**, Vol. 126, No. 19, pp. 5932-5933.

11. Suman and Kumar, A., 2008, "Recent Advances in DNA Biosensor", **Sensors & Transducers**, Vol. 92, No. 5, pp. 122-133.

12. Castañeda, M.T., Alegret, S., and Merkoçi, A., 2007, "Electrochemical Sensing of DNA Using Gold Nanoparticles", **Electroanalysis**, Vol. 19, No. 7-8, pp. 743-753.

13. Pumera, M., Sánchez, S., Ichinose, I., and Tang, J., 2007, "Electrochemical Nanobiosensors", **Sensors and Actuators B: Chemical**, Vol. 123, No. 2, pp. 1195-1205.

14. Wei, F., Lillehoj, P.B., and Ho, C.-M., 2010, "DNA Diagnostics: Nanotechnology-Enhanced Electrochemical Detection of Nucleic Acids", **Pediatric Research**, Vol. 67, No. 5, pp. 458-468.

15. Wang, J., Xu, D., Kawde, A.-N., and Polsky, R., 2001, "Metal Nanoparticle-Based Electrochemical Stripping Potentiometric Detection of DNA Hybridization", **Analytical Chemistry**, Vol. 73, No. 22, pp. 5576-5581.

16. Authier, L., Grossiord, C., Brossier, P., and Limoges, B., 2001, "Gold Nanoparticle-Based Quantitative Electrochemical Detection of Amplified Human Cytomegalovirus DNA Using Disposable Microband Electrodes", **Analytical Chemistry**, Vol. 73, No. 18, pp. 4450-4456.

17. Wang, J., Xu, D., and Polsky, R., 2002, "Magnetically-Induced Solid-State Electrochemical Detection of DNA Hybridization", **Journal of the American Chemical Society**, Vol. 124, No. 16, pp. 4208-4209.

18. Rochelet-Dequaire, M., Limoges, B., and Brossier, P., 2006, "Subfemtomolar Electrochemical Detection of Target DNA by Catalytic Enlargement of the Hybridized Gold Nanoparticle Labels", **Analyst**, Vol. 131, No. 8, pp. 923-929.

19. Pinijsuwan, S., Rijiravanich, P., Somasundrum, M., and Surareungchai, W., 2010, "Attomolar Electrochemical Detection of DNA Hybridization Based on Enhanced Latex/Gold Nanoparticles", **Advanced Engineering Materials**, Vol. 12, No. 11, pp. B649-B653.

20. Rijiravanich, P., Somasundrum, M., and Surareungchai, W., 2008, "Femtomolar Electrochemical Detection of DNA Hybridization Using Hollow Polyelectrolyte Shells Bearing Silver Nanoparticles", **Analytical Chemistry**, Vol. 80, No. 10, pp. 3904-3909.

21. Fatimah, A.I.F., 2011, **Highly Sensitive DNA Hybridizatin Detection Based on Au-Capsule Electrochemical Label**, Master's Thesis (Biotechnology), School of Bioresources and Technology, King Mongkut's University of Technology Thonburi, p. 61.

22. Hsing, I.M., Xu, Y., and Zhao, W., 2007, "Micro- and Nano- Magnetic Particles for Applications in Biosensing", **Electroanalysis**, Vol. 19, No. 7-8, pp. 755-768.

23. Rahman, M. and Elaissari, A., 2010, "Organic–Inorganic Hybrid Magnetic Latex", In **Hybrid Latex Particles**. Herk, A.M. and Landfester, K., Springer Berlin Heidelberg, Germany, pp. 237-281.

24. Beveridge, J.S., Stephens, J.R., and Williams, M.E., 2011, "The Use of Magnetic Nanoparticles in Analytical Chemistry", **Annual Review of Analytical Chemistry**, Vol. 4, No. 1, pp. 251-273.

25. Paniel, N. and Baudart, J., 2013, "Colorimetric and Electrochemical Genosensors for the Detection of *Escherichia coli* DNA without Amplification in Seawater", **Talanta**, Vol. 115, No. 0, pp. 133-142.

26. Luo, C., Lei, Y., Yan, L., Yu, T., Li, Q., Zhang, D., Ding, S., and Ju, H., 2012, "A Rapid and Sensitive Aptamer-Based Electrochemical Biosensor for Direct Detection of *Escherichia coli* O111", **Electroanalysis**, Vol. 24, No. 5, pp. 1186-1191.

27. Geng, P., Zhang, X., Teng, Y., Fu, Y., Xu, L., Xu, M., Jin, L., and Zhang, W., 2011, "A DNA Sequence-Specific Electrochemical Biosensor Based on Alginic Acid-Coated Cobalt Magnetic Beads for the Detection of E. Coli", **Biosensors and Bioelectronics**, Vol. 26, No. 7, pp. 3325-3330.

28. Lívia Maria da Costa Silva, Ana Claudia Sant'Ana Pinto, Andrea Medeiros Salgado, and Coelho., M.A.Z., 2011, "Development of Potentiometric Urea Biosensor Based on Canavalia Ensiformis Urease", In **Biosensors - Emerging Materials and Applications**. Serra, P.A., InTech, pp. 483-498.

29. Chambers, J.P., Arulanandam, B.P., Matta, L.L., Weis, A., and Valdes, J.J., 2008, "Biosensor Recognition Elements.", **Current Issues in Molecular Biology**, Vol. 10, No. 1-2, pp. 1-12.

30. Van Dorst, B., Mehta, J., Bekaert, K., Rouah-Martin, E., De Coen, W., Dubruel, P., Blust, R., and Robbens, J., 2010, "Recent Advances in Recognition Elements of Food and Environmental Biosensors: A Review", **Biosensors and Bioelectronics**, Vol. 26, No. 4, pp. 1178-1194.

31. Monk, D. and Walt, D., 2004, "Optical Fiber-Based Biosensors", **Analytical and Bioanalytical Chemistry**, Vol. 379, No. 7-8, pp. 931-945.

32. Lee, Y.H. and Mutharasan, R., 2005, "Biosensors", In **Sensor Technology Handbook**. Wilson, J.S., Newnes, Burlington, USA, pp. 161-180.

33. Dixon, M.C., 2008, "Quartz Crystal Microbalance with Dissipation Monitoring: Enabling Real-Time Characterization of Biological Materials and Their Interactions", **Journal of Biomolecular Techniques**, Vol. 19, No. 3, pp. 151-158.

34. Johansson, T., 2010, "Affinity Measurements Using Quartz Crystal Microbalance (QCM)", In **Antibody Engineering**. Kontermann, R. and Dübel, S., Springer Berlin Heidelberg, Germany, pp. 683-693.

35. Patel P. N., Mishra, V., and Mandloi A. S., 2010, "Optical Biosensors: Fundamentals & Trends", **Journal of Engineering Research and Studies** Vol. 1, No. 1, pp. 15-34.

36. Chung-Chiun, L., 1999, "Electrochemical Sensors", In **The Biomedical Engineering Handbook**. Bronzino, J.D., 2nd ed., CRC Press, Boca Raton, USA, pp. 1-6.

37. Thévenot, D.R., Toth, K., Durst, R.A., and Wilson, G.S., 2001, "Electrochemical Biosensors: Recommended Definitions and Classification", **Biosensors and Bioelectronics**, Vol. 16, No. 1–2, pp. 121-131.

38. Griffiths, A.J., Miller, J.H., Suzuki, D.T., Lewontin, R.C., and Gelbart, W.M., 2000, **An Introduction to Genetic Analysis**, 7th ed., W.H.Freeman, New York, pp.

39. Tropp, B.E., 2008, **Molecular Biology Genes to Proteins**, 3rd ed., Jones and Bartlett Publishers, Canada, pp. 109-114.

40. Garrett, R.H. and Grisham, C.M., 2008, **Biochemistry**, 4th ed., Mary Finch Publisher, Canada, pp. 330-331.

41. Williams, S.A., Slatko, B.E., and McCarrey, J.R., 2007, **Laboratory Investigations in Molecular Biology**, Jones and Bartlett Publishers, Canada, pp. 227-229.

42. Broude, N.E., 2005, "Molecular Beacons and Other Hairpin Probes", In **Encyclopedia of Medical Genomics and Proteomics**, 1st ed., Marcel Dekker, Inc., New York, USA, pp. 846-850.

43. Broude, N.E., 2002, "Stem-Loop Oligonucleotides: A Robust Tool for Molecular Biology and Biotechnology", **Trends in Biotechnology**, Vol. 20, No. 6, pp. 249-256.

44. Mishra, G., Giri, D., Li, M.S., and Kumar, S., 2011, "Role of Loop Entropy in the Force Induced Melting of DNA Hairpin", **The Journal of Chemical Physics**, Vol. 135, No. 3, pp. 035102-035108.

45. Macdonald, J., Stefanovic, D., and Stojanovic, M.N., 2008, "Smart DNA: Programming the Molecule of Life for Work and Play", In **Scientific American Magazine**. Editor, Scientific American, Inc., New York, USA, pp. 85-88.

46. Ozsoz, M.S., 2012, **Electrochemical DNA Biosensors**, 1st ed., Pan Stanford Publishing Pte.LTd., Singapore, pp. 227.

47. Satterfield, B.C., Bartosiewicz, M., West, J.A.A., and Caplan, M.R., 2010, "Surpassing Specificity Limits of Nucleic Acid Probes Via Cooperativity", **The Journal of Molecular Diagnostics**, Vol. 12, No. 3, pp. 359-367.

48. Fan, C., Plaxco, K.W., and Heeger, A.J., 2003, "Electrochemical Interrogation of Conformational Changes as a Reagentless Method for the Sequence-Specific Detection of DNA", **Proceedings of the National Academy of Sciences**, Vol. 100, No. 16, pp. 9134-9137.

49. Silva, F., Vieira, S., Goulart, L., Boodts, J., Brito-Madurro, A., and Madurro, J., 2008, "Electrochemical Investigation of Oligonucleotide-DNA Hybridization on Poly(4-Methoxyphenethylamine)", **International Journal of Molecular Sciences**, Vol. 9, No. 7, pp. 1173-1187.

50. Guiseppi-Elie, A. and Lingerfelt, L., 2005, "Impedimetric Detection of DNA Hybridization: Towards near-Patient DNA Diagnostics", In **Immobilisation of DNA on Chips I**. Wittmann, C., Springer Berlin Heidelberg, Germany, pp. 161-186.

51. Giusto, D. and King, G., 2005, "Special-Purpose Modifications and Immobilized Functional Nucleic Acids for Biomolecular Interactions", In **Immobilisation of DNA on Chips Ii**. Wittmann, C., Springer Berlin Heidelberg, Germany, pp. 131-168.

52. Avnir, D., Coradin, T., Lev, O., and Livage, J., 2006, "Recent Bio-Applications of Sol-Gel Materials", **Journal of Materials Chemistry**, Vol. 16, No. 11, pp. 1013-1030.

53. Pividori, M.I., Merkoçi, A., and Alegret, S., 2000, "Electrochemical Genosensor Design: Immobilisation of Oligonucleotides onto Transducer Surfaces and Detection Methods", **Biosensors and Bioelectronics**, Vol. 15, No. 5–6, pp. 291-303.

54. Li, Z., Niu, T., Zhang, Z., Feng, G., and Bi, S., 2011, "Studies on the Effect of Solvents on Self-Assembly of Thioctic Acid and Mercaptohexanol on Gold", **Thin Solid Films**, Vol. 519, No. 13, pp. 4225-4233.

55. Bănică, F.G., 2012, "Nucleic Acids in Chemical Sensors", In **Chemical Sensors and Biosensors: Fundamentals and Applications**. Bănică, F.G., 1st ed., John Wiley & Sons, Ltd, UK, pp. 118-134.

56. Yoon, H.C., Hong, M.-Y., and Kim, H.-S., 2001, "Reversible Association/Dissociation Reaction of Avidin on the Dendrimer Monolayer Functionalized with a Biotin Analogue for a Regenerable Affinity-Sensing Surface", **Langmuir**, Vol. 17, No. 4, pp. 1234-1239.

57. Han, X., Cheetham, M.R., Sheikh, K., Olmsted, P.D., Bushby, R.J., and Evans, S.D., 2009, "Manipulation and Charge Determination of Proteins in Photopatterned Solid Supported Bilayers", **Integrative Biology**, Vol. 1, No. 2, pp. 205-211.

58. Kessler, C., Höltke, H.J., Seibl, R., Schmitz, G., Walter, T., Rüger, R., Sagner, G., Burg, J., Mühlegger, K., Haselbeck, A., and Hösel, W., 1992, "The Digoxigenin: Anti-Digoxigenin (Dig) System", In **Nonradioactive Labeling and Detection of Biomolecules**. Kessler, C., Springer Berlin Heidelberg, Germany, pp. 35-69.

59. Schlingman, D.J., Mack, A.H., Mochrie, S.G.J., and Regan, L., 2011, "A New Method for the Covalent Attachment of DNA to a Surface for Single-Molecule Studies", **Colloids and Surfaces B: Biointerfaces**, Vol. 83, No. 1, pp. 91-95.

60. Hejazi, M.S., Pournaghi-Azar, M.H., Alipour, E., and Karimi, F., 2008, "Construction, Electrochemically Biosensing and Discrimination of Recombinant Plasmid (Pethil-2) on the Basis of Interleukine-2 DNA Insert", **Biosensors and Bioelectronics**, Vol. 23, No. 11, pp. 1588-1594.

61. Souza, E., Nascimento, G., Santana, N., Ferreira, D., Lima, M., Natividade, E., Martins, D., and Lima-Filho, J., 2011, "Label-Free Electrochemical Detection of the Specific Oligonucleotide Sequence of Dengue Virus Type 1 on Pencil Graphite Electrodes", **Sensors**, Vol. 11, No. 6, pp. 5616-5629.

62. Rochelet-Dequaire, M., Djellouli, N., Limoges, B., and Brossier, P., 2009, "Bienzymatic-Based Electrochemical DNA Biosensors: A Way to Lower the Detection Limit of Hybridization Assays", **Analyst**, Vol. 134, No. 2, pp. 349-353.

63. Kagan, K., Masaaki, K., and Eiichi, T., 2004, "Recent Trends in Electrochemical DNA Biosensor Technology", **Measurement Science and Technology**, Vol. 15, No. 2, pp. R1–R11.

64. Cagnin, S., Caraballo, M., Guiducci, C., Martini, P., Ross, M., SantaAna, M., Danley, D., West, T., and Lanfranchi, G., 2009, "Overview of Electrochemical DNA Biosensors: New Approaches to Detect the Expression of Life", **Sensors**, Vol. 9, No. 4, pp. 3122-3148.

65. Castañeda, M.T., Alegret, S., Pumera, M., and Merkoçi, A.,2006. "Electrochemical Sensors for Biomedical Applications Based on DNA Hybridization Detection Using Gold Nanoparticle Tags". **Ibero-American Congress on Sensors (IBERSENSOR)**, 27-29 Sep. 2006, Montevideo, Uruguay pp. 1-5.

66. Chen, H., Kou, X., Yang, Z., Ni, W., and Wang, J., 2008, "Shape- and Size-Dependent Refractive Index Sensitivity of Gold Nanoparticles", **Langmuir**, Vol. 24, No. 10, pp. 5233-5237.

67. Henze, G., 2004, **Introduction to Polarography and Voltammetry**, [online], Available: http://www.metrohm.com/com/Search/index.html?identifier=80275003&language=en [2013, March 27].

68. Lee, T.M.-H., Li, L.-L., and Hsing, I.M., 2003, "Enhanced Electrochemical Detection of DNA Hybridization Based on Electrode-Surface Modification", **Langmuir**, Vol. 19, No. 10, pp. 4338-4343.

69. Kawde, A.-N. and Wang, J., 2004, "Amplified Electrical Transduction of DNA Hybridization Based on Polymeric Beads Loaded with Multiple Gold Nanoparticle Tags", **Electroanalysis**, Vol. 16, No. 1-2, pp. 101-107.

70. De Geest, B.G., Sanders, N.N., Sukhorukov, G.B., Demeester, J., and De Smedt, S.C., 2007, "Release Mechanisms for Polyelectrolyte Capsules", **Chemical Society Reviews**, Vol. 36, No. 4, pp. 636-649.

71. Herk, A.M. and Landfester, K., 2010, "Historical Overview of (Mini)Emulsion Polymerizations and Preparation of Hybrid Latex Particles", In **Hybrid Latex Particles**. Herk, A.M. and Landfester, K., Springer Berlin Heidelberg, Germany, pp. 1-18.

72. Pichot, C., 2004, "Surface-Functionalized Latexes for Biotechnological Applications", **Current Opinion in Colloid & Interface Science**, Vol. 9, No. 3–4, pp. 213-221.

73. Zhu, N., Zhang, A., He, P., and Fang, Y., 2004, "DNA Hybridization at Magnetic Nanoparticles with Electrochemical Stripping Detection", **Electroanalysis**, Vol. 16, No. 23, pp. 1925-1930.

74. Dong, X., Zhao, W., Xu, J., and Chen, H., 2011, "Magnetic Particles and Cadmium Sulfide Nanoparticles Tagging for Signal-Amplifying Detection of Nucleic Acids", **Science China Chemistry**, Vol. 54, No. 8, pp. 1304-1310.

75. Leoni, E. and Legnani, P.P., 2001, "Comparison of Selective Procedures for Isolation and Enumeration of Legionella Species from Hot Water Systems", **Journal of Applied Microbiology**, Vol. 90, No. 1, pp. 27-33.

76. Alocilja, E.C. and Radke, S.M., 2003, "Market Analysis of Biosensors for Food Safety", **Biosensors and Bioelectronics**, Vol. 18, No. 5–6, pp. 841-846.

77. Bej, A.K., Mahbubani, M.H., Dicesare, J.L., and Atlas, R.M., 1991, "Polymerase Chain Reaction-Gene Probe Detection of Microorganisms by Using Filter-Concentrated Samples", **Applied and Environmental Microbiology**, Vol. 57, No. 12, pp. 3529-3534.

78. Lazcka, O., Campo, F.J.D., and Muñoz, F.X., 2007, "Pathogen Detection: A Perspective of Traditional Methods and Biosensors", **Biosensors and Bioelectronics**, Vol. 22, No. 7, pp. 1205-1217.

79. Singh, A., Poshtiban, S., and Evoy, S., 2013, "Recent Advances in Bacteriophage Based Biosensors for Food-Borne Pathogen Detection", **Sensors**, Vol. 13, No. 2, pp. 1763-1786.

80. Guillermo López-Campos, Martínez-Suárez, J., Aguado-Urda, M., and López-Alonso, V., 2012, "Introduction to Foodborne Diseases", In **Microarray Detection and Characterization of Bacterial Foodborne Pathogens**. Guillermo López-Campos, et al., Springer Verlag, New York, USA, pp. 1-11.

81. Déjugnat, C., Shchukin, D.G., and Sukhorukov, G.B., 2006, "Microcapsules through Layer-by-Layer Assembly Technique", In **Functional Coatings**, Wiley-VCH Verlag GmbH & Co. KGaA, pp. 67-83.

82. Sanchez-Gaytan, B.L. and Park, S.-J., 2010, "Spiky Gold Nanoshells", **Langmuir**, Vol. 26, No. 24, pp. 19170-19174.

83. Gao, C., Moya, S., Donath, E., and Möhwald, H., 2002, "Melamine Formaldehyde Core Decomposition as the Key Step Controlling Capsule Integrity: Optimizing the Polyelectrolyte Capsule Fabrication", **Macromolecular Chemistry and Physics**, Vol. 203, No. 7, pp. 953-960.

84. Chen, J.-P. and Su, D.-R., 2001, "Latex Particles with Thermo-Flocculation and Magnetic Properties for Immobilization of A-Chymotrypsin", **Biotechnology Progress**, Vol. 17, No. 2, pp. 369-375.

85. Huang, Z. and Tang, F., 2004, "Preparation, Structure, and Magnetic Properties of Polystyrene Coated by Fe3o4 Nanoparticles", **Journal of Colloid and Interface Science**, Vol. 275, No. 1, pp. 142-147.

86. Wu, W., He, Q., and Jiang, C., 2008, "Magnetic Iron Oxide Nanoparticles: Synthesis and Surface Functionalization Strategies", **Nanoscale Research Letters**, Vol. 3, No. 11, pp. 397-415.

87. Tadera, K., Minami, Y., and Chohchi, M., 2003, "Interaction between Acidic Polysaccharides and Proteins", **Bioscience, Biotechnology, and Biochemistry**, Vol. 67, No. 8, pp. 1840-1843.

88. Lukesh, J.C., Palte, M.J., and Raines, R.T., 2012, "A Potent, Versatile Disulfide-Reducing Agent from Aspartic Acid", **Journal of the American Chemical Society**, Vol. 134, No. 9, pp. 4057-4059.

89. Ackerson, C.J., Powell, R.D., and Hainfeld, J.F., 2010, "Site-Specific Biomolecule Labeling with Gold Clusters", In **Methods in Enzymology**. Grant, J.J., Academic Press, Inc., New York, USA, pp. 195-230.

90. Dharuman, V. and Hahn, J.H., 2007, "Effect of Short Chain Alkane Diluents on the Label Free Electrochemical DNA Hybridization Discrimination at the Hs-Ssdna/Diluent Binary Mixed Monolayer in Presence of Cationic Intercalators", **Sensors and Actuators B: Chemical**, Vol. 127, No. 2, pp. 536-544.

91. Chevalier, J., Yi, J., Michel, O., and Tang, X.-M., 1997, "Biotin and Digoxigenin as Labels for Light and Electron Microscopy in Situ Hybridization Probes: Where Do We Stand?", **Journal of Histochemistry & Cytochemistry**, Vol. 45, No. 4, pp. 481-491.

92. Leitch, I. and Pat Heslop-Harrison, J.S., 1994, "Detection of Digoxigenin-Labeled DNA Probes Hybridized to Plant Chromosomes in Situ", In **Protocols for Nucleic Acid Analysis by Nonradioactive Probes**. Isaac, P., Humana Press, Inc., Totowa, USA, pp. 177-185.

93. Bonnet, G., Tyagi, S., Libchaber, A., and Kramer, F.R., 1999, "Thermodynamic Basis of the Enhanced Specificity of Structured DNA Probes", **Proceedings of the National Academy of Sciences**, Vol. 96, No. 11, pp. 6171-6176.

94. Yang, W. and Lai, R.Y., 2011, "Comparison of the Stem-Loop and Linear Probe-Based Electrochemical DNA Sensors by Alternating Current Voltammetry and Cyclic Voltammetry", **Langmuir**, Vol. 27, No. 23, pp. 14669-14677.

95. Liu, G., Wan, Y., Gau, V., Zhang, J., Wang, L., Song, S., and Fan, C., 2008, "An Enzyme-Based E-DNA Sensor for Sequence-Specific Detection of Femtomolar DNA Targets", **Journal of the American Chemical Society**, Vol. 130, No. 21, pp. 6820-6825.

96. Zuker, M., 2003, "Mfold Web Server for Nucleic Acid Folding and Hybridization Prediction", **Nucleic Acids Research**, Vol. 31, No. 13, pp. 3406-3415.

97. Whitlock, S., 2009, **Immunohematology for Medical Laboratory Technicians**, Delmar Cengage Learning, Stamford, USA, pp. 19.

98. Yusoff, N.A., Soin, N., Rahman, N.A., Rahman, R., Kahar, M.K.B.A., and Ibrahim, F.,2009. "Binding Characteristics Study for Dengue Virus Non-Structural Protein 1 of Antigen and Its Antibody by Using Circular Dichroism Technique". **Technical Postgraduates (TECHPOS)**, 14-15 Dec. 2009, Kuala Lumpur, Malaysia. , pp. 1-6.

99. Demirel, G.B., Dilsiz, N., Ergun, M.A., Cakmak, M., and Caykara, T., 2011, "Photocontrollable DNA Hybridization on Reversibly Photoresponsive Surfaces", **Journal of Materials Chemistry**, Vol. 21, No. 28, pp. 10415-10420.

100. Mery, J., Granier, C., Juin, M., and Brugidou, J., 1993, "Disulfide Linkage to Polyacrylic Resin for Automated Fmoc Peptide Synthesis. Immunochemical Applications of Peptide Resins and Mercaptoamide Peptides", **International Journal of Peptide and Protein Research**, Vol. 42, No. 1, pp. 44-52.

101. Han, J.C. and Han, G.Y., 1994, "A Procedure for Quantitative Determination of Tris(2-Carboxyethyl)Phosphine, an Odorless Reducing Agent More Stable and Effective Than Dithiothreitol", **Analytical Biochemistry**, Vol. 220, No. 1, pp. 5-10.

102. Hecker KH. and Roux KH., 1996, "High and Low Annealing Temperatures Increase Both Specificity and Yield in Touchdown and Stepdown PCR.", **Biotechniques**, Vol. 20, No. 3, pp. 478-485.

103. Tinoco Jr, I. and Bustamante, C., 1999, "How RNA Folds", **Journal of Molecular Biology**, Vol. 293, No. 2, pp. 271-281.

104. Owczarzy, R., You, Y., Moreira, B.G., Manthey, J.A., Huang, L., Behlke, M.A., and Walder, J.A., 2004, "Effects of Sodium Ions on DNA Duplex Oligomers: Improved Predictions of Melting Temperatures", **Biochemistry**, Vol. 43, No. 12, pp. 3537-3554.

105. Danilowicz, C., Lee, C.H., Kim, K., Hatch, K., Coljee, V.W., Kleckner, N., and Prentiss, M., 2009, "Single Molecule Detection of Direct, Homologous, DNA/DNA Pairing", **Proceedings of the National Academy of Sciences**, Vol. 106, No. 47, pp. 19824-19829.

106. Kumagai, I. and Tsumoto, K., 2001, "Antigen–Antibody Binding", In **Encyclopedia of Life Sciences**. Group, N.P., Nature Publishing Group, London, UK, pp. 1-7.

107. Reverberi, R. and Reverberi, L., 2008, "Factors Affecting the Antigen-Antibody Reaction", **Blood Transfusion**, Vol. 6, No. 1, pp. 227.

108. Herzer, S. and Englert, D.F., 2002, "Nucleic Acid Hybridization", In **Molecular Biology Problem Solver**. Gerstein, A.S., John Wiley & Sons, Ltd., New York, USA, pp. 399-460.

109. Pinijsuwan, S., Rijiravanich, P., Somasundrum, M., and Surareungchai, W., 2008, "Sub-Femtomolar Electrochemical Detection of DNA Hybridization Based on Latex/Gold Nanoparticle-Assisted Signal Amplification", **Analytical Chemistry**, Vol. 80, No. 17, pp. 6779-6784.

110. Boateng, J., Peek, J., Zahorchak, R., and Chittur, K., 2012, "Dendron-Modified Surfaces Provide an Ideal Environment for Stem–Loop DNA Probes", **Analytical Biochemistry**, Vol. 430, No. 1, pp. 39-44.

111. Kolpashchikov, D.M., 2012, "An Elegant Biosensor Molecular Beacon Probe: Challenges and Recent Solutions", **Scientifica**, Vol. 2012, No., pp. 17.

112. Berk, Z., 2009, "Reaction Kinetics", In **Food Process Engineering and Technology**. Berk, Z., Academic Press, Inc., San Diego, USA, pp. 115-127.

113. Farrokh, C., Jordan, K., Auvray, F., Glass, K., Oppegaard, H., Raynaud, S., Thevenot, D., Condron, R., De Reu, K., Govaris, A., Heggum, K., Heyndrickx, M., Hummerjohann, J., Lindsay, D., Miszczycha, S., Moussiegt, S., Verstraete, K., and Cerf, O., (in press), Review of Shiga-Toxin-Producing *Escherichia coli* (Stec) and Their Significance in Dairy Production. **International Journal of Food Microbiology**.

114. Ghosh, S., Chakraborty, R., Chatterjee, G., and Raychaudhuri, U., 2012, "Study on Fermentation Conditions of Palm Juice Vinegar by Response Surface Methodology and Development of a Kinetic Model", **Brazilian Journal of Chemical Engineering**, Vol. 29, No. 30, pp. 461-472.

115. Manel, Z., Sana, M.h., Nedia, K., Moktar, H., and Ali, F., 2011, "Microbiological Analysis and Screening of Lactic Acid Bacteria from Tunisian Date Palm Sap", **African Journal of Microbiology Research**, Vol. 5, No. 19, pp. 2929-2936.

116. Liu, M., 2010, **Understanding the Mechanical Strength of Microcapsules and Their Adhesion on Fabric Surfaces**, Chemical Engineering, The University of Birmingham, UK, p. 256.

APPENDIX

APPENDIX A: ANALYTICAL MATHODS

1. The preparation of spiky gold capsule for the cross-section TEM images

The cross-section image of spiky gold capsules were used to observer the loading of gold nanoparticle into the capsule. Their preparation was adapted from microcapsule preparation in literature [116].

Briefly, 200 μL of spiky gold capsule were centrifuged at 14,000 rpm for 1 min, and the supernatant was discarded. Then, 1.5 mL of 2.5 % glutaraldehyde in PB (pH 7.0) was added and incubated at 4 ◦C for 1 h, followed by replacing the supernatant with 1.5 mL of 50% ethanol. After mixed 30 min and centrifuged at 14,000 rpm for 1 min, the spiky gold capsule were mixed with 70% and 100% ethanol, respectively. A mixture of ethanol/acrylic resin (1:1 volume ratio) was added into the precipitated spiky gold capsule and incubated for 12 h before being embedded in acrylic resin, and then continued incubation for 2 days. After that, a spiky gold capsule/acrylic resin mixture and hardner solution were mixed with the volume ratio was 5:1 and then added into gelatin capsule. The gelatin capsule was dried in an oven at 60 ◦C for 12 h. An ultramicrotome was used to trim and section it for observed TEM.

2. The calculation of the PAA encapsulated in microcapsule

The method to calculate the mass of a hollow shell polyelectrolyte microcapsule and PAA-capsule will be explained in this section. The diameter and thickness of both capsules could be measured by using TEM. The diameter of the hollow shell polyelectrolyte was 425.19 nm and shell thickness was 48.04 nm. Therefore, the volume of the hollow polyelectrolyte microcapsule can be calculated, by using the volume formula for a sphere ($\frac{4}{3}\pi r^3$) and the inner diameter of the capsule, to be 2.16×10^{-14} cm^3. From the equation for density ($\rho = \frac{m}{V}$) the mass of one capsule could be estimated to be 2.37×10^{-14} g (the density of the polyelectrolyte shell was 1.1 g cm^3). In the reaction for PAA-capsule preparation, we use 2.50×10^{-2} g of hollow shell polyelectrolyte microcapsule which it can be estimated to be 1.05×10^{12} particles.

The mass of one PAA-capsule can be estimated from the excess PAA after loading into hollow shell polyelectrolyte microcapsule, as measured by the UV absorbance of PAA (210 nm). The total mass of PAA used for loading was 1.16 g and the remaining PAA mass was 1.02 g. Hence, the mass of PAA encapsulated in hollow shell polyelectrolyte microcapsule was 0.14 g. Since we know the amount of hollow shell polyelectrolyte microcapsule, the mass of PAA loaded was about 1.30×10^{-13} g. The mass of one PAA-capsule was 1.54×10^{-13} g.

3. The calculation of the amount of gold ions loaded into PAA-capsule.

The amount of Au^{3+} ions encapsulated per capsule was estimated by ASV using a liner calibration curve concentration, as shown in Figure 4.7:

$$i_{pa} = (1.0 \times 10^{-6})c - (3 \times 10^{-7})$$

where c is the Au^{3+} ions concentration in bulk solution (μM) and i_{pa} is the anodic peak current of the Au^{3+} ions

5 μL of sample (spiky gold capsule) were added to the bulk solution of HBr/Br_2, thus the total concentration of the Au^{3+} ions in spiky gold capsule can be calculated as follow equation:

$$\text{Total concentration of } Au^{3+}\text{ions} = \frac{c \times V_{bulk}}{5\ \mu L}$$

where c is the Au^{3+} ions concentration, V_{bulk} is the total volume in bulk reaction (μL). As we know the amount of PAA-capsule used in the preparation of the spiky gold capsules, assuming no capsules are lost, the quantity of Au^{3+}ions encapsulated can be calculated from:

$$\text{Molecule of } Au^{3+}\text{ions encapsulated per capsule} = \frac{\text{Concentration of } Au^{3+}\text{ions} \times 6.023 \times 10^{23}}{\text{amount of PAA-capsule used, (P L}^{-1})}$$

APPENDIX B: ANALYTICAL RESULTS

Table B.1 The t-test result of the DNA hybridization detection current response based on platform I (for Figure 4.18)

	0 pM	1 pM
Mean	4.3165E-06	4.7110E-06
Variance	1.8982E-13	3.3289E-13
Observations	6	6
Pearson Correlation	0.1983	
Hypothesized Mean Difference	0	
df	5	
t Stat	-1.4857	
P(T<=t) one-tail	0.0987	
t Critical one-tail	2.0150	
P(T<=t) two-tail	0.1975	
t Critical two-tail	2.5706	

Table B.2 The t-test result of the DNA hybridization detection current response based on platform II (for Figure 4.21)

	0 pM	1 pM
Mean	5.2760E-06	6.2978E-06
Variance	2.9169E-14	2.3179E-14
Observations	5	5
Pearson Correlation	0.2413	
Hypothesized Mean Difference	0	
df	4	
t Stat	-11.4528	
P(T<=t) one-tail	0.0002	
t Critical one-tail	2.1318	
P(T<=t) two-tail	0.0003	
t Critical two-tail	2.7764	

Table B.3 The ANOVA result of current response from effect of SL-DNA concentration (for Figure 4.32)

SUMMARY

Groups	*Count*	*Sum*	*Average*	*Variance*
1nM	5	9.8264	1.9653	0.0975
10nM	5	9.6517	1.9303	0.0052
100nM	5	10.1524	2.0305	0.1873
1uM	5	10.4877	2.0975	0.4054

ANOVA

Source of Variation	*SS*	*df*	*MS*	*F*	*P-value*	*F crit*
Between Groups	0.0818	3	0.0273	0.1569	0.9237	3.2389
Within Groups	2.7814	16	0.1738			
Total	2.8632	19				

Table B.4 ANOVA result of DNA hybridization detection current response based on different genomic DNA extraction methods. (for Figure 4.36)

SUMMARY

Groups	*Count*	*Sum*	*Average*	*Variance*
Test Kit_*E. coli* BL21	5	2.61E-05	5.22E-06	3.14E-13
Heat shock_*E. coli* BL21	5	1.88E-05	3.77E-06	1.25E-13
Test Kit_*E. coli* ATCC8739	5	2.74E-05	5.48E-06	1.34E-13
Heat shock_*E. coli* ATCC8739	5	2.13E-05	4.27E-06	1.01E-13

ANOVA

Source of Variation	*SS*	*df*	*MS*	*F*	*P-value*	*F crit*
Between Groups	9.74E-12	3	3.25E-12	19.2720	1.46E-05	3.2389
Within Groups	2.69E-12	16	1.68E-13			
Total	1.24E-11	19				

Table B.5 ANOVA result of DNA hybridization detection current response of *E. coli* BL21, ATCC8739 and O157:H7 genomic DNA in milk sample. (for Figure 4.38)

SUMMARY of *E. coli* BL21

Groups (CFU mL^{-1})	*Count*	*Sum*	*Average*	*Variance*
3.20E+03	3	9.0456	3.0152	1.2322
3.20E+04	3	10.2187	3.4062	0.5205
3.20E+05	3	15.3667	5.1222	2.5262
3.20E+06	3	17.6560	5.8853	3.3869
3.20E+07	3	24.0478	8.0159	1.9404

Source of Variation	*SS*	*df*	*MS*	*F*	*P-value*	*F crit*
Between Groups	49.0041	4	12.2510	6.3766	0.0081	3.4780
Within Groups	19.2125	10	1.9212			
Total	68.2166	14				

SUMMARY of *E. coli* ATCC8739

Groups (CFU mL^{-1})	*Count*	*Sum*	*Average*	*Variance*
4.48E+03	3	9.2045	3.0682	0.3947
4.48E+04	3	13.3142	4.4381	0.2974
4.48E+05	3	16.7182	5.5727	0.7996
4.48E+06	3	17.5187	5.8396	1.2153
4.48E+07	3	22.4165	7.4722	4.3930

Source of Variation	*SS*	*df*	*MS*	*F*	*P-value*	*F crit*
Between Groups	32.4162	4	8.1040	5.7071	0.0117	3.4780
Within Groups	14.2000	10	1.4200			
Total	46.6162	14				

SUMMARY of *E. coli* O157:H7

Groups (CFU mL^{-1})	*Count*	*Sum*	*Average*	*Variance*
1.48E+03	3	8.8208	2.9403	0.1697
1.48E+04	3	10.4308	3.4769	1.2197
1.48E+05	3	14.1981	4.7327	5.5527
1.48E+06	3	15.5818	5.1939	0.4269
1.48E+07	3	18.2421	6.0807	0.6385

Source of Variation	*SS*	*df*	*MS*	*F*	*P-value*	*F crit*
Between Groups	19.5380	4	4.8845	3.0500	0.0695	3.4780
Within Groups	16.0149	10	1.6015			
Total	35.5529	14				

Table B.6 ANOVA result of DNA hybridization detection current response of *E. coli* BL21, ATCC8739 and O157:H7 genomic DNA in fermented palm juice sample. (for Figure 4.39)

SUMMARY of *E. coli* BL21

Groups (CFU mL^{-1})	*Count*	*Sum*	*Average*	*Variance*
3.20E+03	3	9.5216	3.1739	0.6539
3.20E+04	3	12.9749	4.3250	1.3592
3.20E+05	3	15.4305	5.1435	0.2931
3.20E+06	3	18.3440	6.1147	0.0328
3.20E+07	3	21.7380	7.2460	4.6800

Source of Variation	*SS*	*df*	*MS*	*F*	*P-value*	*F crit*
Between Groups	29.6903	4	7.4226	5.2875	0.0150	3.4780
Within Groups	14.0380	10	1.4038			
Total	43.7283	14				

SUMMARY of *E. coli* ATCC8739

Groups (CFU mL^{-1})	*Count*	*Sum*	*Average*	*Variance*
4.48E+03	3	9.5985	3.1995	1.0541
4.48E+04	3	12.7456	4.2485	1.1089
4.48E+05	3	15.3741	5.1247	0.3351
4.48E+06	3	18.7880	6.2627	0.9424
4.48E+07	3	21.2793	7.0931	0.9300

Source of Variation	*SS*	*df*	*MS*	*F*	*P-value*	*F crit*
Between Groups	28.87507	4	7.2188	8.2585	0.0033	3.4780
Within Groups	8.741028	10	0.8741			
Total	37.6161	14				

SUMMARY of *E. coli* O157:H7

Groups (CFU mL^{-1})	*Count*	*Sum*	*Average*	*Variance*
1.48E+03	3	8.0503	2.6834	1.5668
1.48E+04	3	12.1792	4.0597	0.1161
1.48E+05	3	15.3868	5.1289	0.8221
1.48E+06	3	17.7862	5.9287	0.4051
1.48E+07	3	19.9497	6.6499	9.3330

Source of Variation	*SS*	*df*	*MS*	*F*	*P-value*	*F crit*
Between Groups	29.3745	4	7.3436	2.9991	0.0724	3.4780
Within Groups	24.4864	10	2.4486			
Total	53.8609	14				

CURRICULUM VITAE

NAME	Miss Naphat Khunrattanaporn
DATE OF Birth	25 April 1988
EDUCATIONAL RECORD	
High School	Chakkhamkhanathon School, 2005
Bachelor's Degree	B.S. (Agro-Industrial Biotechnology), Chiang Mai University, 2009
Master's Degree	M.Sc. (Biotechnology), King Mongkut's University of Technology Thonburi (KMUTT), 2012
SCHOLARSHIP	School of Bioresources and Technology, King Mongkut's University of Technology Thonburi (2010-2011)
	National Nanotechnology Center (2011-2012)
	National Research Council of Thailand (2012-2013)
ORAL PRESENTATION	N. Khunrattanaporn, P. Rijiravanich, M. Somasundrum, W. Surarengchai, 2012, "Novel electrochemical label based on synthetic gold nanostructures in microcapsule", **PACCON 2012-CHEMISTRY BEYOND BOUNDARIES**, 11-13 Jan. 2012, The Empress Convention Center, Chiang Mai, Thailand.